Stephen F. Austin State University

SFA ScholarWorks

Spring 5-13-2017

THE REGULATION OF ROTAVIRUS−INFECTED HT29.F8 AND MA104 CELLS TREATED WITH ARACHIDIN 1 OR ARACHIDIN 3

Caleb M. Witcher
Stephen F Austin State University, calebwitcher@students.rossu.edu

Follow this and additional works at: https://scholarworks.sfasu.edu/etds

Part of the Cell Biology Commons, Therapeutics Commons, and the Virus Diseases Commons
Tell us how this article helped you.

THE REGULATION OF ROTAVIRUS–INFECTED HT29.F8 AND MA104 CELLS
TREATED WITH ARACHIDIN 1 OR ARACHIDIN 3

Creative Commons License

THE REGULATION OF ROTAVIRUS–INFECTED HT29.F8 AND MA104 CELLS

TREATED WITH ARACHIDIN 1 OR ARACHIDIN 3

By

CALEB MICHAEL WITCHER, B.S IN ANIMAL SCIENCE

Presented to the Faculty of Graduate School of

Stephen F. Austin State University

In Partial Fulfillment

Of the Requirements

For the Degree of

Master of Science in Biology

STEPHEN F. AUSTIN STATE UNIVERSITY

May 20, 2017

THE REGULATION OF ROTAVIRUS–INFECTED HT29.F8 AND MA104 CELLS

TREATED WITH ARACHIDIN 1 OR ARACHIDIN 3

By

CALEB MICHAEL WITCHER, B.S IN ANIMAL SCIENCE

APPROVED:

_____
Rebecca D. Parr, Ph.D., Thesis Director

_____
Beatrice Clack, Ph.D., Committee Member

_____
Josephine Taylor, Ph.D., Committee Member

_____
Donald Pratt, Ph.D., Committee Member

_____
Richard Berry, D.M.A.
Dean of the Graduate School

ABSTRACT

Rotavirus (RV) infections cause severe life threatening diarrhea in young children and immunocompromised individuals. Several effective vaccines have been developed for young children but are not protective against all strains of RV, and there are no anti-RV therapeutics. Our laboratory has discovered a decrease in the number of infectious simian RV particles (SA114f) in human intestinal cell line, HT29.f8 cells with the addition of either of two stilbenoids, arachidin-1 (A1) or arachidin-3 (A3). This suggests effects on the host cell and RV replication. We examined the cellular effects of human RV strain (Wa) on a human intestinal cell line (HT29.f8) and an African green monkey kidney cell line (MA104) treated with/without either arachidin. Both cell lines demonstrated apoptotic characteristics that were modulated with the addition of either A1 or A3, and the size and population of the released virus particles were significantly altered. Likewise, the number of infectious virus particles released from the arachidin treated cells were significantly reduced. This data supports the RV therapeutic potential of A1 and A3.

In dedication to Norris Linvel Witcher (1928-2013),

Who always had faith in me no matter the situation, and helped make me who I

am today

ACKNOWLEDGEMENTS

Completing this thesis project was a great milestone in my life and it couldn't have been done without the help and support of many colleagues, professors, friends and family.   Individuals in the Parr and Clack labs have helped me in more ways than I can mention, and I wish to extend my sincere thanks to them. There have been countless occasions throughout my research when I wanted to give up, however God reminds me I can accomplish anything if I put my mind to it.

I would like to express my special thanks to Dr. Rebecca Parr, for her taking me in under her wing and instructing her knowledge and expertise in this study as well as guidance throughout my graduate career. Furthermore, I would like to thank Dr. Beatrice Clack, Dr. Josephine Taylor and Dr. Donald Pratt for their valued suggestions as well for the encouragement and support along the way as my committee members.

A special thanks to my parents, Mike and Eva Witcher, who have offered continuous support and motivation throughout my academic career. Lastly, I would like to thank Sara Witcher, for being patient and supportive throughout all my research.

TABLE OF CONTENTS

LIST OF FIGURES

CHAPTER ONE

A TIME COURSE STUDY OF ROTAVIRUS-INFECTED CELLS TREATED WITH STILBENOIDS AND THE REGULATION OF CELL DEATH PATHWAYS

CHAPTER TWO

Arachidin 1 and Arachidin 3 Regulations of Rotavirus-infected MA104 Cells

LIST OF TABLES

CHAPTER ONE

A TIME COURSE STUDY OF ROTAVIRUS-INFECTED CELLS TREATED WITH STILBENOIDS AND THE REGULATION OF CELL DEATH PATHWAYS

CHAPTER TWO

Arachidin 1 and Arachidin 3 Regulations of Rotavirus-infected MA104 Cells

LIST OF ABBREVIATIONS

Symbol	Description
A1	Arachidin 1
A3	Arachidin 3
ANOVA	Analysis of variance
BSA	Bovine serum albumin
CB	Cannabinoids
CBR	Cannabinoid Receptors
cDNA	Complementary DNA
Ct	Threshold cycle
DLP	Double Layered Particles
DMEM	Dulbecco's Modified Eagle's Medium
DNA	Deoxyribose Nucleic Acid
dNTP	Deoxy ribonucleotide triphosphate
dsRNA	Double stranded Ribonucleic Acid
ENS	Enteric nervous system
ER stress	Endoplasmic reticulum stress
$_e$RV	Enveloped Rotavirus particle
FBS	Fetal bovine serum

GI	Gastrointestinal
HPCCC	High Performance Countercurrent Chromatography
HPI	Hours post infection
HT29	Human colon adenocarcinoma cell line
HT29.f8	Spontaneously polarizing human colon adenocarcinoma cell line
IBS	Irritable bowel syndrome
MA104	African green monkey kidney cell line
MEM	Minimum essential media
MOI	Multiplicity of infection
mRNA	Messenger Ribonucleic Acid
$_{ne}$RV	Non-enveloped Rotavirus particle
NV	No Virus
PCR	Polymerase chain reaction
PFU	Plaque Forming Unit assay
qRT-PCR	Quantitative real time polymerase chain reaction
RdRP	RNA-dependent RNA polymerase
RNA	Ribonucleic acid
RRV	Rhesus Rotavirus
RV	Rotavirus

RV+A3	Rotavirus with 20μM A3
SA11.4f	Simian rotavirus strain
SD	Standard Deviation
SDS	Sodium dodecyl sulfate
TEM	Transmission Electron Microscopy
TLP	Triple layered particles
TRPS	Tunable Resistive Pulse Sensing Technology
VP	Viral protein
Wa	Human rotavirus strain

INTRODUCTION

Rotavirus

Rotavirus (RV) is a major cause of infantile gastroenteritis, which accounts for 20% of deaths in children less than 5 years of age. RV also causes severe diseases in pediatric and adult immunocompromised individuals, patients on chemotherapy, and transplantation patients. RV belongs to the family Reoviridae that infects humans and several other mammals including cattle, pigs, mice, and primates (Desselberger, 2014; Hall, Bridger, Chandler, & Woode, 1976; Mebus et al., 1976). The ubiquitous nature of RV and the health risks it poses for a wide range of hosts has made it a heavily studied pathogen for the past 70 years. One of the earliest studies dates to 1943 at Johns Hopkins University in Baltimore. Gnotobiotic calves were inoculated with stool samples from children experiencing gastroenteritis. Although the technology to identify the infectious agent was not available at that time, signs and symptom of lethargy and watery diarrhea were observed in the calves. In later years with the development of transmission electron microscopy (TEM), micrographs of intestinal epithelium from infant mice with diarrhea demonstrated spherical particles that were about 75 nm in diameter (Adams & Kraft, 1963). In 1973, stool samples from several severe gastroenteritis

cases in young children at the Royal Children's Hospital in London, England were submitted for electron microscopy (EM), and the same type of spherical particles observed by Adams and Kraft were detected (Bishop, Davidson, Holmes, & Ruck, 1973). It was the first confirmation in humans and led to further use of EM for diagnostics of RV infections. Preserved fecal samples from the 1943 study by Light and Hodes were viewed with EM in 1976 and "reovirus" like particles were seen (Light & Hodes, 1943; Mebus et al., 1976). Since then polyacrylamide gel electrophoresis (PAGE), enzyme linked immunosorbent assays (ELISA), and latex agglutination tests have been developed as more rapid and sensitive assays to test for RV infections.

Globally, where temperature varies according to seasonality, RV is more common in the cooler months, but the seasonal peaks of the infections can vary broadly (Cook, Glass, LeBaron, & Ho, 1990). This seasonality is not well understood and is uncommon among most enteric pathogens. It became increasingly important to discover epidemiological patterns of RV infections. One study looked at RV contaminated freshwater and its ability to maintain infectious RV particles (Rzeżutka & Cook, 2004). It was discovered that at 20°C, RV remained infectious for approximately 10 days; however, at 4°C the virus was infectious for 32 days. Another study examined the occurrence of nosocomial RV infections. Fingertips of healthy individuals were inoculated with the human RV strain (Wa) and the survival of the virus was monitored at multiple time points for

260 minutes (Rzeżutka & Cook, 2004). It was found that RV retains infectivity for several hours on skin, and can remain infectious on various clinical and environmental fomites.   This indicates sterility and aseptic techniques are extremely important for care of newborns in hospital settings as they are highly susceptible to RV infections (Berardi *et al.*, 2009). Furthermore, RV-infected infants can begin showing symptoms within 1-2 days after birth, exhibiting watery diarrhea, vomiting, and fever that can last 4-8 days (Bernstein, 2009). Trans placental antibodies are passed from mother to infant at the time of birth, however, these maternally derived IgG antibodies provide limited protection and will be absent in the child by five months of age (Bobek *et al.*, 2010).

There have been up to 600,000 deaths associated with RV infections per year worldwide, with the majority of the deaths occurring in Africa and Asia (Bernstein, 2009; Parashar & Glass, 2009). RV is transmitted by the fecal-oral route and is extremely contagious during the diarrheal stage of infection (Cook et al., 1990). Once infected a person can remain asymptomatic or have an acute gastroenteritis (AGE) with mild to severe diarrhea, and vomiting. This combination of symptoms leads to a massive electrolyte imbalance causing severe dehydration. Dehydration and cardiac failure are the main causes of death due to RV infections (Desselberger, 2014; Tate et al., 2012). According to the Centers for Disease Control (CDC) and the World Health Organization (WHO), the fatality rates associated with diarrheal disease have fallen sharply since 1980, due to the aid of

RV vaccines and effective treatment practices (Bishop, 2009; Jiang, Jiang, Tate, Parashar, & Patel, 2010). However, recently there have been 114 million RV diarrheal episodes worldwide per year (Greenberg & Estes, 2009). Of these cases, approximately 2.4 million are hospitalized and over 500,000 children under the age of five succumb to the RV infection (Greenberg & Estes, 2009). Although the RV disease burden has been significantly decreased in Western Europe and the United States, both countries reported that 50% of gastroenteritis emergency cases presented in children were caused by RV infections (Greenberg & Estes, 2009).

In 1973, RV particles were visualized using EM by Ruth Bishop and her colleagues at the Department of Medicine, Melbourne University, Australia (Bishop et al., 1973). One of her collaborators, Thomas Flewett, and his team suggested the Latin name rota, meaning wheel, due to its unique microscopic appearance (Flewett & Woode, 1978). Four years later, the International Committee on Taxonomy of Viruses agreed to officially name the pathogen, rotavirus (Matthews, 1979). Infectious RV particles (virions) are approximately 75-80 nanometers in diameter, non-enveloped, with three concentric icosahedral protein layers that encapsulate 11 double stranded RNA segments. RV structure is composed of three structural, viral proteins, VP2, VP6 and VP7. The inner core or single layered particle is made up of 60 dimers of VP2. This layer encloses the complete viral genome as well as viral RNA dependent RNA polymerase, VP1 and the capping

4

enzyme VP3 (Desselberger, 2014; Patton, 1995; Payne et al., 2006). The intermediate capsid layer is composed of VP6 and is arranged in lattice form with 260 trimers forming its icosahedral layer. Immature virus particles with only VP6 as their outside protein coat are typically referred to as noninfectious double layered particles (DLPs) however they are transcriptionally competent during the replication process. The outermost layer consists of an icosahedral capsid made of VP7. One unique feature of rotavirus particles is the presence of large channels that penetrate through the VP7 and VP6 layers, allowing for the passage of aqueous materials in and out of the capsid (Payne et al., 2006). When an RV particle contains VP4 and VP7, it is considered a triple layered particle (TLP) and is infectious due to 60 projecting spikes that are made up of VP4 dimers used by virions for cell entry (D. Payne et al., 2006). When RV particles make contact with a host cell they attach with VP4 before it is cleaved by trypsin present in the small intestine. This produces a conformational change leading to the production of VP5 and VP8 that are necessary for viral entry into the host (M K Estes, Graham, & Mason, 1981). Low calcium levels in endosomes make it possible for direct membrane penetration due to the removal of the outer capsid protein, VP7 (Desselberger, 2014). The newly assembled DLPs are released into the cytoplasm of the infected cell and are transcriptionally active (Gardet et al., 2006). Once DLPs have made their way to a specialized structure called the viroplasm, viral replication begins to take place (Patton, 1995). Viroplasms are usually

adjacent to the nucleus and can vary in shape and size depending on the stage of the replication cycle (Desselberger, 2014). After new DLPs have been produced they bind to NSP4 found on the endoplasmic reticulum (ER). As VP4 and VP7 assemble, the ER membranes are removed, resulting in a mature TLP (Greenberg & Estes, 2009). Mature virions are released by lysis (McNulty et al,1976), or they can be delivered to the plasma membrane in polarizing cells.

There are two licensed RV attenuated vaccines, RotaTeq® (Merck) and Rotarix® (GlaxoSmithKline) in the United States, that prevent severe diarrhea, and Rotavac® which was recently released in India by Hyderabad-based Bharat Biotech International. However, the vaccines' efficacies are dependent on the timing of vaccination, and are designed to protect against common RV strains in specific areas of the world. Consequently, they are dependent on the genetic stability of the virus with rearrangements randomly occurring resulting in new infectious RV strains. Furthermore, the vaccines are contraindicated for immunosuppressed individuals, and there are no antiviral therapeutic agents currently available for RV infections. Besides the possibility of contracting RV-induced diarrhea directly from the attenuated vaccines, there are documented cases of horizontal transmission of vaccine RV among immunocompromised household contacts from vaccinated children who shed the vaccine virus. RV vaccines have been introduced in many countries around the world; however, it still remains an important cause of mortality in children.

Recent studies in the Parr laboratory have shown that stilbenoids, natural products from peanut hairy root cultures, notably decrease the production of infectious RV particles and significantly affect RV replication (Ball et al., 2015). This demonstrates the potential for the development of these stilbenoids as antiviral therapeutics.

Stilbenoids

Stilbenoids are secondary metabolites that act as phytoalexins produced by plants such as grapes, berries, and peanuts in response to pathogens (Huang et al., 2010; Moss et al., 2013). Phytoalexin substances synthesized by plants accumulate rapidly at areas of infections and demonstrate anti-oxidative properties (Chong et al., 2009; Jeandet et al., 2010).

Resveratrol, a common stilbenoid, has received a great deal of interest due to its wide range of biological activities with potential impact on human health, including anti-oxidant, anti-inflammatory, cardio protective, antiviral, anticancer, and anti-aging properties (Huang et al., 2010; Sobolev et al., 2006; Velayudhan et al., 2014). Many *in vitro* and *in vivo* studies have demonstrated significant, advantageous, biological effects of resveratrol (Berardi et al., 2009; Nakamura et al., 2010; Palamara et al., 2005), however due to limited oral bioavailability, resveratrol does not live up to its full potential (Gambini et al., 2015; Vitaglione et al., 2005). This may be due to rapid absorption and metabolism leading to the

formation of various metabolites such as resveratrol glucuronides and sulfates that are quickly released from the body (Gambini et al., 2015; Vitaglione et al., 2005). In peanuts, the majority of the known stilbenoids are prenylated, harboring an isopentenyl, hydrophobic moiety as in A1 and A3 (Sobolev et al., 2006).

Arachidins

Peanut (*Arachis hypogaea*) hairy root cultures produce multiple stilbenoids upon their exposure to abiotic (environmental) and biotic (caused by living organisms) stresses (Chong et al., 2009). Among these compounds the analogues of piceatannol and resveratrol, A1 and A3, respectively, possess anti-inflammatory, anti-cancer and anti-proliferative properties similar to resveratrol (Chang et al., 2006; Djoko et al., 2007).

One study suggests that the increased therapeutic activity of these natural products likely results from the increased ability to dissolve fats, oils, and non-polar solvents imparted by single or multiple prenyl groups present within their structure (Huang et al., 2010). It was proposed that the greater lipophilicity of the prenylated arachidins may allow for easier interaction between these substances and cell membranes. This would enhance associations with potential membrane-bound molecular targets responsible for the beneficial actions of these compounds (Huang et al., 2010). Another study suggests that the lipophilic side chain (3-methyl-1-butenyl group) might hinder the addition of glucuronic acid to a substrate

and thereby slow metabolism which enhances the bioavailability of the analogues piceatannol or resveratrol, A1 and A3 (Brents et al., 2012). Additionally, A3 also exhibits higher biological activities both *in vitro* when compared to resveratrol, as well as demonstrating antiviral activity (Ball et al., 2015).

Our first paper summarizes the progression of the RV infection with and without the arachidins using a time course study at 12, 14, 16, and 18 hours post infection (hpi) in a human intestinal cell line, HT29.f8.   Cell ultrastructurewas characterized and morphometric analysis of maturing virus particles were performed using transmission electron microscopy (TEM). Progeny infectious RV particles were measured using plaque forming assays (PFUs). At the same time points, released virus particles were evaluated for concentration and size distribution by tunable resistive pulse sensing (TRPS) analysis with the qNano instrument (IZON). Furthermore, the nucleus to cytoplasmic ratios were measured to observe the cells' progression to apoptosis. While performing the study on nucleus to cytoplasm ratios the presence of autophagosomes were reported to note the regulation and cross talk between apoptosis and autophagy. Likewise, qRT-PCR experiments were implemented to determine which transcripts associated with apoptosis and autophagy are being modulated with the addition of the arachidins.

CHAPTER ONE

A TIME COURSE STUDY OF ROTAVIRUS-INFECTED CELLS TREATED WITH STILBENOIDS AND THE REGULATION OF CELL DEATH PATHWAYS

Caleb M Witcher[1,] Hannah N Lockwood[1,2], Rebekah Napier-Jameson[1], Macie N Mattila[1], Essence B Strange[1], Josephine Taylor[1], Beatrice Clack[1], Fabricio Medina-Bolivar[3], Judith M Ball[3] and Rebecca D Parr[1*]

[1] Department of Biology, Stephen F Austin State University, Nacogdoches, TX 75962; [2] Hannah N. Lockwood, Tyler, TX, [3] Department of Biological Sciences & Arkansas Biosciences Institute, Arkansas State University, Jonesboro, AR 72401; [4] Department of Biological and Environmental Sciences, Texas A&M University-Commerce, Commerce, TX 77843, *e-mail: parrr1@sfasu.edu

ABSTRACT

Rotavirus (RV) infections cause severe diarrhea in young animals, children and immunocompromised individuals. Two vaccines for young children have been developed that are effective in reducing symptoms of specific RV strains commonly found in the United States, but are not protective against diarrhea caused by certain RV strains in other areas of the world. Therefore, understanding the mechanisms of RV pathogenesis, along with how the host responds to RV infections, will support the discovery of new strategies to use against RV infections. Our laboratory has shown that two natural products from peanut hairy root cultures, arachidin-1 (A1) and arachidin-3 (A3), significantly inhibit simian RV (SA114f) replication. Although the molecular mechanism(s) of action are not known, the decrease in infectious virus particles suggests antiviral activity. The objectives of this study were to determine if the arachidins have the same effects on a human (Wa) RV infection as previously described with the simian RV, and to perform a time course analysis of the changes in RV-infected cells and RV particles. Cell viability assays showed the arachidins alone had no effect on the cells, and virus plaque assays demonstrated a significant decrease in virus progeny similar to the simian RV study. Transmission electron microscopy (TEM) was used to observe the gross distribution of RV particles and the effects on cell ultrastructure. Two populations of significantly different sizes of RV particles were measured. A time

course of the ratios of the nucleus to the cytoplasm in RV-infected cells was compared to the ratios of RV-infected cells with the addition of the arachidins. Cells treated with the arachidins displayed an ultrastructure similar to control cells by 18 hpi. Tunable resistive pulse sensing technology (TRPS) was used to quantify and determined the distribution of sizes of all the virus particles in the supernatants of the treated and untreated cells at each time point. Supernatants collected from arachidin treated cells revealed a shift in population from non-enveloped, mature RV particles to enveloped particles by 18 hpi. Furthermore, slot blot assays of the HT29.f8 cell lysates demonstrate the presence of both cannabinoid receptors 1 and 2 which have been shown to bind to both A1 and A3. Taken together, these data demonstrate that Wa RV replication in HT29.f8 cells was affected by A1 and A3, with consistent patterns in cell morphology throughout the time course. The mechanism of action may be through binding of the arachidins to the cannabinoid receptors, however, the prominence of autophagosomes in A1 treated cells, but not in cells treated with A3 suggests different signaling pathways are activated. The arachidins appeared to hinder the progress of the RV infection, thus showing promise to be RV therapeutic agents.

1. Introduction

Rotavirus (RV) is one of the leading causes of severe gastroenteritis in infants and young children around the world (Bernstein, 2009; Stokley et al., 2014; World Health Organization, 2013). RV is in the family Reoviridae and infects humans and several mammals. The ubiquitous nature of RV and the health risks it poses for a wide range of hosts has made it a heavily studied pathogen for the past 70 years. With the development of transmission electron microscopy (TEM), micrographs of intestinal epithelium from infant mice with diarrhea demonstrate spherical particles that ranged from 65 to 75 nm in diameter and are identified as reo-like viruses (Adams & Kraft, 1963).

RV-infected infants can begin showing symptoms within 1-2 days after birth, exhibiting watery diarrhea, vomiting, and fever that can last 4-8 days (Bernstein, 2009). While trans placental antibodies transfer from mother to infant at the time of birth; these maternally derived IgG antibodies provide limited protection and will be absent in the child by 5 months of age (Bobek et al., 2010). RV is transmitted by the fecal-oral route and is extremely contagious during the diarrheal stage of infection (Cook et al., 1990). Once infected, a person can remain asymptomatic or have acute gastroenteritis (AGE) with mild to severe diarrhea, and vomiting. This combination of symptoms leads to a massive electrolyte imbalance causing severe dehydration. Dehydration and cardiac failure are the main causes of death

13

due to RV infections (Desselberger, 2014; Tate et al., 2012). Worldwide, there are only three licensed live vaccines available that prevent severe diarrhea; however, they are only effective against specific strains (Bhandari et al., 2014; Glass et al., 2014). Furthermore, the zoonotic nature of RV infections supports the likelihood that reassortment events will take place, decreasing the efficacy of the vaccines and warranting the need for novel therapeutic agents against RV infections (Desselberger, 2014).

Our laboratory is investigating the effects of highly purified prenylated stilbenoids extracted from peanut (*Arachis hypogea*) hairy root cultures on RV infections (Ball et al., 2015). Previously, four stilbenoids were tested and the two prenylated stilbenoids, arachidin-1 (A1) and arachidin- 3 (A3), were shown to significantly inhibit the production of infectious simian RV (SA114f) virions (Ball et al., 2015). Stilbenoids are secondary metabolites derived from plants, such as grapes, berries and peanuts, that have antioxidant, anticancer, antifungal and anti-inflammatory properties (Aggarwal et al., 2004; Athar et al., 2007; Roupe et al., 2006). They are phytoalexins that are produced *de novo* in plants in response to environmental stresses and accumulate rapidly at areas of pathogen infections

---

[1] **Abbreviations:** Rotavirus (RV), Plaque forming units (PFU), hours post infection (hpi), dimethyl sulfoxide (DMSO), fetal bovine serum (FBS), Dulbecco's Modified Eagle's medium (DMEM), arachidin-1 (A1), arachidin-3 (A3), multiplicity of infection (MOI), tissue culture (TC), MSV (modified Murashige and Skoog medium), phosphate buffered saline (PBS), analysis of variance (ANOVA), transmission electron microscopy (TEM), tunable resistance pulse sensing (TRPS), endoplasmic reticulum (ER), plasma membrane (PM).

(Hammerschimidt & Dann, 1999; Huang et al., 2010; Moss et al., 2013). Although the molecular mechanism(s) of action for A1 and A3 on RV infections are unknown, the decrease in infectious virus particles suggests an effect on viral maturation and replication. Earlier studies demonstrated that RV dampens the innate immune response via modulation by NSP1 (Holloway & Coulson, 2013). This study investigated the effects of A1 and A3 on the clonally derived human intestinal cell line, HT29.f8, infected with the human RV strain, Wa.

Virus plaque forming assays were performed to quantify and compare the amount of infectious RV particles produced in human RV Wa-infected MA104 cells with and without A1 or A3. Tunable resistive pulse sensing technology (TRPS) using the qNano system by Izon was employed to quantify and determine the size distribution of all the virus particles in arachidin-treated and untreated HT29.f8 cells. Likewise, morphometric analyses of the cellular ultrastructure and gross distribution of RV particles was performed using transmission electron microscopy (TEM). This study demonstrated that A1 and A3 decreased the number of Wa, RV infectious virus particles produced. The size of the population of RV particles shifted from that of infectious RV particles to that of larger immature RV particles with arachidin treatment. These sizes correspond to the measured enveloped and non-enveloped RV particles observed in the cells. Also, changes in cell structure were observed that are characteristic of apoptosis and autophagy, and HT29.f8 cells were shown to be positive for both cannabinoid receptor 1 and receptor 2.

This study suggests a mechanism of action of the arachidins on RV-infected intestinal cells and the potential anti-RV therapeutic activity of A1 and A3.

2. Materials and Methods

2.1 Cells, Virus, Reagents and Bioproduction of Stilbenoids

2.1.1 Cell Lines and Virus

MA104 cells were obtained from ATCC (Rockville, MD) and the HT29.F8 cells, a spontaneously polarizing cell line, were derived from the parent human adenocarcinoma (HT29) intestinal line (Mitchell & Ball, 2004). The cell line was confirmed to be free of mycoplasma contamination using the MycoFind mycoplasma PCR kit version 2.0 (Clongen Laboratories, LLC). RV Wa (G[1] P[8] genotype) (Matthijnssens et al., 2008) was amplified, viral titers determined by plaque forming unit (PFU) assays in MA104 cells, and stored at -80°C. Arachidin efficacies against RV were tested using HT29.f8 cells obtained from Dr. Judith Ball (Texas A&M University, College Station, Tx). The cell line was maintained in Dulbecco's Modified Eagle Medium (DMEM; Gibco, Grand Island, NY) supplemented with 5% fetal bovine serum (FBS), glutamine (2 mM), penicillin-streptomycin (100 µg/mL) and non-essential amino acids (1X) (Sigma, St. Louis, MO) (Mitchell & Ball, 2004).

2.1.2 Bioproduction of stilbenoids in peanut hairy root cultures

A1 and A3 were purified from methyl-β-cyclodextrin (CD)-elicited peanut (*A. hypogea*) hairy root cultures as recently described (Abbott et al., 2010; Condori et al., 2010; Yang et al., 2015). Briefly, 9-day peanut hairy root cultures, line 3 (Condori et al. 2010), were elicited with methyl-β-cyclodextrin (fresh MSV medium with 9 g/L methyl-β-cyclodextrin (Cavasol® W7 M)) (Medina-Bolivar et al. 2007; Medina-Bolivar et al. 2010). Cultures were incubated in the dark at 28°C for an additional 72 hours to induce synthesis and secretion of stilbenoids into the culture medium (Abbott et al., 2010; Yang et al., 2015). After the elicitation period, the culture medium was removed from each flask and combined. This pooled medium was mixed with an equal volume of ethyl acetate in a separator funnel to extract the stilbenoids as described previously (Jose Condori et2 al., 2010). The ethyl acetate phase was recovered and dried in a rotavapor (Buchi), and A1 and A3 was purified from the extract with HPCCC. Fractions were collected every 30 seconds, dried in a speed-vac and selected fractions were checked for purity by mass spectrometry using an UltiMate 3000 ultrahigh performance liquid chromatography (UHPLC) system (Dionex, Thermo Scientific) coupled with a LTQ XL linear ion trap mass spectrometer (Thermo Scientific) as previously described (Marsh et al., 2014). HPCCC fractions containing A1 and A3 with over 95% purity based on HPLC analysis (UV 340 nm) were combined, dried under a nitrogen stream and used for viral assays. The dry mass of the purified stilbenoids were reconstituted

in 0.02% DMSO with 1 μg/ml trypsin (Worthington Biochemical, Lakewood, NJ) in MEM medium.

2.2 Viability Assay

Viability assays were performed with RV alone, RV with 0.002% DMSO, RV with 20 μM A1 or A3, A1 alone, A3 alone, and cells without treatments (NV-no virus) using the trypan blue cell exclusion assay (Ball et al., 2015; Freshney, 1994). Briefly, HT29.f8 cells were grown to 80% confluence in 6-well tissue culture plates (Corning Life Sciences); starved for fetal bovine sera 12 hours prior to the addition of DMSO, DMSO with 20 μM concentrations of the arachidins, RV and RV with 20 μM concentrations of the arachidins. At 18 hours after the treatments, a suspension of ~10^6 cells/mL was diluted 1:1 with a 0.4% trypan blue solution, and loaded onto a hemocytometer. The number of stained dead cells and total number of cells were counted, and the calculated percentage of live cells was reported. Each treatment was performed in triplicate, data was expressed as the mean $\pm$ 1 standard deviation (SD), and comparisons were statistically evaluated by analysis of variance (ANOVA) and Student t tests using Excel (significance level, $p \leq 0.05$).

2.3 RV Infections in HT29.f8 Cells

To test the biological activity of A1 and A3 on RV infections in HT29.f8 cells, the cells were grown to 80% confluence in T25 tissue culture flasks (Corning Life Sciences); starved for fetal bovine sera 12 hours prior to infection, and then

infected with RV Wa as previously described (Arnold et al., 2009; Ball et al., 2015; Yakshe et al., 2015). Briefly, Wa RV stock was sonicated 5 minutes using a cup horn attachment and ice bath in a Misonix Sonicator 3000 (Misonix, Inc, Farmingdale, NY) and incubated in serum-free DMEM with 1 µg/mL trypsin (Worthington Biochemical, Lakewood, NJ) for 45 min at 37°C. The activated viral inoculum was incubated with the cells for 1 hour at 37°C in 5% CO_2 at an MOI of 0.002. At the scheduled collection times, cells were washed with PBS and released from the flasks using a 0.25% trypsin-EDTA solution. The supernatants were collected, clarified at 300*xg* for 5 minutes, and stored at -80°C for plaque assays and TRPS analysis (see below). The cells were washed in 1X cold Dulbecco's PBS (Caisson Laboratories, Smithfield, UT), fixed with 5% glutaraldehyde and used for TEM analysis as described below.

2.4 Infectious RV particle quantification

Plaque forming unit (PFU) assays were performed in triplicate as previously described (Arnold et al., 2009; Ball et al., 2015; Yakshe et al., 2015). Briefly, 10-fold dilutions of RV alone and RV with 20 µM of A1 or A3 were added to serum starved MA104 cells for 1 hour. The virus inoculum was replaced with 3 mL of a medium overlay consisting of a 1:1 mixture of 1.2% agarose (Apex Low Melting Point Agarose, Genesee Scientific Inc) and complete MEM containing 0.5 µg/mL trypsin and incubated at 37°C in 5% CO_2 for 3 to 4 days or until plaques became

visible. A neutral red overlay consisting of a 1:1 mixture of 1.2% agarose with an equal volume of serum-free MEM containing 50 µg/mL neutral red was prepared and 2 mL per well of stain overlay was added on top of the first agarose/medium overlay. The six-well plates were incubated at 37°C until plaques were visible (approximately 3 to 4 days). The individual plaques were counted, and the titers were calculated as follows: Number of plaques x 1/dilution factor x 1/ (mL of inoculum) = PFU/mL. Plaque forming assays were performed in triplicate as outlined above. Data were expressed as mean $\pm$ SD, and comparisons were statistically evaluated by analysis of variance (ANOVA) and Student t tests using Excel (significance level, $p \leq 0.05$).

2.5 Morphometric analysis of Arachidin Treated RV-infected HT29.f8 cells

TEM analysis was performed on RV-infected HT29.f8 cells to visualize the effects of A1 and A3 on progeny virus and cellular morphology as described by Wright (2000). Briefly, RV-infected HT29.f8 cells with and without 20 µM A1 or A3 were incubated for 12, 14, 16 and 18 hpi, washed with PBS and then trypsinized. Cells were pelleted and fixed with 5% glutaraldehyde and refrigerated overnight. The cells were post-fixed with 2% osmium tetroxide followed by an overnight incubation in a uranyl acetate solution. Cells were dehydrated with a graded ethanol series, and acetone was used for the transitional solvent, then samples were infiltrated and embedded in Spurr's resin. Thin sections were obtained with

an RMC MT-X ultra-microtome and stained with uranyl acetate and lead citrate. Samples were examined and photographed with a Hitachi H-7000 transmission electron microscope operating at 75 KeV (Wright, 2000), negatives were digitized at 800 dpi, and image analysis was performed using Macnification Version 2 (Orbicule, Inc., www.orbicule.com). The mean ratio of the cell nucleus to cytoplasm was determined using 10 micrographs of cells from each treatment to compare between test and control groups. The average diameter of enveloped and non-enveloped RV particles was determined (n=23 for each group). Ten micrographs of cells from each treatment at all four time points (see above) were scored for presence or absence of autophagosomes.

2.6 Quantification and Size Distribution of RV Particles

After observing enveloped RV ($_e$RV) and non-enveloped RV ($_{ne}$RV) particles with TEM, TRPS analysis using the qNano system (Izon Science, Cambridge, MA) was performed on the RV-infected cell supernatants to display the concentration of virus particles/mL, diameter of RV particles and size distribution of particles. TRPS is based on a coulter counter that is composed of two fluid reservoirs filled with an electrolyte or other conductive medium and separated by a membrane containing a nanopore (Kozak et al., 2011; Weatherall et al., 2016). When an electrical field is applied across the pore, the resistance to the resulting ionic current is indirectly proportional to the cross-sectional area of the pore. When a

non-conducting particle passes through the pore, the increase in resistance is proportional to the particle volume relative to pore size. This change in resistance is detected as a pulse in an ionic current. The pulse frequency is proportional to particle flow rate and particle concentration (DeBlois, 1970). This system provides a quick and accurate way to measure sizes of individual nanoparticles and their volume in a solution. All qNano experiments were performed using the manufacturer's established protocols (Bo et al., 2014; Jones, 2015; Vogel et al., 2011). Briefly, prior to measuring, samples were purified using a qEV size exclusion column from Izon, and were suspended in PBS with 0.025% Tween 20 to reduce particle aggregation and ease the wetting of the nanopore. A 1:1000 dilution of the sample was placed on the qNano size-tunable nanopore (NP100, Izon) and each sample was measured as a transient change in the ionic current flow. This was denoted as a blockade event with its amplitude representing the blockade magnitude. Because the blockade magnitude is proportional to the particle size, accurate particle sizing was achieved after calibration with particles of a known size (CPC100B, Izon) using identical settings. The size distribution and concentration analysis was performed using IZON proprietary software v3.2.2.268 (Izon).

2.7 Quantification of Transcripts for Cell Death Pathway genes in HT29.f8 Cells

The structural changes observed by TEM were validated by quantitative real-time polymerase chain reaction (qRT-PCR) assays. RNA was extracted from each experimental set described above. The PureLink® RNA Mini Kit (Ambion by Life Technologies; Foster City, CA) was used to extract and purify total RNA according to the manual protocol (Chirgwin et al., 1979; Vogelstein & Gillespie, 1979). Briefly, an equal volume of 70% ethanol was added to 5 µg of total RNA of each sample and vortexed. The samples were then transferred to a spin cartridge and centrifuged for 15 seconds at 12,000 xg at room temperature. Then the sample was washed and centrifuged with 700 µL of wash buffer I for 15 seconds at 12,000 xg. A second wash was performed with 500 µL of wash buffer II for 15 seconds at 12,000 xg. A final spin was performed at 12,000 xg for 2 min to dry the membrane containing the bound RNA. The RNA was eluted from the membrane with 50 µL of nuclease free water. Total RNA was analyzed using a full spectrum analysis at 240 nm-320 nm in the Cary 50 spectrophotometer (Agilent, Corp.). The total RNA was stored at -80°C for future studies. A conversion factor of 40 µg/mL was used to convert the A_{260} to concentration and the value of 10 corrected for path length of 0.1 mm (Sean and Wiley, 2008). The concentration of RNA was calculated using the formula as follows: Concentration of RNA= A260 x 40 µg/mL x 10 x Dilution factor. cDNA was then synthesized using the Thermo Scientific Verso cDNA Synthesis Kit from each experimental set using 5 µg of purified total

RNA. A Master Mix was prepared as described in the manufacturer's protocol as shown in Table 1 (2015 Thermo Fisher Scientific, Inc.). The samples were then placed into the BioRad Real-Time System C1000 Thermal Cycler Instrument (Hercules, CA) for the following cycle (Table 2).

The qRT-PCR experiment was performed using a CFX96 Touch Real-Time PCR Detection System (BioRad, Des Plaines, IL). For all experiments, reactions were performed in triplicate with Apex qPCR GREEN Master Mix without ROX (Genesee Scientific) that contained all necessary components to perform a DNA-binding dye base real-time DNA amplification experiment (Table 3). Primers were purchased from Sigma-Aldrich (St. Louis, MO) with the sequences, Tm, and base pairs sizes of the products shown in Table 4.

Each reaction mixture contained 10 μL of Apex qPCR GREEN Master Mix, 0.5 μL of 10 μM forward/reverse primers, 3 μL template cDNA and nuclease-free water to a final volume of 20 μL. GAPDH and β-actin were used as housekeeping genes to normalize for relative expression analyses. The cycle threshold (Ct) value or cycle number obtained from a single reaction for each standard reaction were all values that fell within a linear portion of the standard curve. The obtained Ct values from the qRT-PCR experiment were exported to Excel for data analyses. Fold change in signals of expression of the genes of interest relative to GAPDH and β-Actin were determined by using the $\Delta\Delta$Ct method. The results were expressed as mean $\pm$ SD.

2.8 Protein quantification and Slot blot assays

A cell lysate was prepared from the HT29.f8 cells, and quantified using a micro-BCA protein assay. Cell lysates (10, 5, 2.5, 1.25 µg) were added to nitrocellulose membranes, probed with a 1:1000 dilution of rabbit anti-CNR1/2 antibodies (Antibodies Online, Atlanta, GA) and reactive bands were visualized by the addition and excitation of goat anti-rabbit antibodies Alexa Fluor®546 (Life Technologies) using the Typhoon 9500 Plus laser scanner (GE Life Sciences, Marlborough, MA).

3. RESULTS

Our first experiments using the human RV (Wa) to infect a human intestinal cell line, HT29.f8, with A1 or A3 treatments and control cells (no virus, A1 and A3 only) were performed at 18 hpi. There were ultrastructural differences between RV-infected and RV-infected, arachidin-treated cells, including changes in the size of mitochondria, PM blebbing, and enlarged nuclei in RV-infected cells (Fig. 1). The viability assay of the cells at 18 hpi showed no adverse effects of the arachidins (Fig. 2). Also, two populations of RV particles were observed with cells collected from all RV treatments (with/without arachidins), enveloped RV particles ($_e$RV) and non-enveloped RV particles ($_{ne}$RV) (Fig. 3). The viroplasm (V), was a prominent component in RV-infected cells and is the site where newly formed immature $_e$RV particles are assembled and bud into the endoplasmic reticulum

(ER). Once $_e$RV particles lose the ER envelope and condense to the $_{ne}$RV form they either obtain the VP4 in the ER or at the PM to become mature infectious RV particles that are approximately 75-80 nm in diameter (M.K. Estes & Greenberg, 2013). The plaque forming assays confirmed that the Wa RV strain had similar decreases in the production of infectious virus particles at 18 hpi with arachidin treatment (Fig. 4). Furthermore, a shift in the size of the released viral populations from $_{ne}$RV to $_e$RV with decreased viral titers with the addition of the arachidins was observed using TRPS analysis (Fig. 5 a, b, c). Therefore, a time course study was implemented to observe any significant temporal changes at 12, 14, 16 and 18 hpi.

3.1 Viability of HT29.f8 cells during an RV infection at 18 hpi

Percent live/dead cells were calculated using the trypan blue exclusion dye assay as previously described (Ball et al 2015). Briefly, at 18 hpi, the cells treated with A1, A3, NV, and NV+DMSO all had cell viabilities of at least 93.5%. Cells infected with RV alone had a viability of 91.7% and cells with RV and 0.02% DMSO had a viability of 91.3% (Fig. 2). RV-infected cells treated with the A1 and A3 showed an increased viability of 94.5% and 93.7%, respectively.

3.2 RV particle size measurements with TEM

From the low magnification micrographs viewed for autophagosome content and nucleus to cytoplasm ratios, RV particles of two different populations were observed, $_e$RV and $_{ne}$RV (Fig. 3A). Twenty-three RV particles from each

group were measured from higher magnification micrographs and the diameter expressed as mean ± SD statistical evaluation by analysis of variance (ANOVA) demonstrated that $_{e}$RV and $_{ne}$RV virus particles represented two populations with average diameters of $_{ne}$RV 115 nm and $_{e}$RV 78 nm p = 1.50E-30 (Fig. 3B)

3.3 Production of infectious virus particles with the addition of A1 and A3

Supernatants collected at 18 hpi from the RV-infected and RV-infected with 20 µM concentrations of A1 or A3 were used for plaque forming assays to quantify the amount of infectious viral progeny produced (Arnold et al., 2009). The PFU assays demonstrated statistically significant differences between RV and RV+A1 (p = 2.39E-5) and RV and RV+A3 (p = 2.38E-5); representing 79-fold change decrease in PFU with A1 treatment and a 94-fold change decrease in PFU with A3 treatment (Fig. 4).

3.4 Quantification of RV particles and size distribution by TRPS analysis

The concentration of particles in RV-only samples gradually increased to 2.13E13 particles/mL at 18 hpi (Fig. 5). Also, the particles had a dispersed range in diameter until the 16 and 18 hpi time points, when the average particle size was 74 nm (Fig. 5A). RV-infected cells treated with A1 displayed a pattern of increasing particle concentration over the time course to 1.05E13 particles/mL at 18 hpi. At 12 hpi, the RV particles averaged 110 nm in size, but at 14, 16 and 18 hpi a scattered distribution was observed with an average diameter of 103 nm (Fig. 5B).

Furthermore, RV-infected cells treated with A3 demonstrated a gradual increase in particle concentration to 2.01E13 particles/mL at 18 hpi. At 12, 14, and 16 hpi a wide range of RV particle sizes were displayed averaging 104 nm; however, at 18 hpi a shift to a population of larger particles (116 nm) was revealed (Fig. 5C).

3.5 TEM Analysis of RV-infected HT29.f8 Cells with/without A1/A3

HT29.f8 cells were infected with RV (Fig. 6 panel 1A-D), RV with A3 (Fig. 6 panel 2A-D), and RV with A1 (Fig. 6 panel 3A-D). These were compared to the three controls, NV, A3, and A1 (Fig. 6 panel 4A-C). With RV only (Fig. 6 panel 1A-D), at 12 hpi, RV particles were present and by 14 hpi, and the cytoplasm had numerous vesicles present. By 16 hpi, the nuclei increased in size and by 18 hpi, the cells appeared apoptotic with PM blebbing and large nuclei. RV treated with A3 (Fig. 6 panel 2A-D) by 18 hpi, the cells appeared to have normal-sized nuclei with numerous vesicles in the cytoplasm. With the RV treated with A1 (Fig. 6 panel 3A-D) there were numerous autophagosomes present in the cytoplasm and by 18 hpi, the nuclei appeared to be similar in size to the control cells. TRPS analysis of the extracellular particles was performed and the populations of viral particles by size were charted (Fig. 6 panel 5a-c and panel 6a-d). Particles from RV-infected cells demonstrated a wide range in diameter at 12 hpi that narrowed to a range of smaller sizes by 18 hpi. RV-infected cells treated with A3 contained large particles, and the diameter range remained consistent throughout the study (Fig. 6 panel

5B). Figure 6 panel 5C represents the diameters of RV particles from RV-infected cells treated with A1 from 12 to 18 hpi; RV diameter distribution appeared to increase over the time course.

TRPS graphs were overlaid for the different treatments at the same time points (Fig. 6 panel 6A-D). At 12 hpi, all three treatments displayed similar distributions of their viral particle populations, but by 14 hpi, RV only and RV with A1 treated particles began to show a distribution of smaller particles typical of the mature form of RV. By 16-18 hpi, all three treatments revealed different distributions of RV particle diameters. RV only showed a distribution of small particles, RV with A1 showed a broad distribution of particle sizes, and the distribution of RV particles from A3 treated cells was unchanged from that observed at 12 hpi. Figure 6 panel 7A illustrates the presence of autophagosomes in RV-infected cells treated with A1 Figure 6 panel 7B demonstrated a viroplasm where immature RV particles were assembled, then released into the ER where they acquire the ER membrane envelope.

At 18 hpi, the ultrastructural appearance and mean nuclear to cytoplasm ratios of the control cells with A1 (0.56) and A3 (0.50) were similar to the cells with no treatment (0.46) (Fig. 7 E). An increase in the number of mitochondria, autophagosomes, RV particles and viroplasms was demonstrated in RV-infected cells, and RV-infected cells treated with A1 or A3 (Fig. 7 A-D).

At 12 hpi, RV cells had a mean nuclear to cytoplasmic ratio of 0.83 and a more apoptotic appearance with rounded nucleus and membrane blebbing (Superti et al., 1996). RV-infected cells treated with A1 exhibited a more normal ultrastructure and had a mean nuclear to cytoplasmic ratio of 0.42 (Fig. 7A), comparable to uninfected cells at 0.46 (Fig. 7E). Cellular ultrastructure of RV-infected cells treated with A3 correlated with normal cells; however, the mean nucleus to cytoplasm ratio was much smaller at 0.20 (Fig. 7A).

At 14 hpi, RV-infected cells demonstrated large abnormal mitochondria (large, with poorly defined cristae) and increased numbers of vacuoles. Additionally, the mean ratio of nucleus to cytoplasm was 0.55 (Fig. 7B) slightly reduced from the ratio at 12 hpi (Fig. 7A). However, with the addition of A1, the mean nucleus to cytoplasm ratio was increased to 0.91 (Fig. 7B). RV-infected cells treated with A3 at 14 hpi had an average ratio of 0.73 (Fig. 7B) and had a relatively normal ultrastructure similar to control cells.

At 16 hpi, the mean ratio of RV-infected cells was 0.41, similar to the control cells (NV, A1 and A3 alone) as shown in figure 7C. At the same time point, RV-infected cells treated with A1 had a large average ratio of 1.48 (Fig. 7C) and displayed a pyknotic ultrastructure often seen in apoptotic cells (Nikoletopoulou, Markaki, Palikaras, & Tavernarakis, 2013). RV+A3 cells had similar ratios at 14 and 16 hpi (0.73 and 0.77) (Fig. 7B, C).

At 18 hpi, the RV-infected cells demonstrated an increased nucleus to cytoplasm ratio and apoptotic characteristics as seen in figure 7D (Elmore, 2007). RV-infected cells treated with either arachidin had similar mean ratios, 0.41 and 0.42, respectively, and both A1 or A3 treatments showed normal ultrastructure (Fig. 7D).

3.6 Autophagosome content in RV infected cells present 12-18 hpi

The time course analysis quantified the number of cells with autophagosomes present (n≥ 13 cells/treatment). NV, A1 and A3 only treated HT29.f8 cells were compared to RV-infected cells with or without A1 or A3 treatment (Fig. 8). The percentage of cells that had autophagosomes increased over the time course (12, 14, 16, 18 hpi) for RV-infected cells (15%, 27%, 31%, and 46%, respectively). A similar, increasing pattern was observed with the A1-treated, RV-infected cells at 12, 14, 16 and 18 hpi, displaying 54%, 62%, 82% and 92% of cells with autophagosomes, respectively (Fig. 8). The percent cells positive for autophagosomes with A3-treated, RV-infected cells were similar to the RV-only cells, displaying an increase in the number of positive cells to 46% at 16 hpi; however, at 18 hpi there was a dramatic decrease to 8% cells (Fig. 8). Control cells (NV = no virus and A3 only) presented 7% and 15% cells positive for autophagosome, respectively (Fig. 8). Conversely, 45% of A1-treated cells were

positive for autophagosomes, similar to the RV-infected rate at 18 hpi and RV-infected with A3 at 16 hpi.

3.7 Quantification of Transcripts for HT29.f8 cells treated with arachidins

Multiple connections exist between autophagy and apoptosis (Dang et al., 2015; Kroemer & Levine, 2009; Nikoletopoulou et al., 2013; Wanget al., 2015). The presence of both pathways as observed with TEM, led to exploration of the molecular and functional connections between the apoptosis and autophagy pathways in RV-infected HT29.f8 cells with and without the arachidins. The expression of caspases that initiate the apoptosis death pathway (initiator caspase-8 and -9) and genes that execute the apoptosis death pathway (caspase-3 and -7). Also, we detected the presence of genes (Beclin-1, Bcl-2, atg 3, atg 5) that are decisive in the progression to autophagy (Noguchi & Hirata, 2015). In our experiments, both initiator caspases (caspase-8 and -9) showed a two-fold increase in transcripts with RV infection that was statistically reduced with the addition of both A1 and A3 (Fig. 9A and C). Also, two of the executioner caspases, cas-3 and cas-7, showed a two-fold increase in transcripts with RV infection that was statistically reduced with the addition of A3 (Fig. 9A and C). Likewise, the autophagy proteins that are important in the crosstalk between autophagy and apoptosis, Beclin-1 and Bcl-2, demonstrated a two-fold increase in transcripts with a RV infection that was statistically reduced with the addition of A1 or A3, while

ATG-3 and *ATG-5* were not significantly affected by RV, A1 or A3 (Fig. 9 B and D). The manipulation of the two death pathways could initiate the regulation of RV infection, leading to the observed antiviral activity of A1 and A3.

3.8 Slot Blot confirmation of the presence of cannabinoid receptors

The slot blot data confirmed the presence of both cannabinoid receptor 1 (CBR1) and cannabinoid receptor 2 (CBR2) on HT29.f8 cells (Fig. 10).

4. DISCUSSION

Previous experiments using the simian RV, SA11.4f, demonstrated an antiviral effect of both A1 and A3 that decreased the amount of released infectious RV and suggested a reduction in viral replication (Ball et al 2015). This study investigated the effects of A1 and A3 on the clonally derived human intestinal cell line, HT29.f8, infected with the human RV strain, Wa. Time course experiments (12, 14, 16 and 18 hpi) were performed to observe the intracellular patterns of the host cell and production of RV particles in RV-infected cells with/without the arachidins. At the same time points, the intracellular and extracellular RV particles were examined to determine the diameter size of the population.

Viability assay data showed that the arachidins did not adversely affect the host cells whether they were infected with human RV (Wa) or not (Fig. 2). This implies that the arachidins are not toxic to the cells, and that any effects observed

in this study can be attributed to the mechanism of action of the arachidins on RV and viable HT29.f8 cells.

TEM analysis of the diameters of the intracellular RV particles revealed two distinct populations of particles, $_{ne}$RV and $_e$RV. Correspondingly, TRPS analysis demonstrated varying populations of both $_{ne}$RV and $_e$RV. The viral titers from RV-only cells, quantifying the population of extracellular particles, had a large population of $_{ne}$RV, whereas viral titers from RV-infected, arachidin treated cells were dominated by $_e$RV particles. Other studies suggest that $_{ne}$RV particles be termed infectious due to the shedding of the ER membrane (Ruiz et al., 2009), while $_e$RV particles are non-infectious particles (Teimoori et al., 2014). Verification from electron micrographs showed two distinct populations of virus particles present in RV-infected cells. $_e$RV representing immature virus and $_{ne}$RV, more mature virus particles (Fig. 3A and B) which corresponds to previously reported sizes of infectious and noninfectious RV particles (Ruiz et al., 2009; Teimoori et al., 2014).

PFU assays are commonly used to determine titers (PFU/mL) for infectious virus particles (Arnold et al., 2012). Previously, we reported a statistically significant change in the amount of infectious RV produced using the simian RV, SA11.4f (Ball et al 2015). This is the first report to demonstrate that the human RV (Wa)-infected cells treated with A1 and A3 produced significantly fewer infectious RV particles than untreated RV-infected cells (Fig.4). This demonstrates that A1

and A3 have antiviral activity against both a simian RV (SA11.4f) and a human RV (Wa).

TRPS analysis showed that early during an RV infection without A1 or A3 treatment, RV particles averaged 78 nm in diameter, consistent with the $_{ne}$RV range, with a wide distribution of diameters in the $_{e}$RV range as well (Fig. 5A). However, as the infection progressed RV particle size was reduced to a $_{ne}$RV-only size distribution with 74 nm diameter average size, similar to that of mature RV particles in other studies (Ruiz et al., 2009). Treatment with A1 caused a decrease in viral progeny but broadened the size distribution of RV particles in the $_{e}$RV population, averaging 96 nm (Fig.5B). Similar findings were observed for the A3-treated, RV-infected cells with a broad distribution of virus particles at 12, 14, and 16 hpi. Interestingly, at 18 hpi the population was minimized to a diameter within the $_{e}$RV range, 116 nm (Fig. 5C).

The time course study demonstrated changes in the ultrastructure of the RV-infected cells treated with the arachidins. When comparing RV to RV with A3, there appeared to be a 2-hour delay in the appearance of numerous vesicles in the cytoplasm. This was not observed with RV with A1, but with this treatment many autophagosomes were seen by 18 hpi. Apoptotic characteristics were not observed in arachidin-treated, RV-infected cells, indicating different pathways were regulated by the two arachidins.

The RV-infected cells revealed approximately equal amounts of nucleus and cytoplasm at 12 hpi, but at 14 to 16 hpi the area of the cytoplasm was twice that of the nucleus. At 12, 14 and 16 hpi, the arachidin treated, RV-infected cells followed a different pattern. At 12 hpi, the area of the cytoplasm was twice that of the nucleus which changed at 14 and 16 hpi to equal amounts of cytoplasm and nucleus. However, there was a dramatic switch by 18 hpi with RV-infected cells having a larger nucleus than cytoplasm, and the arachidin-treated, RV-infected cells having twice as much cytoplasm as nucleus. This implies that there is a switch between 16 and 18 hpi that is regulated by the arachidins, with treated cells similar in appearance to uninfected controls (Fig. 7).

In addition, ultrastructure and morphometric analysis of human RV (Wa)-infected HT29.f8 cells revealed different cellular alterations at the time points observed in this study (12, 14, 16 and 18 hpi). TEM observations of the ultrastructure of the RV-infected cells revealed the appearance of abnormal mitochondria, cellular vesicles, and increased nuclear sizes that suggested a progression to apoptosis by 18 hpi (Fig. 1 and 7); whereas the arachidin-treated, RV-infected cells showed very different patterns over time with more normal appearing mitochondria and nuclei by 18 hpi. The increased presence of autophagosomes in A1-treated cells, as compared to A3 treated, (Fig. 8) suggests that A1 and A3 have different mechanism of actions.

Previous reports have shown that RV infections lead to cell death using the apoptosis cellular death pathway (Frias et al. , 2012). However, recent studies have suggested that the RV nonstructural protein 4 (NSP4) alone triggers the cells to produce autophagosomes, suggesting a change to an autophagy pathway that may be arrested at the autophagosomal stage of development (Crawford et al., 2012). The data presented here show ultrastructural changes in human intestinal cells that indicate the apoptosis pathway is activated with an RV infection, and that the addition of A1 or A3 causes major changes in the RV-infected cells, leading to the absence of apoptotic features and an increase of autophagosomes (Fig. 9 panel 7A). More A3 treated cells contained autophagosomes at 16 hpi, followed by a dramatic reduction at 18 hpi similar to uninfected cells (Fig. 8). A different pattern was observed in the A1 treatments with 92% of cells positive for autophagosomes by 18 hpi, again suggesting that A1 and A3 have different mechanisms of action.

An examination of the effects of the various treatments on the expression of apoptosis and autophagy genes important in the modulation of both cell death pathways by qRT-PCR demonstrated a significant decrease in apoptosis transcripts in RV-infected cells with the addition of either A1 or A3 (Fig. 9 A-D). Similarly, a significant decrease in the transcripts for *Beclin-1* and Bcl-2 shows a regulation of RV-infected cells that can change the outcome of an infection. Previous studies observing different infectious agents and host systems have

revealed that autophagy and apoptosis can cooperate, antagonize or assist each other and affect the fate of the cell, and is well documented that the crosstalk between autophagy and apoptosis is mediated, at least in part, by the functional and structural interaction between *Beclin*-1 and the anti-apoptotic proteins BCL-2 (Nikoletopoulou et al., 2013; Pattingre et al., 2005).

A previous study demonstrated the binding of A1 and A3 to cannabinoid receptors 1 and 2 (Brents et al., 2012). The presence of these receptors on our cells suggests a signaling pathway that could be used in HT29.f8 cells to modulate an RV infection.

Altogether, the data suggests the addition of A1 or A3 to RV infections has a protective effect on host cells, and that a crosstalk between apoptosis and autophagy inhibits RV morphogenesis. These findings indicate the possibility that RV modulates the switch between autophagy and apoptosis to facilitate their own replication in untreated cells, and suggests that A1 and A3 restore cellular homeostasis, producing a protective response that has potential therapeutic antiviral activity.

TABLES

Table 1. cDNA Master Mix.

	Volume	Final Concentration
5x cDNA synthesis buffer	4µL	1x
dNTP Mix	2µL	500µM each
Anchored oligo dT	1µL	
Verso Enzyme Mix	1µL	
Template (RNA)	5µL	5µg
Nuclease-free Water	7µL	
Total Volume	20µL	

Table 2. cDNA synthesis thermocycler parameters.

	Temperature	Time	Number of cycles
cDNA synthesis	42°C	30 min	1 cycle
Inactivation	95°C	2 min	1 cycle

Table 3. PCR cycle conditions used for qRT-PCR.

Initial denaturation	94°C	3 minutes
PCR (34 cycles)	94°C	30 seconds
	58°C	30 seconds
	72°C	1 minute

Table 4. Primers for autophagy and apoptosis

Genes	Primer name	Primer sequence (5'-3')[a]	Size (bp)
GAPDH	GAPDHfor	GAGTCCACTGGCGTCTTCA	190
	GAPDHrev	GGGGTGCTAAGCAGTTGGT	
β-Actin	β-Actin for	ATCCTCACCCTGAAGTACCC	183
	β-Actin rev	TAGAAGGTGTGGTGCCAGAT	
Caspase 3	Casp3for	GAGTCCATTGATTCGCTTCC	209
	Casp3rev	TCTGGTTTTCGGTGGGTG	
Caspase 7	Cas7for2	TCAGTGGATGCTAAGCCAGA	230
	Cas7rev2	GAACGCCCATACCTGTCACT	
Caspase 8	NCIcasp8for	GGTCACTTGAACCTTGGGAA	146
	NCIcasp8rev	CGGAATGTAGTCCAGGCTCA	
Caspase 9	NCIcasp9for	CACGGCAGAAGTTCACATTG	148
	NCIcasp9rev	ACACCCAGACCAGTGGACAT	
Caspase 10	NCIcasp10for	GGGAGGTAAAGCTGTGGTTG	182
	NCIcasp10rev	GCCGAGTCGTATCAAGGAGA	
Bcl-2	BCL2 For	CAGTTGGGCAACAGAGAACCAT	171
	BCL2 Rev	AGCCCTTGTCCCCAATTTGGAA	
ATG 3	atg3 For	ACATCAGTCAGGATCATGTGAAGA	206
	atg3 Rev	CGTTAACAGCCATTTTGCCA	
ATG 5	atg5 For	ATGTGCTTCGAGATGTGTGGT	220
	atg5 Rev	CATTTCAGTGGTGTGCCTTCA	
Beclin-1	beclin-1 For	AGCCAGACGCTGTTTGGAG	189
	beclin-1 Rev	TGATCCAGTCTCTCAGCCTCA	

40

FIGURES

Figure 1.

Figure 2.

Figure 3.

HT29.f8 Viability Assay at 18hpi

Figure 4.

PFU/ml for HT29.f8 w/without arachidins
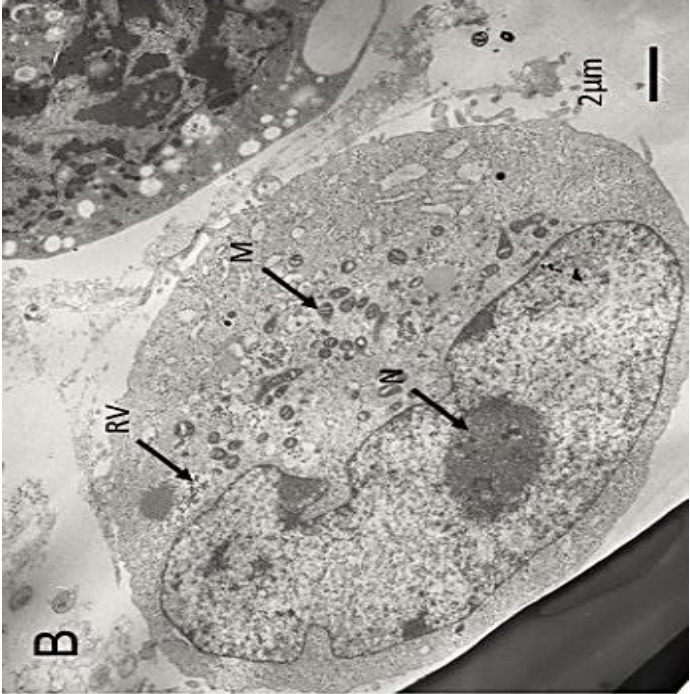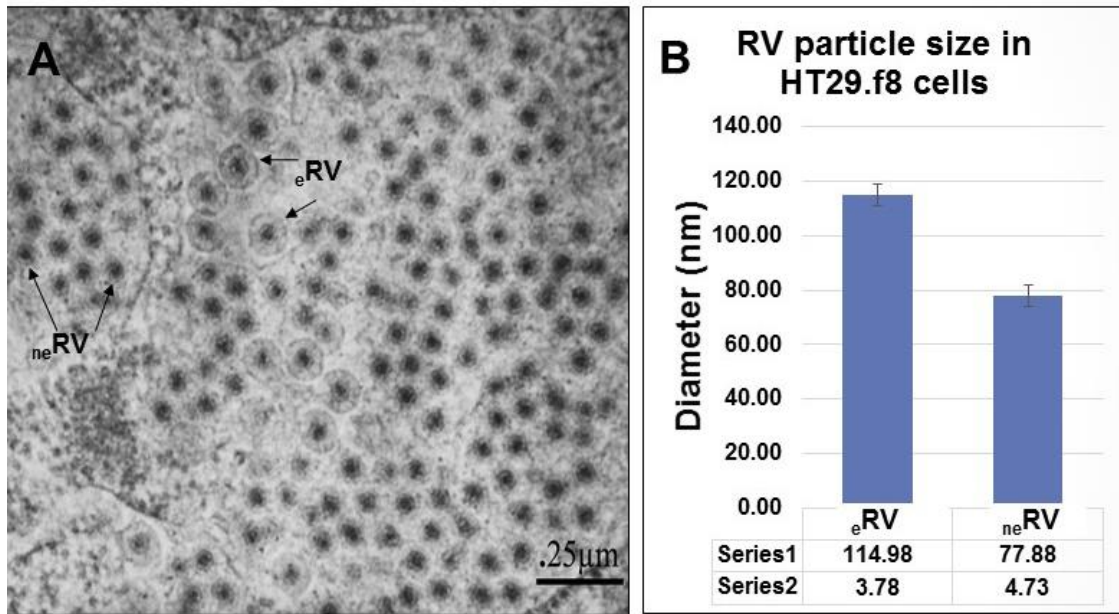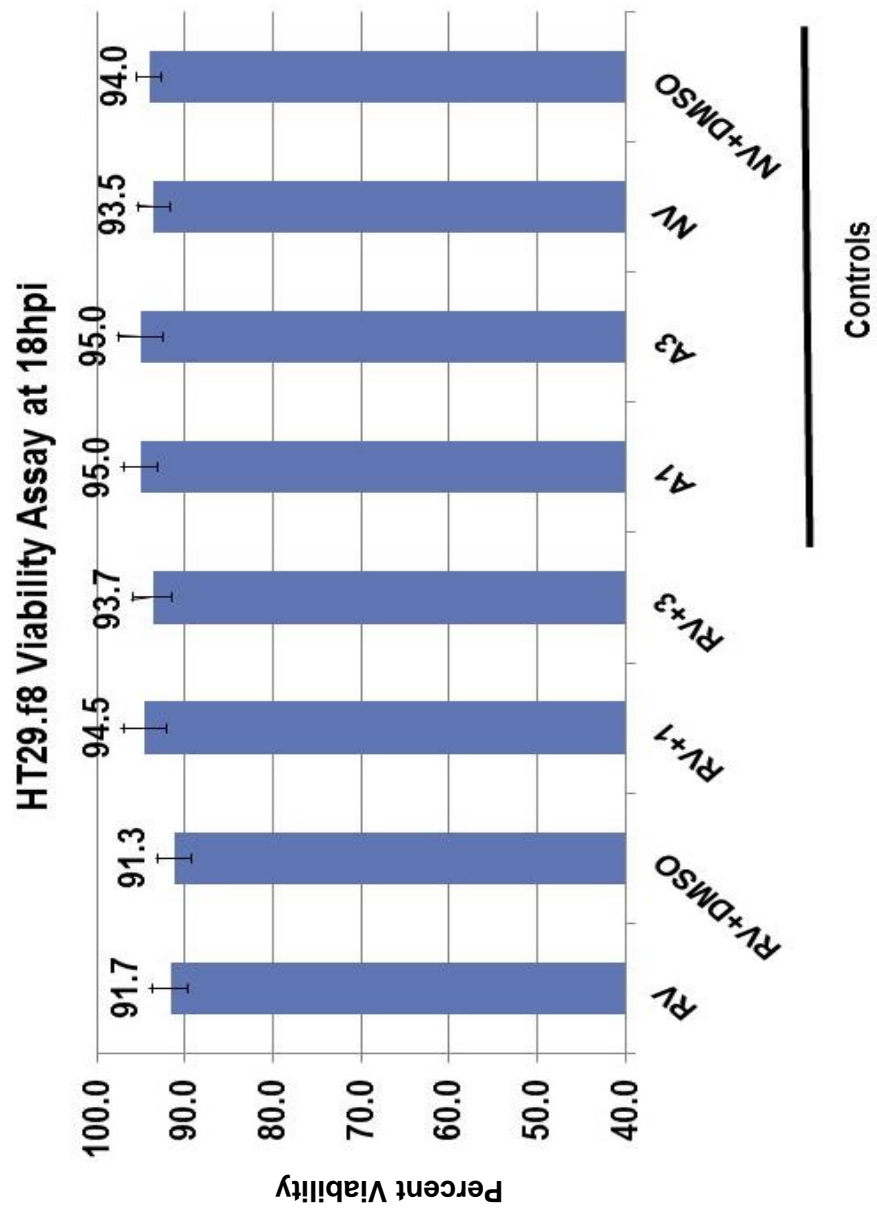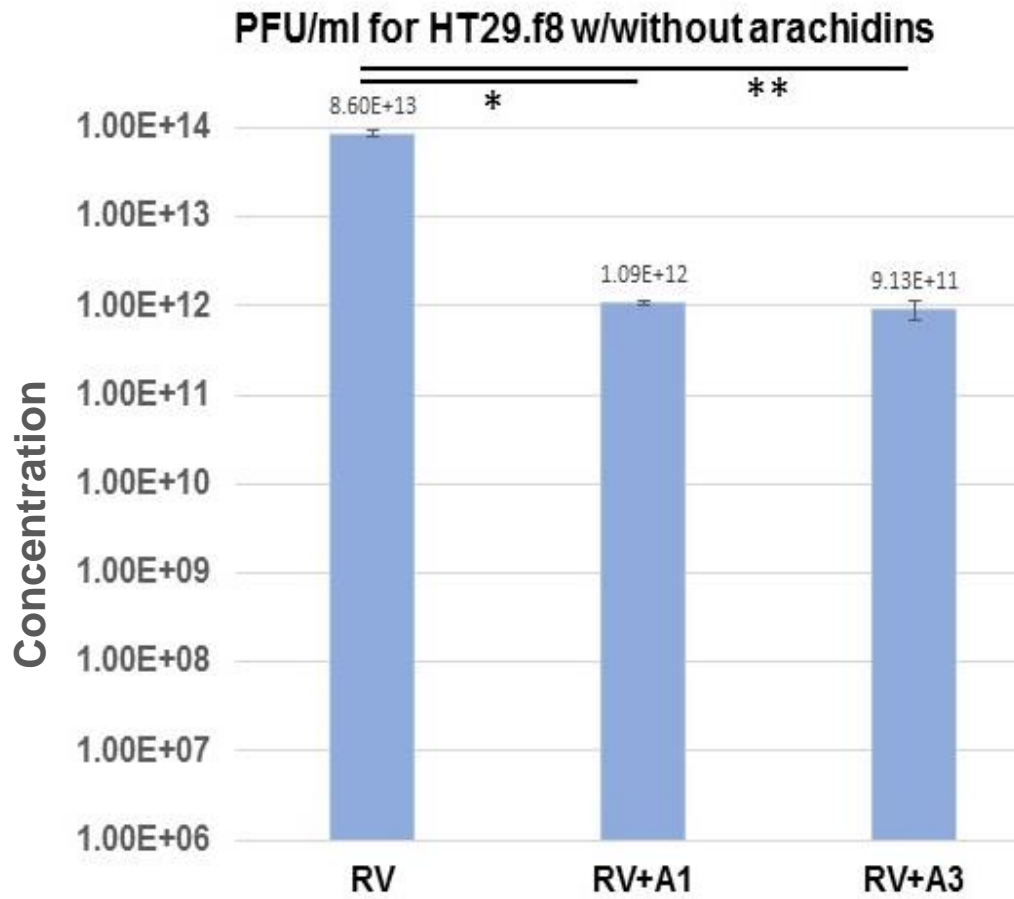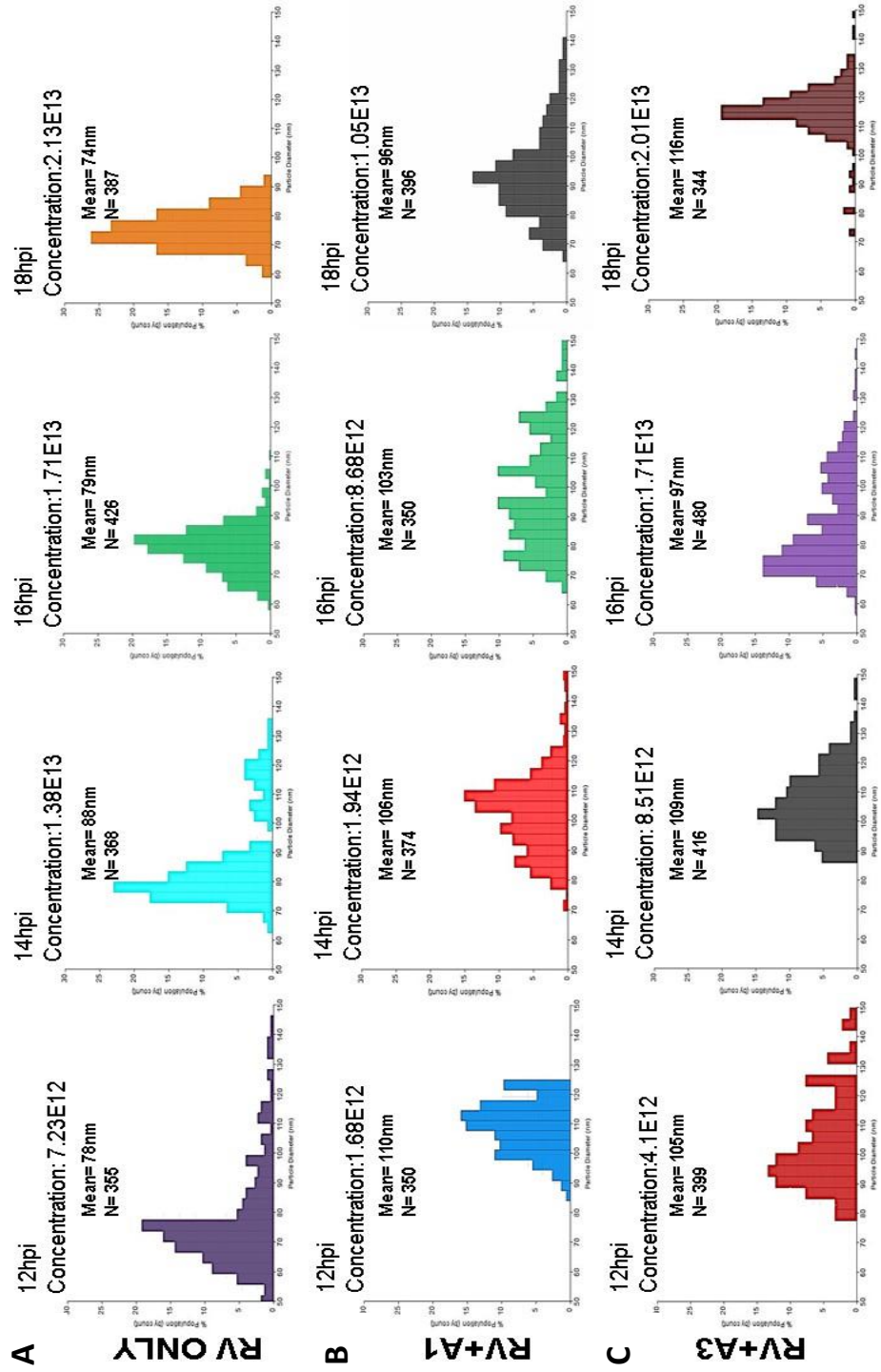
Figure 5.

Figure 6.

Figure 7.

Figure 8.

Percent Autophagosomes in HT29.f8 cells

Figure 9.

Quantification of Transcripts for Apoptosis and Autophagy Genes in HT29.f8 Cells Treated with and without Arachidins

Figure 10.

FIGURE LEGENDS

Fig. 1. Electron micrographs of rotavirus-infected HT29.f8 cells A) rotavirus (Wa) only infected HT29.f8 cells at 18 hpi. Mitochondria (M) and autophagosomes (AP) are indicated by arrows. Final Magnification = 7,800x. B) Rotavirus (Wa) infected HT29.f8 cells treated with A3 at 18 hpi. Mitochondria (M), rotavirus particles (RV), and a nucleolus (N) are indicated by arrows. Final Magnification = 8,300x.
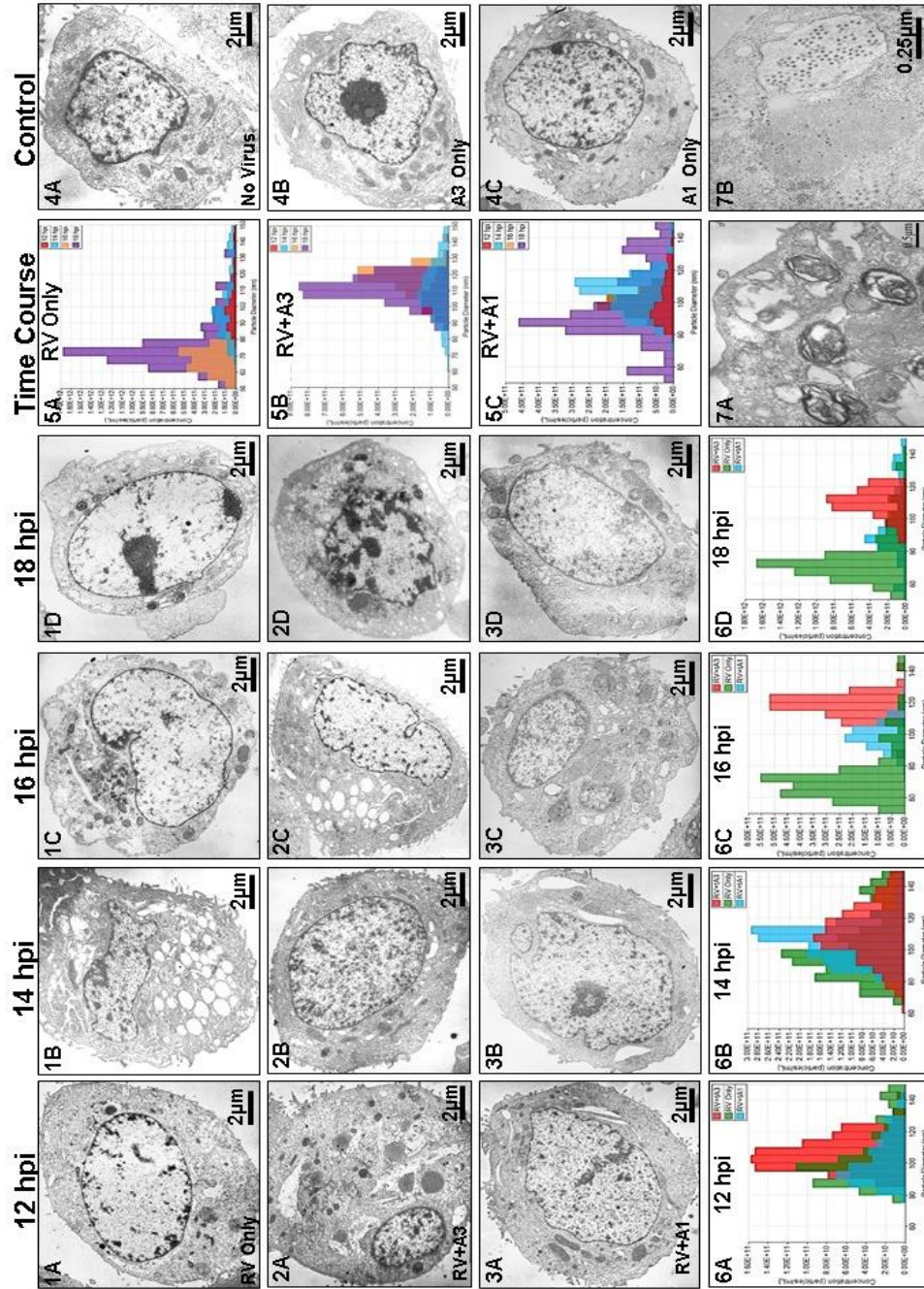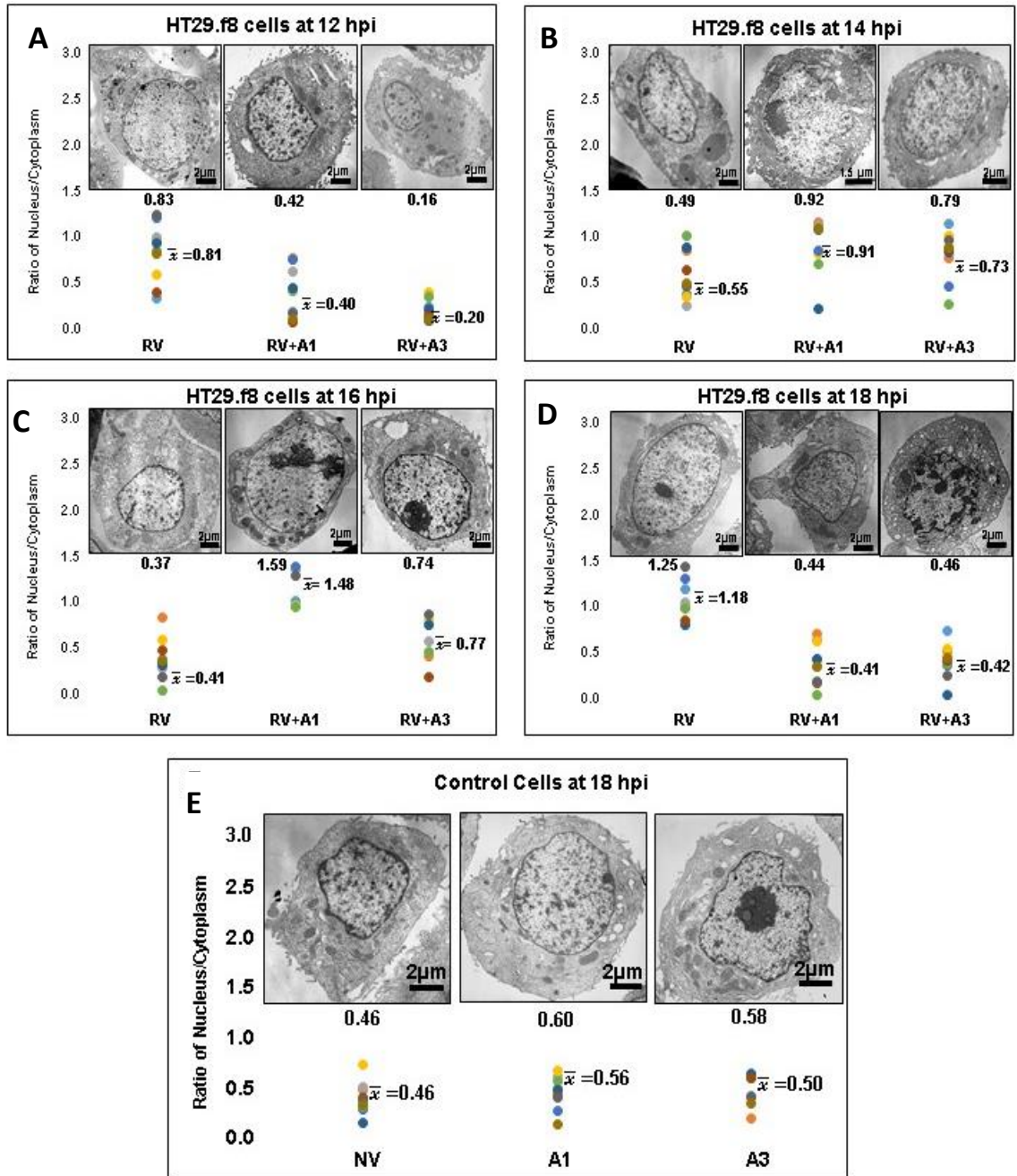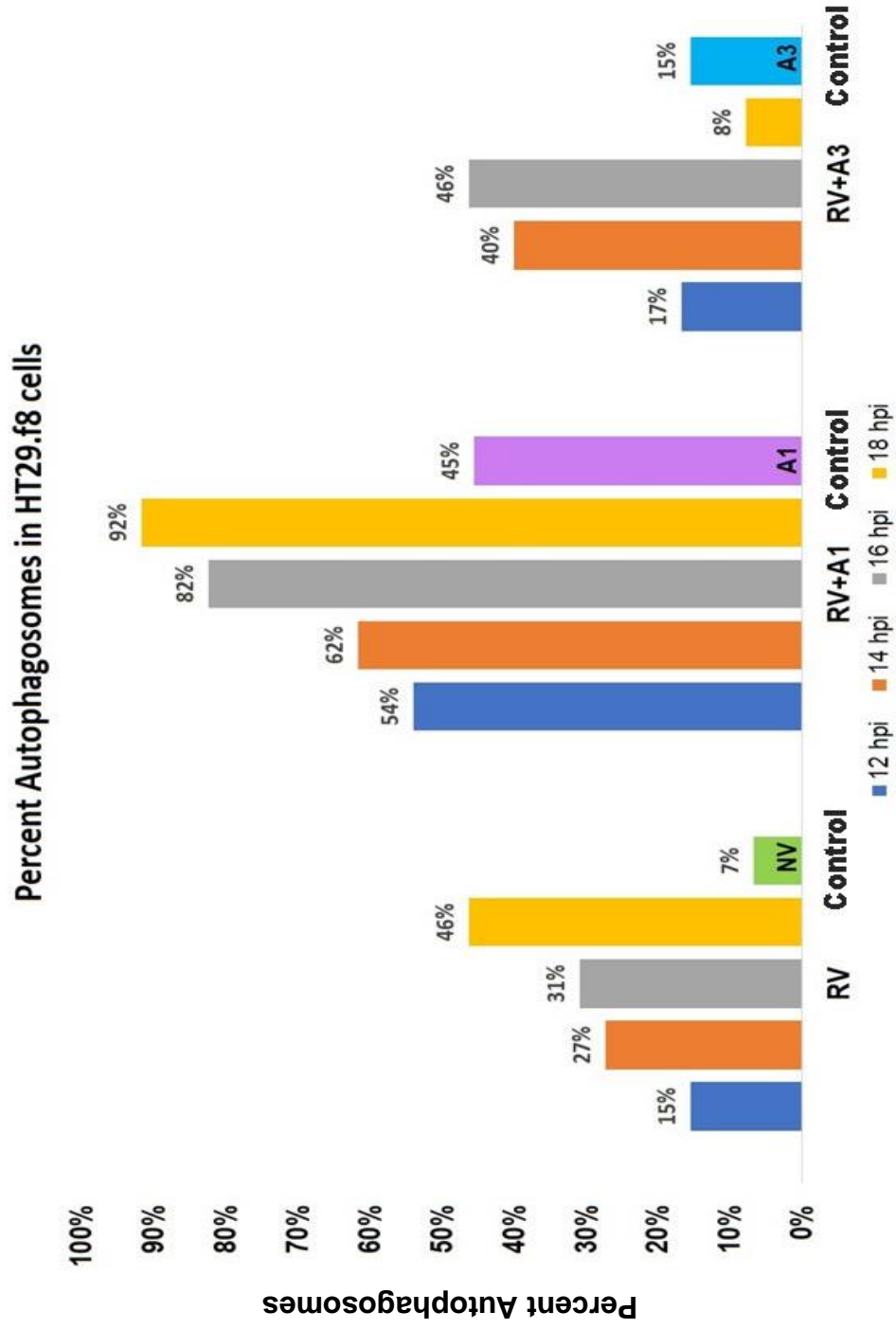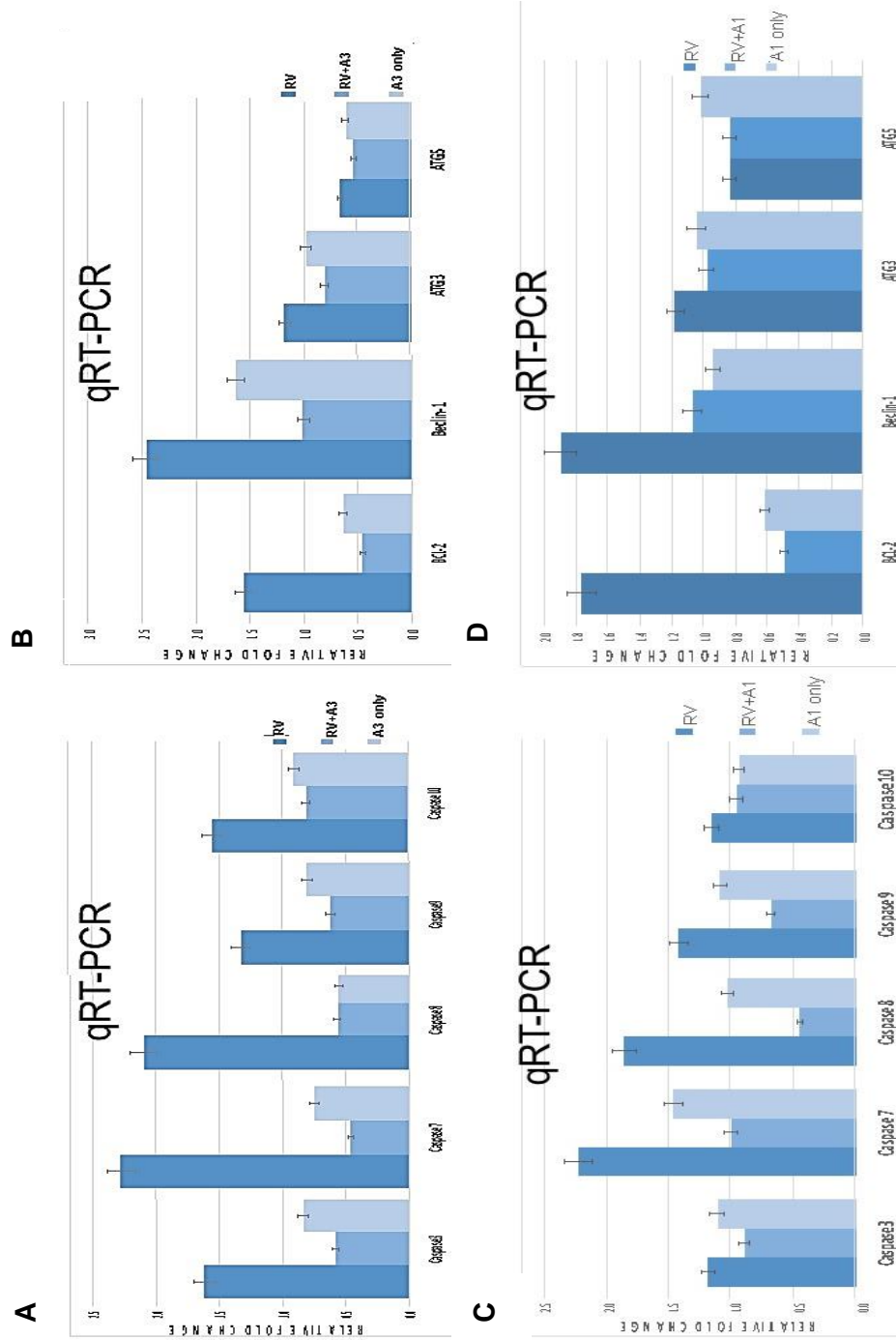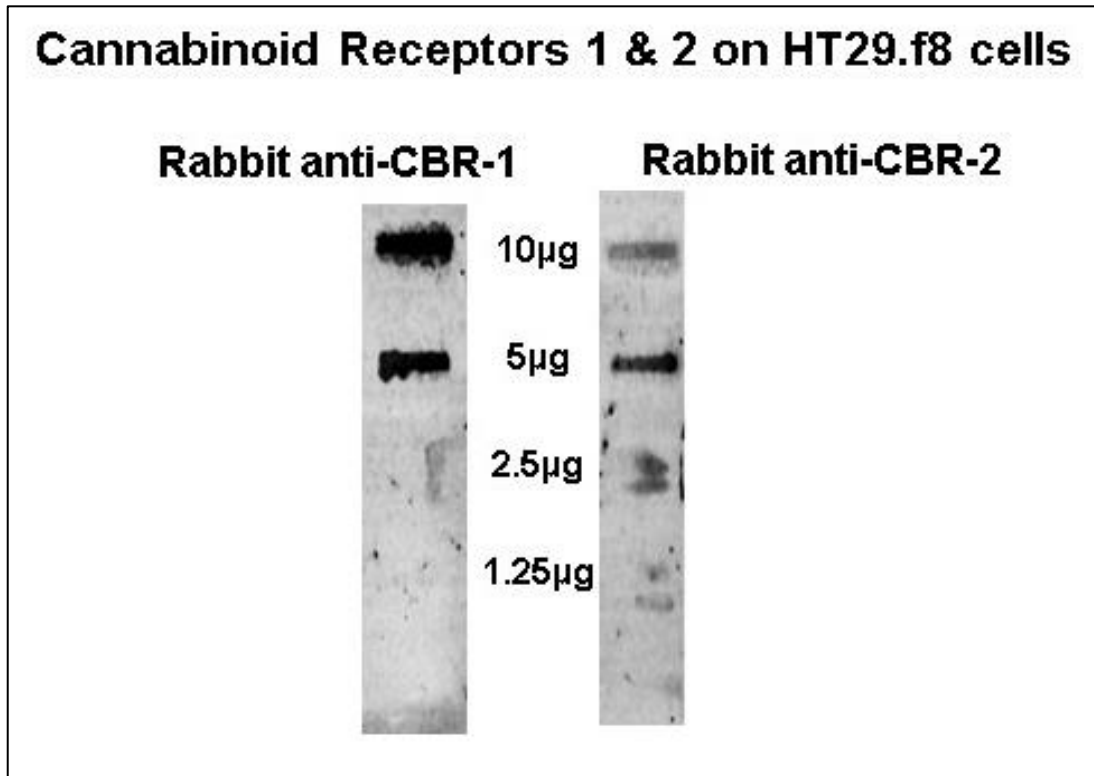
Fig. 2. HT29.f8 cell viability assay. Using a Trypan blue exclusion dye assay, the cells were counted in triplicate with and without treatments (DMSO, A1 or A3) at 18 hpi and percent live/dead cells were calculated. Data was statistically evaluated by Student's t-tests and expressed as mean ± SD (significance level, $p \leq 0.05$).

Fig. 3. Measurement of RV particle sizes. A) RV-infected HT29.f8 cells with 20µM A3 were processed for TEM at 18 hpi. The two different sized RV particles were observed and measured to determine the average RV particle diameter.   B) Measurements of RV particles in HT29.f8 cells infected with RV at 18 hpi. N=23 per group. *Statistically significantly different population, p = 1.50E-30.

Fig. 4. Quantification of infectious Wa RV particles using plaque forming assays (PFU/mL) at 18 hpi. HT29.f8 cells were infected with RV, RV+20 µM A1, or RV +20 µM A3. At 18 hpi, the supernatants were collected, clarified by centrifugation, and used in plaque forming assays. The RV titer was 8.6E13, RV with A1 titer was

1.09E12, and RV with A3 titer was 9.13E11. Statistically analysis showed there was a significant difference between RV and RV with A1 (p = 2.39E-5), likewise there was a significant difference between RV and RV with A3 (p =2.38E-5).

Fig. 5. TRPS time course study of arachidin treated HT29.f8 cells. The size variations, virus concentrations and population distribution of extracellular RV particles were measured from supernatants of RV-infected cells treated with/without A1 and A3 at 12, 14, 16 and 18 hpi. A) Supernatants collected from RV-infected cells B) Supernatants collected from RV-infected cells treated with 20 μM A1 C) Supernatants collected from RV-infected cells treated with 20 μM A3.

Fig. 6. Electron microscopic and TRPS time course study of RV-infected HT29.f8 cells and supernatants treated with and without arachidins. Rows 1-3 are micrographs of RV-infected HT29.f8 cells treated with A1 and A3 from 12-18 hpi. Control cells (NV, A1, and A3) were collected at 18 hpi and are displayed in panel 4. Panel 5 and 6 demonstrate TRPS experiments from 12-18 hpi that are overlain together. Autophagosomes (7A) and RV particles exiting a viroplasm into the ER (7B) in RV-infected HT29.f8 cells at 18 hpi.

Fig. 7. Time course analysis of HT29.f8 nuclear to cytoplasm ratio are shown at higher magnification using transmission electron microscopy. A) Electron micrographs of cells collected at 12 hpi, B) Electron micrographs of cells collected at 14 hpi, C) Electron micrographs of cells collected at 16 hpi, D) Electron

micrographs of cells collected at 18 hpi, Micrographs collected from control cells (NV, A1, A3) at 18 hpi. n = 10 for each treatment.

Fig. 8. Percent of HT29.f8 cells with autophagosomes over time. RV TEMs (n=13 for each time point) were compared to the no virus (NV) control. RV with A1 TEMS were compared to the A1 only control, and RV with A3 TEMS were compared to the A3 only.

Fig. 9. Real-time quantitative PCR (qRT-PCR) investigation of apoptosis and autophagy signaling pathways. Total RNA at 8 hpi was extracted from HT29.f8 cells with RV, RV+20µM A1, RV+20µM A3, 20µM A1 or 20µM A3 at 8 hpi. cDNA for each treatment was synthesized and used for qRT-PCR experiments. Fold change in expression of the genes of interest relative to GAPDH and β-actin were determined using the $2^{\Delta\Delta CT}$ method. The results are expressed as mean ± SD from three separate experiments.

Fig. 10. Presence of cannabinoid receptors on uninfected HT29.f8 cells. Cell lysates (10, 5, 2.5, 1.25 µg) were added to nitrocellulose membranes, probed with a 1:1000 dilution of rabbit anti-CNR1/2 antibodies from Antibodies Online (Atlanta, GA) and reactive bands were visualized by the addition and excitation of goat anti-rabbit antibodies Alexa Fluor®546 (Life Technologies) using the Typhoon 9500 laser scanner.

Conflict of interest

The authors have no conflict of interest to declare.

Aknowledgement

Style: Virus Research

References

Abbott, J. A., Medina-Bolivar, F., Martin, E. M., Engelberth, A. S., Villagarcia, H., Clausen, E. C., & Carrier, D. J. (2010). Purification of resveratrol, arachidin-1, and arachidin-3 from hairy root cultures of peanut (Arachis hypogaea) and determination of their antioxidant activity and cytotoxicity. *Biotechnology Progress*, *26*(5), 1344–1351. http://doi.org/10.1002/btpr.454

Adams, W. R., & Kraft, l. M. (1963). Epizootic diarrhea of infant mice: indentification of the etiologic agent. *Science (New York, N.Y.)*, *141*(3578), 359–360.

Aggarwal, B. B., Bhardwaj, A., Aggarwal, R. S., Seeram, N. P., Shishodia, S., & Takada, Y. (2004). Role of resveratrol in prevention and therapy of cancer: preclinical and clinical studies. *Anti- Cancer Research*, *24*, 2783–2840.

Anderson, E. J., & Weber, S. G. (2004). Rotavirus infection in adults. *The Lancet Infectious Diseases*, *4*(February), 91–99.

Arnold, M., Patton, J. T., & McDonald, S. M. (2009). Culturing, storage, and quantification of rotaviruses. *Current Protocols in Microbiology*, *SUPPL. 15C*. http://doi.org/10.1002/9780471729259.mc15c03s15

Arnold, M., Patton, J. T., & Mcdonald, S. M. (2012). Culturing, Storage, and Quantification of Rotavirus. *Current Protocols in Microbiology*, *15C.3*, 1–29. http://doi.org/10.1002/9780471729259.mc15c03s15.Culturing

Athar, M., Back, J. H., Tang, X., Kim, K. H., Kopelovich, L., Bickers, D. R., & Kim, A. L. (2007). Resveratrol: a review of preclinical studies for human cancer prevention. *Toxicology and Applied Pharmacology*, *224*, 274–283.

Ayala-Breton, C., Arias, M., Espinosa, R., Romero, P., Arias, C. F., & López, S. (2009). Analysis of the kinetics of transcription and replication of the rotavirus genome by RNA interference. *Journal of Virology*, *83*(17), 8819–8831. http://doi.org/10.1128/JVI.02308-08

Bakare, N., Menschik, D., Tiernan, R., Hua, W., & Martin, D. (2010). Severe combined immunodeficiency (SCID) and rotavirus vaccination: Reports to the Vaccine Adverse Events Reporting System (VAERS). *Vaccine*, *28*(40), 6609–6612. http://doi.org/10.1016/j.vaccine.2010.07.039

Ball, J. M., Medina-Bolivar, F., Defrates, K., Hambleton, E., Hurlburt, M., Fang, L., Parr, R. (2015). Investigation of stilbenoids as potential therapeutic agents for rotavirus gastroenteritis. *Advances in Virology*.

Berardi, V., Ricci, F., Castelli, M., Galati, G., & Risuleo, G. (2009). Resveratrol exhibits a strong cytotoxic activity in cultured cells and has an antiviral action against polyomavirus: potential clinical use. *Journal of Experimental & Clinical Cancer Research : CR*, *28*, 96. http://doi.org/10.1186/1756-9966-28-96

Bernstein, D. I. (2009). Rotavirus overview. *The Pediatric Infectious Disease Journal*, *28*, S50–S53. http://doi.org/10.1097/INF.0b013e3181967bee

Bhandari, N., Rongsen-Chandola, T., Bavdekar, A., John, J., Antony, K., Taneja, S., Bhan, M. K. (2014). Efficacy of a monovalent human-bovine (116E) rotavirus vaccine in Indian infants: A randomised, double-blind, placebo-controlled trial. *The Lancet*, *383*(9935), 2136–2143. http://doi.org/10.1016/S0140-6736(13)62630-6

Bishop, R. (2009). Discovery of rotavirus: Implications for child health. *Journal of Gastroenterology and Hepatology*, *24 Suppl 3*, S81–S85. http://doi.org/10.1111/j.1440-1746.2009.06076.x

Bishop, R., Davidson, G. P., Holmes, I. H., & Ruck, B. J. (1973). Virus particles in epithelial cells of duodenal mucosa from children with acute non-bacterial gastroenteritis. *The Lancet*, *302*(7841), 1281–1283.

Bo, A. N., Pol, E. Van Der, & Grootemaat, A. E. (2014). Single-step isolation of extracellular vesicles by size-exclusion chromatography. *Journal of Controlled Release : Official Journal of the Controlled Release Society*, *1*, 1–11. http://doi.org/10.3402/jev.v3.23430

Bobek, V., Kolostova, K., Pinterova, D., Kacprzak, G., Adamiak, J., Kolodziej, J., Hoffman, R. M. (2010). A clinically relevant, syngeneic model of spontaneous, highly metastatic B16 mouse melanoma. *Anticancer Research*, *30*(12), 4799–4804. http://doi.org/10.1002/jmv

Brents, L. K., Medina-Bolivar, F., Seely, K. a., Nair, V., Bratton, S. M., Ñopo-

Olazabal, L., Radominska-Pandya, A. (2012). Natural prenylated resveratrol analogs arachidin-1 and -3 demonstrate improved glucuronidation profiles and have affinity for cannabinoid receptors. *Xenobiotica*, *42*(2), 139–156. http://doi.org/10.3109/00498254.2011.609570

Chang, J. C., Lai, Y. H., Djoko, B., Wu, P. L., Liu, C. D., Liu, Y. W., & Chiou, R. Y. Y. (2006). Biosynthesis enhancement and antioxidant and anti-inflammatory activities of peanut (Arachis hypogaea L.) arachidin-1, arachidin-3, and isopentadienylresveratrol. *Journal of Agricultural and Food Chemistry*, *54*(26), 10281–10287. http://doi.org/10.1021/jf0620766

Chong, J., Anne, P., & Hugueney, P. (2009). Metabolism and roles of stilbenes in plants. *Plant Science*, *177*(3), 143–155.

Condori, J., Sivakumar, G. Hubstenberger, J., Dolan, M. C., Sobolev, V. S., & Medina-Bolivar, F. (2010). Induced biosynthesis of resveratrol and the prenylated stilbenoids arachidin-1 and arachidin-3 in hairy root cultures of peanut: effects of culture medium and growth stage. *Plant Physiology and Biochemistry*, *48*(5), 310–318.

Cook, S. M., Glass, R. I., LeBaron, C. W., & Ho, M. S. (1990). Global seasonality of rotavirus infections. *Bulletin of the World Health Organization*, *68*(2), 171–177.

Crawford, S. E., Hyser, J. M., Utama, B., & Estes, M. K. (2012). Autophagy

hijacked through viroporin-activated calcium/calmodulin-dependent kinase kinase-β signaling is required for rotavirus replication. *Proceedings of the National Academy of Sciences of the United States of America*, *109*(50), E3405–13. http://doi.org/10.1073/pnas.1216539109

Dang, S., Yu, Z., Zhang, C., Zheng, J., Li, K., Wu, Y., Wang, R. (2015). Autophagy promotes apoptosis of mesenchymal stem cells under inflammatory microenvironment. *Stem Cell Research & Therapy*, 1–9. http://doi.org/10.1186/s13287-015-0245-4

DeBlois, R. W. (1970). Counting and Sizing of Submicron Particles by the Resistive Pulse Technique. *Review of Scientific Instruments*, *41*(7), 909. http://doi.org/10.1063/1.1684724

Desselberger, U. (2014). Rotaviruses. *Virus Research*, *190*, 75–96. http://doi.org/10.1016/j.virusres.2014.06.016

Di Fiore, I. J. M., Holloway, G., & Coulson, B. S. (2015). Innate immune responses to rotavirus infection in macrophages depend on MAVS but involve neither the NLRP3 inflammasome nor JNK and p38 signaling pathways. *Virus Research*, *208*, 89–97. http://doi.org/10.1016/j.virusres.2015.06.004

Djoko, B., Chiou, R. Y. Y., Shee, J. J., & Liu, Y. W. (2007). Characterization of immunological activities of peanut stilbenoids, arachidin-1, piceatannol, and resveratrol on lipopolysaccharide-induced inflammation of RAW 264.7

macrophages. *Journal of Agricultural and Food Chemistry*, *55*(6), 2376–2383. http://doi.org/10.1021/jf062741a

Elmore, S. (2007). Apoptosis: a review of programmed cell death. *Toxicologic Pathology*, *35*(4), 495–516. http://doi.org/10.1080/01926230701320337

Estes, M. K., Graham, D. Y., & Mason, B. B. (1981). Proteolytic enhancement of rotavirus infectivity: molecular mechanisms. *Journal of Virology*, *39*(3), 879–888. http://doi.org/10.1016/0042-6822(80)90456-0

Estes, M. K., & Greenberg, H. . (2013). Rotaviruses. In *Fields Virology* (6th ed., pp. 1347–1401). Wolters Kluwer Health/Lippincott Williams & Wilkins, Philadelphia, PA.

Flewett, T. H., & Woode, G. N. (1978). The rotaviruses. *Archives of Virology*, *57*(1), 1–23.

Freshney, R. I. (1994). *Culture of Animal Cells: A Manual of Basic Technique.* (3rd ed.). New York: Wiley-Liss.

Frias, A. H., Jones, R. M., Fifadara, N. H., Vijay-Kumar, M., & Gewirtz, A. T. (2012). Rotavirus-induced IFN-β promotes anti-viral signaling and apoptosis that modulate viral replication in intestinal epithelial cells. *Innate Immunity*, *18*(2), 294–306. http://doi.org/10.1177/1753425911401930

Gambini, J., Inglés, M., Olaso, G., Abdelaziz, K. M., Vina, J., & Borras, C. (2015).

Properties of Resveratrol: In Vitro and In Vivo Studies about Metabolism, Bioavailability, and Biological Effects in Animal Models and Humans. *Oxidative Medicine and Cellular Longevity*.

Gardet, A., Breton, M., Fontanges, P., Trugnan, G., & Chwetzoff, S. (2006). Rotavirus spike protein VP4 binds to and remodels actin bundles of the epithelial brush border into actin bodies. *Journal of Virology*, *80*(8), 3947–3956. http://doi.org/10.1128/JVI.80.8.3947-3956.2006

Glass, R. I., Parashar, U., Patel, M., Gentsch, J., & Jiang, B. (2014). Rotavirus vaccines: Successes and challenges. *Journal of Infection*, *68*, S9–S19. http://doi.org/10.1016/j.jinf.2013.09.010

Greenberg, H. B., & Estes, M. K. (2009). Rotaviruses: From Pathogenesis to Vaccination. *Gastroenterology*, *136*(6), 1939–1951. http://doi.org/10.1053/j.gastro.2009.02.076

Halasz, P., Holloway, G., Turner, S. J., & Coulson, B. S. (2008). Rotavirus replication in intestinal cells differentially regulates integrin expression by a phosphatidylinositol 3-kinase-dependent pathway, resulting in increased cell adhesion and virus yield. *Journal of Virology*, *82*(1), 148–160. http://doi.org/10.1128/JVI.01980-07

Hall, G. A., Bridger, C., Chandler, R. L., & Wwde, G. N. (1976). Gnotobiotic Piglets Experimentally Infected with Neonatal Calf Diarrhoea Reovirus-Like Agent

(Rotavirus), *210*, 197–210.

Hammerschimidt, R., & Dann, E. K. (1999). The role of phytoalexins in plant protection. *Novartis Foundation Symposium*, *223*, 175–87. http://doi.org/223

Holloway, G., & Coulson, B. S. (2006). Rotavirus activates JNK and p38 signaling pathways in intestinal cells, leading to AP-1-driven transcriptional responses and enhanced virus replication. *Journal of Virology*, *80*(21), 10624–10633. http://doi.org/10.1128/JVI.00390-06

Holloway, G., & Coulson, B. S. (2013). Innate cellular responses to rotavirus infection. *Journal of General Virology*, *94*(Pt_6), 1151–1160. http://doi.org/10.1099/vir.0.051276-0

Hsieh, Y. C., Wu, F. T., Hsiung, C. A., Wu, H. S., Chang, K. Y., & Huang, Y. C. (2014). Comparison of virus shedding after lived attenuated and pentavalent reassortant rotavirus vaccine. *Vaccine*, *32*(10), 1199–1204. http://doi.org/10.1016/j.vaccine.2013.08.041

Huang, C.-P., Au, L.-C., Chiou, R. Y.-Y., Chung, P.-C., Chen, S.-Y., Tang, W.-C., Lin, S.-B. (2010). Arachidin-1, a peanut stilbenoid, induces programmed cell death in human leukemia HL-60 cells. *Journal of Agricultural and Food Chemistry*, (16), 12123–12129. http://doi.org/10.1021/jf102993j

Jeandet, P., Delaunois, B., Conreux, A., Donnez, D., Nuzzo, V., Cordelier, S., Courot, E. (2010). Biosynthesis, metabolism, molecular engineering, and

biological functions of stilbene phytoalexins in plants. *BioFactors*, *36*(5), 331–341.

Jiang, V., Jiang, B., Tate, J., Parashar, U. D., & Patel, M. M. (2010). Performance of rotavirus vaccines in developed and developing countries. *Human Vaccines*, *6*(7), 532–542. http://doi.org/10.4161/hv.6.7.11278

John M Chirgwin, Przybyla, A. E., MacDonald, R. J., & Rutter, W. J. (1979). Isolation of biologically active ribonucleic acid from sources enriched in ribonuclease. *Biochemistry*, *18*(24), 5294–5299. http://doi.org/10.1021/bi00591a005

Jones, C. L. (2015). Characterization of Vesicular stomatitis virus populations by tunable resistive pulse sensing Fulya, *33*(4), 395–401. http://doi.org/10.1038/nbt.3121.ChIP-nexus

Kozak, D., Anderson, W., Vogel, R., & Trau, M. (2011). Advances in resistive pulse sensors: Devices bridging the void between molecular and microscopic detection. *Nano Today*, *6*(5), 531–545. http://doi.org/10.1016/j.nantod.2011.08.012

Kroemer, G., & Levine, B. (2009). Autophagic cell death: the story of a misnomer. *Apoptosis*, *9*(12), 1004–1010. http://doi.org/10.1038/nrm2527.

Leshem, E., Lopman, B., Glass, R., Gentsch, J., Banyai, K., Parashar, U., & Patel, M. (2014). Distribution of rotavirus strains and strain-specific ectiveness of the

rotavirus vaccine after its introduction: a systematic review and meta-analysis.

Light, J. S., & Hodes, H. L. (1943). Studies on epidemic diarrhea of the new-born: isolation of a filtrable agent causing diarrhea in calves. *American Journal of Public Health*, *33*(12), 1451.

Marsh, Z., Yang, T., Nopo-Olazabal, L., Wu, S., Ingle, T., Joshee, N., & Medina-Bolivar, F. (2014). Effect of light, methyl jasmonate and cyclodextrin on production of phenolic compounds in hairy root cultures of Scutellaria lateriflora. *Phytochemistry*, *107*, 50–60. http://doi.org/http://dx.doi.org/10.1016/j.phytochem.2014.08.020

Matthews, R. (1979). The classification and nomenclature of viruses. *Intervirology*, *11*, 133–135.

Matthijnssens, J., Ciarlet, M., Heiman, E., Arijs, I., Delbeke, T., McDonald, S. M., Van Ranst, M. (2008). Full genome-based classification of rotaviruses reveals a common origin between human Wa-Like and porcine rotavirus strains and human DS-1-like and bovine rotavirus strains. *Journal of Virology*, *82*(7), 3204–3219. http://doi.org/10.1128/JVI.02257-07

McNulty, M., Curran, W., & McFerran, J. (1976). The morphogenesis of a cytopathic bovine rotavirus in Madin-Darby bovine kidney cells. *Journal of General Virology*, *33*(3), 503–508.

Mebus, C. A., Wyatt, R. G., Sharpee, R. L., Sereno, M. M., Kalica, A. R., &

Twiehaus, M. J. (1976). Diarrhea in gnotobiotic calves caused by the reovirus-like agent of human infantile Diarrhea in Gnotobiotic Calves Caused by the Reovirus-Like Agent of Human Infantile Gastroenteritis1, *14*(2), 471–474.

Mitchell, D. M., & Ball, J. M. (2004). Characterization of a spontaneously polarizing HT-29 cell line, HT-29/cl.f8. *In Vitro Cellular & Developmental Biology. Animal*, *40*(10), 297–302. http://doi.org/10.1290/04100061.1

Moss, R., Mao, Q., Taylor, D., & Saucier, C. (2013). Investigation of monomeric and oligomeric wine stilbenoids in red wines by ultra-high-performance liquid chromatography/electrospray ionization quadrupole time-of-flight mass spectrometry. *Rapid Communications in Mass Spectrometry*, *27*, 1815–1827. http://doi.org/10.1002/rcm.6636

Nakamura, M., Saito, H., Ikeda, M., Hokari, R., Kato, N., Hibi, T., & Miura, S. (2010). An antioxidant resveratrol significantly enhanced replication of hepatitis C virus. *World Journal of Gastroenterology*, *16*(2), 184–192. http://doi.org/10.3748/wjg.v16.i2.184

Nikoletopoulou, V., Markaki, M., Palikaras, K., & Tavernarakis, N. (2013). Crosstalk between apoptosis, necrosis and autophagy. *Biochimica et Biophysica Acta - Molecular Cell Research*, *1833*(12), 3448–3459. http://doi.org/10.1016/j.bbamcr.2013.06.001

Noguchi, M., & Hirata, N. (2015). Intersection of apoptosis and autophagy cell

Death pathways. *Austin Journal of Molecular and Cellular Biology*, *2*(1), 1–7.

Otto, P. H., Reetz, J., Eichhorn, W., Herbst, W., & Elschner, M. C. (2015). Isolation and propagation of the animal rotaviruses in MA-104 cells—30 years of practical experience. *Journal of Virological Methods*, *223*, 88–95. http://doi.org/10.1016/j.jviromet.2015.07.016

Palamara, A. T., Nencioni, L., Aquilano, K., De Chiara, G., Hernandez, L., Cozzolino, F., Garaci, E. (2005). Inhibition of influenza A virus replication by resveratrol. *The Journal of Infectious Diseases*, *191*, 1719–1729. http://doi.org/10.1086/429694

Parashar, U. D., & Glass, R. I. (2009). Rotavirus Vaccines — Early Success, Remaining Questions. *New England Journal of Medicine*, *360*(11), 1063–1065. http://doi.org/10.1056/NEJMp0810154

Park, M., Yun, Y. J., Woo, S. Il, Lee, J. W., Chung, N. G., & Cho, B. (2015). Rotavirus-associated hemophagocytic lymphohistiocytosis (HLH) after hematopoietic stem cell transplantation for familial HLH. *Pediatrics International*, *57*(2), e77–e80. http://doi.org/10.1111/ped.12567

Patel, N. C., Hertel, P. M., Estes, M. K., de la Morena, M., Petru, A. M., Noroski, L. M., Abramson, S. L. (2010). Vaccine-acquired rotavirus in infants with severe combined immunodeficiency. *The New England Journal of Medicine*, *362*(4), 314–9. http://doi.org/10.1056/NEJMoa0904485

Pattingre, S., Tassa, A., Qu, X., Garuti, R., Xiao, H. L., Mizushima, N., Levine, B. (2005). Bcl-2 antiapoptotic proteins inhibit Beclin 1-dependent autophagy. *Cell*, *122*(6), 927–939. http://doi.org/10.1016/j.cell.2005.07.002

Patton, J. T. (1995). Structure and function of the rotavirus RNA-binding proteins. *Journal of General Virology*, *76*(11), 2633–2644. http://doi.org/10.1099/0022-1317-76-11-2633

Patton, J. T. (2012). Rotavirus diversity and evolution in the post-vaccine world. *Discovery Medicine*, *13*(68), 85–97. Retrieved from http://www.pubmedcentral.nih.gov/articlerender.fcgi?artid=3738915&tool=pmcentrez&rendertype=abstract

Payne, C., Thomas, B., Skillicorn, C., & Charles, G. (2012). Anti-Apoptotic and Pro-Apoptotic Molecular and Cellular Pathways Induced by Viral Agents of Human and Animal Gastroenteritis: A Comprehensive Review. Retrieved from http://www.viralem.com/wp-content/uploads/2012/08/How-G.I.-Viruses-Kill-Cells.pdf

Payne, D., Staat, M., Edwards, K., Szilagyi, P., Gentsch, J., Stockman, L., Parashar, U. (2006). Rotavirus Proteins: Structure and Assembly. *CTMI*, *309*, 189–219.

Roupe, K. A., Remsberg, C. M., Yanez, J. A., & Davies, N. M. (2006). Pharmacometrics of stilbenes: seguing towards the clinic. *Current Clinical*

Pharmacology, *1*, 81–101.

Ruiz, M. C., Leon, T., Diaz, Y., & Michelangeli, F. (2009). Molecular biology of rotavirus entry and replication. *TheScientificWorldJournal*, *9*, 1476–1497. http://doi.org/10.1100/tsw.2009.158

Rzeżutka, A., & Cook, N. (2004). Survival of human enteric viruses in the environment and food. *FEMS Microbiology Reviews*, *28*(4), 441–453. http://doi.org/10.1016/j.femsre.2004.02.001

Saxena, K., Blutt, S. E., Ettayebi, K., Zeng, X., Broughman, J. R., Crawford, S. E., Estes, K. (2016). Human Intestinal Enteroids : a New Model To Study Human Rotavirus Infection , Host Restriction , and Pathophysiology, *90*(1), 43–56. http://doi.org/10.1128/JVI.01930-15.Editor

Sobolev, V. S., Potter, T. L., & Horn, B. W. (2006). Prenylated stilbenes from peanut root mucilage. *Phytochemical Analysis*, *17*(5), 312–322. http://doi.org/10.1002/pca.920

Stokley, S., Jeyarajah, J., Yankey, D., Cano, M., Gee, J., Roark, J., Markowitz, L. (2014). Human papillomavirus vaccination coverage among adolescents, 2007-2013, and postlicensure vaccine safety monitoring, 2006-2014 - United States. *MMWR. Morbidity and Mortality Weekly Report*, *63*(29), 620–4. Retrieved from http://www.ncbi.nlm.nih.gov/pubmed/25055185

Superti, F., Ammendolia, M. G., Tinari, A., Bucci, B., Giammarioli, A. M., Rainaldi,

G., Donelli, G. (1996). Induction of apoptosis in HT-29 cells infected with SA-11 rotavirus. *Journal of Medical Virology*, *50*(4), 325–334. http://doi.org/10.1002/(SICI)1096-9071(199612)50

Takacs-Vellai, K., Vellai, T., Puoti, A., Passannante, M., Wicky, C., Streit, A., Müller, F. (2005). Inactivation of the autophagy Gene bec-1 triggers apoptotic cell death in C. elegans. *Current Biology*, *15*(16), 1513–1517. http://doi.org/10.1016/j.cub.2005.07.035

Tate, J. E., Burton, A. H., Boschi-Pinto, C., Steele, A. D., Duque, J., & Parashar, U. D. (2012). 2008 estimate of worldwide rotavirus-associated mortality in children younger than 5 years before the introduction of universal rotavirus vaccination programmes: a systematic review and meta-analysis. *The Lancet. Infectious Diseases*, *12*(2), 136–141. http://doi.org/10.1016/S1473-3099(11)70253-5

Teimoori, A., Soleimanjahi, H., & Makvandi, M. (2014). Characterization and transferring of human rotavirus double-layered particles in MA104 cells. *Jundishapur Journal of Microbiology*, *7*(6), 1–5. http://doi.org/10.5812/jjm.10375

Uzri, D., & Greenberg, H. B. (2013). Characterization of Rotavirus RNAs That Activate Innate Immune Signaling through the RIG-I-Like Receptors. *PLoS ONE*, *8*(7), 1–15. http://doi.org/10.1371/journal.pone.0069825

Velayudhan, L., Van Diepen, E., Marudkar, M., Hands, O., Suribhatla, S., Prettyman, R., Bhattacharyya, S. (2014). Therapeutic potential of cannabinoids in neurodegenerative disorders: a selective review. *Current Pharmaceutical Design*, *20*(13), 2218–30. http://doi.org/10.2174/13816128113199990434

Vitaglione, P., Sforza, S., & Galaverna, G. (2005). Bioavailability of trans-resveratrol from red wine in humans. *Molecular Nutrition*, *49*(5), 495–504.

Vogel, R., Willmott, G. ., Kozak, D., Roberts, G. S., Anderson, W., Groenewegen, L., Trau, M. (2011). Quantitative Sizing of Nano/ Microparticles with a Tunable Elastomeric Pore Sensor. *Analytical Chemistry*, *83*(9), 3499–3506.

Vogelstein, B., & Gillespie, D. (1979). Preparative and analytical purification of DNA from agarose. *Proceedings of the National Academy of Sciences of the United States of America*, *76*(2), 615–619. http://doi.org/10.1073/pnas.76.2.615

Wang, H., Ramakrishnan, A., Fletcher, S., Prochownik, E. V, & Genetics, M. (2015). Current questions and possible controversies in autophagy. *Cell Death Discov.*, *2*(2), 1–20. http://doi.org/10.14440/jbm.2015.54.A

Ward, R. L. (1996). Mechanisms of protection against rotavirus in humans and mice. *The Journal of Infectious Diseases*, *174 Suppl* (3), S51–S58. http://doi.org/10.1097/INF.0b013e3181967c16

Weatherall, E., Hauer, P., Vogel, R., & Willmott, G. R. (2016). Pulse Size Distributions in Tunable Resistive Pulse Sensing. *Anal. Chem*, *88*(17), 8648–8656. http://doi.org/10.1021/acs.analchem.6b01818

Weinberg, G. a., Teel, E. N., Mijatovic-Rustempasic, S., Payne, D. C., Roy, S., Foytich, K., Bowen, M. D. (2013). Detection of novel rotavirus strain by vaccine postlicensure surveillance. *Emerging Infectious Diseases*, *19*(8), 1321–1323. http://doi.org/10.3201/eid1908.130470

World Health Organization. (2013). Weekly epidemiological record Relevé épidémiologique hebdomadaire. *Weekly Epidemiological Record*, (5), 49–64. Retrieved from http://www.who.int/wer/2013/wer8805.pdf

Wright, R. (2000). Transmission electron microscopy of yeast. *Microsc Res Tech.*, *51*(6), 496–510.

Yakshe, K. a, Franklin, Z. D., & Ball, J. M. (2015). *Rotaviruses: Extraction and Isolation of RNA, Reassortant Strains, and NSP4 Protein. Current Protocols in Microbiology.* http://doi.org/10.1002/9780471729259.mc15c06s37

Yang, T., Fang, L., Nopo-Olazabal, C., Condori, J., Nopo-Olazabal, L., Balmaceda, C., & Medina-Bolivar, F. (2015). Enhanced Production of Resveratrol, Piceatannol, Arachidin-1, and Arachidin-3 in Hairy Root Cultures of Peanut Co-treated with Methyl Jasmonate and Cyclodextrin. *Journal of Agricultural and Food Chemistry*, *63*, 3942–3950. http://doi.org/10.1021/jf5050266

Yen, C., Tate, J. E., Hyde, T. B., Cortese, M. M., Lopman, B. A., Jian, B., Parashar, U. D. (2014). RV Vaccines.

Yin, Y., Metselaar, H. J., Sprengers, D., Peppelenbosch, M. P., & Pan, Q. (2015). Rotavirus in organ transplantation: Drug-virus-host interactions. *American Journal of Transplantation*, *15*(3), 585–593. http://doi.org/10.1111/ajt.13135

CHAPTER TWO

To compare results observed from two cell lines our second study used African green monkey kidney cells (MA104) that were infected with human RV, Wa, and treated with A1 or A3. Based on results from the first study, experiments were conducted at 18 hpi.

Arachidin 1 and Arachidin 3 Regulations of Rotavirus-infected MA104 Cells

Caleb M Witcher[1,] Hannah N Lockwood[1,2], Rebekah Napier-Jameson[1], Macie N Mattila[1], Essence B Strange[1], Josephine Taylor[1], Beatrice Clack[1], Fabricio Medina-Bolivar[3], Judith M Ball[3] and Rebecca D Parr[1*]

[1] Department of Biology, Stephen F Austin State University, Nacogdoches, TX 75962; [2] Hannah N. Lockwood, Tyler, TX, [3] Department of Biological Sciences & Arkansas Biosciences Institute, Arkansas State University, Jonesboro, AR 72401; [4] Department of Biological and Environmental Sciences, Texas A&M University-Commerce, Commerce, TX 77843

Corresponding author: *e-mail: parrr1@sfasu.edu

Abbreviations: Rotavirus (RV), Plaque forming units (PFU), Western blots (WB), NSP4 (nonstructural protein 4), hours post infection (hpi), DMSO (dimethylsulfoxide), FBS (fetal bovine serum), MEM (Miminal essential medium), A1 (arachidin-1), A3 (arachidin-3), multiplicity of infection (MOI), tissue culture (TC), MSV (modified Murashige and Skoog's medium), PBS (phosphate buffered saline), analysis of variance (ANOVA), Transmission electron microscopy (TEM), Scanning electron microscopy (SEM), (qRT-PCR), Tunable resistive pulse sensing (TRPS), cycle threshold (Ct)

Abstract

Rotavirus (RV) causes severe life threatening diarrhea in young children and immunocompromised individuals. Several effective vaccines for young children have been developed, but there are no vaccines or antiviral therapeutics for RV infected immunocompromised patients of any age. Our laboratory has discovered a decrease in the numbers of infectious RV particles and the RV non-structural protein 4, NSP4, in a simian RV-infected human intestinal cell line, HT29.f8, with the addition of either of two stilbenoids, arachidin-1 or arachidin-3 (A1 and A3). This suggests effects on both the cells and RV replication. This study examined the effects of A1 and A3 using the human RV, Wa, to infect the kidney cell line, MA104. Plaque forming assays measured progeny infectious RV particles, and tunable resistance pulse sensing (TRPS) analysis quantified RV particles and determined their particle size distribution. Morphometric analysis of the cells was performed using transmission electron microscopy (TEM), and quantitative reverse transcription polymerase chain reaction (qRT-PCR) measured specific autophagy and apoptosis gene transcripts. Plaque assays demonstrated a decrease in infectious RV particles with the addition of A1 or A3. TRPS analysis showed a shift in the population of virus particles from an average size of 70nm to 110nm that corresponded to non-enveloped and enveloped RV particle sizes, respectively, observed with TEM. Likewise, the signs of apoptosis and autophagy observed with TEM, were validated with qRT-PCR. This study confirms that RV-infected MA104 cells and progeny RV particles are altered with the addition of the A1 or A3. Furthermore, interactions among the genes associated with apoptosis and autophagy suggest complex cross-talk between the two pathways. Future studies will further define the cellular pathways affected by the arachidins to evaluate their potential broad antiviral activity.

Introduction

Rotaviruses (RV) are members of the Reoviridae family that causes infantile gastroenteritis in children less than 5 years of age (Ward, 1996), and severe diseases in pediatric and adult immunocompromised individuals (Anderson & Weber, 2004; Bakare et al., 2010; Park et al., 2015; Patel et al., 2010; Yin, Metselaar, Sprengers, Peppelenbosch, & Pan, 2015). There are two licensed RV attenuated vaccines, RotaTeq® (Merck) and Rotarix® (GlaxoSmithKline), in the United States that prevent severe diarrhea (Leshem et al., 2014; Yen et al., 2014), and an attenuated RV vaccine, Rotavac®, in India (Bhandari et al., 2014). However, the vaccines efficacies are dependent on the timing of vaccination, and are designed to protect against common RV strains in specific areas of the world (Jiang et al., 2010; Patton, 2012). Consequently, they are dependent on the genetic stability of the virus (Patton, 2012), but reassortments are common and result in new infectious RV strains (Patton, 2012; Weinberg et al., 2013). Furthermore, the vaccines are contraindicated for immunosuppressed individuals, and there are no antiviral therapeutic agents currently available for RV infections. Besides the possibility of contracting RV-induced diarrhea directly from the attenuated vaccines, there are documented cases of horizontal transmission of vaccine RV among immunocompromised household contacts from vaccinated children who shed the vaccine virus (Hsieh et al., 2014; Patel et al., 2010; Yen et al., 2015)

RV replication occurs in mature enterocytes of the villi of the small intestine, leading to structural and functional changes in the epithelium. RV is transmitted by the fecal-oral route and is extremely contagious (Cook et al., 1990). The incubation period is 24 to 48 hours. Symptoms consist of watery diarrhea, vomiting, and fever lasting up to 4-8 days (Bernstein, 2009). Development of effective antiviral drugs that affect a wide-range of RV strains and reduce the burden of disease is an important strategy for the prevention of RV disease, especially in immunocompromised individuals. Likewise, the discovery of antiviral mechanism(s) that act upon other viruses could lead to the development of an antiviral compound with a broad range of activity.

Our laboratory is investigating the effects of highly purified prenylated stilbenoids extracted from peanut (*Arachis hypogea*) hairy root cultures on RV infections (Ball et al., 2015). Previously, we tested four stilbenoids, and demonstrated that the two prenylated stilbenoids, arachidin-1 (A1) and arachidin- 3 (A3), significantly inhibit the production of infectious simian RV (SA114f) virions (Ball, et al., 2015). Stilbenoids are secondary metabolites derived from plants that have antioxidant, anticancer, antifungal and anti-inflammatory properties, having been shown to have many human health benefits (Aggarwal et al., 2004; Athar et al., 2007; Roupe et al., 2006). They are products of the phenylpropanoid/ acetate pathway and act as phytoalexins produced by plants such as grapes, berries, and peanuts in response to pathogens (Huang et al., 2010; Moss et al., 2013).

Phytoalexins are antioxidative substances synthesized by plants that accumulate rapidly at areas of pathogen infections (Hammerschimidt & Dann, 1999). Although the molecular mechanism(s) of action for A1 and A3 on RV infections are not known, the decrease in infectious virus particles suggests an effect on viral replication that corresponds to a reduction in the viral nonstructural protein, NSP4, which is critical for viral replication (Ayala-Breton et al., 2009; Ball et al., 2015). Earlier studies have demonstrated that other cell lines from different tissues activate different pathways with RV infections (Di Fiore et al., 2015; Halasz et al., 2008; Gavan et al., 2006; Otto, Reetz, Eichhorn, Herbst, & Elschner, 2015;

Saxena et al., 2016; Uzri & Greenberg, 2013). This study investigated the mechanism of action(s) of A1 and A3 on the African green monkey kidney cell line, MA104, infected with the heterologous human RV strain, Wa.

Virus plaque forming assays were performed to quantify and compare the amount of infectious RV particles produced in human RV Wa-infected MA104 cells with and without A1 or A3. Tunable resistive pulse sensing technology (TRPS) using the qNano system by Izon was employed to quantify and determine the size distribution of all the virus particles in arachidin treated and untreated MA104 cells. Cellular ultrastructure and gross distribution of RV particles was analyzed using transmission electron microscopy (TEM). To corroborate the TEM observations, quantitative real time polymerase chain reactions (qRT-PCR) were performed using Rhesus macaque (*Macaca mulatta*)-specific primers for caspase and autophagy genes that encode proteins that are essential elements in apoptosis and autophagy pathways. We demonstrate that A1 and A3 decrease the amount of infectious RV particles produced, and the population of virus particles is changed from that of enveloped to non-eveloped particles with arachidin treatments. Also, significant changes in cell structure were observed that correspond to the changes in apoptosis and autophagy gene transcripts, induced by these compounds suggesting potential anti-RV therapeutic activity of A1 and A3.

Materials and Methods

Cell lines and virus.

MA104 cells were obtained from ATCC (Rockville, MD) and maintained in Eagle Modified Essential Medium (MEM; Gibco, Grand Island, NY) supplemented with 5% fetal bovine serum (FBS), glutamine (2 mM), penicillin-streptomycin (100 ug/mL) and non-essential amino acids (1X) (Sigma, St. Louis, MO). The cell line was confirmed to be free of mycoplasma contamination using the MycoFind mycoplasma PCR kit version 2.0 (Clongen Laboratories, LLC). RV Wa (G[1] P[8] genotype)(Matthijnssens et al., 2008) was amplified, viral titers were determined in MA104 cells, followed by storage at -80 °C. Stilbenoids efficacies against RV were tested using MA104 cells.

Bioproduction of stilbenoids in hairy root cultures of peanuts.

To produce the stilbenoids A1 and A3, a previously established hairy root line 3 from peanut cv. Hull was used that is capable of synthesizing and secreting A1 and A3 into the culture medium upon treatment with the elicitors sodium acetate or methyl-β-cyclodextrin (CD) (Cavasol® W7 M) (Condori et al., 2010; Yang et al., 2015). A 72-hour treatment of 9 g/L CD was selected based on the production of the highest levels of A1. At day nine of the hairy root culture, the spent medium from each flask was removed and replaced with elicitation medium (fresh MSV medium with 9 g/L methyl-β-CD and incubated in the dark at 28°C for an additional 72 h to induce synthesis and secretion of stilbenoids into the culture medium as recently described (Abbott et al., 2010; Yang et al., 2015). After the elicitation period, the culture medium was removed from each flask and combined. This pooled medium was mixed with an equal volume of ethyl acetate in a separator funnel to extract the stilbenoids as described previously (Condori et al., 2010). The ethyl acetate phase was recovered and was dried in a rotavapor (Buchi), and A1 and A3 were purified from the extract by HPCCC as follows. The dried ethyl acetate extract was suspended in HPCCC solvent system (hexane:ethyl

acetate:methanol:water [4:5:3:3]) and injected into a Spectrum[TM] (Dynamic Extractions) HPCCC system. HPCCC fractions containing A1 and A3 with over 95% purity based on HPLC analysis (UV 340 nm) were combined, dried under a nitrogen stream and used for viral assays (Abbott et al., 2010). As previously demonstrated, A1 and A3 were the major stilbenoids present in the culture medium (Ball et al., 2015). The dry mass of each stilbenoids was reconstituted in 0.002% DMSO with 1 µg/mL trypsin (Worthington Biochemical, Lakewood, NJ) in MEM medium.

Viability Assay.

Viability assays were performed with 0.002% DMSO only (NV + DMSO) that was used to solubilize the hydrophobic arachidins (A1 and A3), RV only, RV + DMSO, RV + 20 µM A1 , RV + 20 µM A3, 20 µM A3, 20 µM A1 and NV (no virus) using the trypan blue cell exclusion assay (Ball et al., 2015; Freshney, 1994). Briefly, MA104 cells were grown to 80% confluence in 6-well tissue culture plates (Corning Life Sciences), and starved for fetal bovine sera 12 hours prior to the addition of DMSO or DMSO with varying concentrations of the arachidins. At 18 hours after the addition of the solutions, a suspension of approximately 10^6 cells/ml was diluted 1:1 with a 0.4% trypan blue solution, and loaded onto a hemocytometer. The number of stained cells and total number of cells were counted, and the calculated percentage of unstained cells was reported as the percentage of viable cells. Each treatment was performed in triplicate, and data was expressed as the mean +/-standard deviation (SD), and comparisons were statistically evaluated by analysis of variance (ANOVA) and Student t tests using Excel (significance level, $p \leq 0.05$).

RV Infection.

To test the biological activity of the stilbenoids on RV infections, MA104 cells were grown to 80% confluence in 6 well tissue culture plates (Corning Life Sciences); starved for fetal bovine sera 12 hours prior to infection then infected with RV Wa as previously described (Arnold et al., 2009; Ball et al., 2015; Yakshe et al., 2015). Briefly, Wa RV stock was sonicated (5 min using a cup horn attachment and ice bath in a Misonix Sonicator 3000; Misonix, Inc, Farmingdale, NY) and incubated in serum-free MEM with 1 µg/mL trypsin (Worthington Biochemical, Lakewood, NJ) for 30 min at 37°C. The activated viral inoculum was incubated with cells for 1 h at 37°C in 5% CO_2 at an MOI of 0.002. The inoculum was replaced with serum-free MEM supplemented with 1 µg/mL trypsin and incubated for 18 hpi. The supernatants were collected, clarified at 300 x *g* for 5 min, and stored at -80°C for plaque assays and TRPS analysis (see below). The cells were washed in cold Dulbecco's PBS, 1X (Caisson Laboratories, Smithfield, UT), and released from the plates using a 0.25% Trypsin-EDTA Solution (1X) (Caisson Laboratories, Smithfield, UT). After the addition of MEM with 5% FBS, the cells were suspended in cold PBS and dilutions were prepared for live/dead cell counts (see above in Viability Assays). Cells were washed with PBS and incubated in Modified Eagle's Medium and trypsin (1µg/ml) without Fetal Bovine Serum for 18 hours at 37ºC in 5% CO_2 (Arnold et al., 2009; Ball et al., 2015; Yakshe et al., 2015). Supernatants were collected and used for TRPS and PFU assays. Some of the cells were fixed with 5% glutaraldehyde for TEM analysis as described below.

Infectious RV quantification.

PFU assays were performed in triplicate as previously described (Arnold et al., 2009; Ball et al., 2015; Yakshe et al., 2015). Briefly, ten-fold dilutions of RV alone and RV with 0.002% DMSO and 20 µM A1 or A3 were added to the serum starved MA104 cells for one hour infection as described above. The virus inoculum was replaced with 3 mL of a medium overlay (1:1 mixture of 1.2% agarose [Apex Low Melting Point Agarose, Genesee Scientific Inc] and complete MEM containing 0.5 µg/mL trypsin and incubated at 37°C in 5% CO_2 for 3 to 4 days or until plaques became visible. A neutral red overlay (1:1 mixture of 1.2% agarose with an equal volume of serum-free MEM containing 50 µg/mL neutral red) was prepared and 2 mL per well of stain overlay was added on top of the first agarose/medium overlay. The six-well plates were incubated at 37°C until plaques were visible (approximately 12 to 72 h). The individual plaques were counted, and the titers were calculated as follows: Number of plaques x 1/dilution factor x 1/ (mL of inoculum) = PFU/mL. Plaque forming assays were performed in triplicate with data are expressed as mean +/-SD. Comparisons were statistically evaluated by analysis of variance (ANOVA) and Student t tests using Excel (significance level, $p \leq 0.05$).

Quantification and Size Distribution of RV Particles.

To determine the concentration and size of RV particles in the samples (RV, RV+A1 and RV+A3), TRPS analysis using the qNano system (Izon Science, Cambridge, MA) was employed. TRPS is based on a coulter counter that is composed of two fluid reservoirs filled with an electrolyte or other conductive media and separated by a membrane containing a pore (Kozak et al., 2011; Weatherall et al., 2016). When an electrical field is applied across the pore, the resistance to the resulting ionic current is indirectly proportional to the cross-sectional area of the pore. When a non-conducting particle passes through the pore, the increase in resistance is proportional to the particle volume relative to pore size. This change in resistance is detected as a pulse in an ionic current. The pulse frequency is proportional to particle flow rate and particle concentration (DeBlois, 1970). This system provides a quick and accurate way to measure individual sizes of nanoparticles and their volume in a solution. All qNano experiments were performed using the manufacturer's established protocols (Bo et al., 2014; Jones, 2015; Vogel et al., 2011). Briefly, prior to measuring, samples were purified using a qEV size exclusion column from Izon, and were then suspended in PBS with 0.025% Tween 20 to reduce aggregation. A dilution of 1:1000 was placed on the qNano size-tunable nanopore (NP100, Izon) with particles detected one at a time as a transient change in the ionic current flow. This was denoted as a blockade event with its amplitude representing the blockade magnitude. Because the blockade magnitude is proportional to the particle size, accurate particle sizing was achieved after calibration with particles of a known size (CPC100B, Izon) using identical settings. The size distribution and concentration analysis was performed using IZON proprietary software v3.2.2.268 (Izon).

Morphometric analysis of RV-infected MA104 cells.

TEM analysis was performed on RV-infected MA104 cells to visualize the effects of the A1 and A3 on progeny virus and cellular morphology. Samples were prepared as described by Wright (2000). Briefly, RV-infected MA104 cells with and without 20µM A1 or A3 were incubated for 18 hpi, washed with PBS and then trypsinized. Cells were pelleted and fixed

with 5% glutaraldehyde overnight at 4^0C. The cells were post-fixed with 2% osmium tetroxide, dehydrated with a graded ethanol series, infiltrated and embedded in epoxy resin. Thin sections were stained with uranyl acetate and lead citrate and were examined with a Hitachi H-7000 electron microscope operating at 75KeV. Negatives were digitized at 800 dpi and analyzed using Macnification Version 2 (Orbicule, Inc., www.orbicule.com). The mean ratio of the cell nucleus: cytoplasm was determined using twelve micrographs of each treatment, and the data was graphed for comparisons between tests and control groups.

Quantification of apoptosis and autophagy gene transcripts.

The PureLink® RNA Mini Kit (Ambion by Life Technologies; Foster City, CA) was used to extract and purify total RNA according to the manual protocol (Chirgwin et al., 1979)·(Vogelstein & Gillespie, 1979). Briefly, an equal volume of 70% ethanol was added to 5µg of total RNA for each sample, and vortexed. The samples were then transferred to a spin cartridge and centrifuged for 15 seconds at 12,000xg at room temperature. The sample was then washed and centrifuged with 700 µL of wash buffer I for 15 seconds at 12,000xg. A second wash was performed with 500 µL of wash buffer II for 15 seconds at 12,000xg. A final spin was performed at 12,000xg for 2 min to dry the membrane containing the bound RNA. The RNA was eluted from the membrane with 50 µL of nuclease free water. Total RNA was analyzed using a full spectrum analysis at 240nm-320nm using the Cary 50 spectrophotometer (Agilent, Corp.). The pure RNA was stored at -80°C for future studies. A conversion factor of 40 µg/mL was used to convert the A_{260} to concentration and the value of 10 corrected for a path length of 0.1 mm (Sean and Wiley, 2008). The concentration of RNA was calculated using the formula as follows: Concentration of RNA= A260 x 40 µg/mL x 10 x Dilution factor. cDNA was then synthesized from each experimental set using the Thermo Scientific Verso cDNA Synthesis Kit using five micrograms of purified total RNA. A Master Mix was prepared as described in the manufacturer's protocol as shown in table 1. The samples were then placed into the BioRad Real-Time System C1000 Thermal Cycler Instrument (Hercules, California) for the following cycle (table 2). The qRT-PCR experiment was performed using a CFX96 Touch Real-Time PCR Detection System (BioRad). For all experiments, reactions were performed in triplicate with Apex qPCR GREEN Master Mix without ROX (Genesee Scientific, San Diego, California) that contained all necessary components to perform a DNA-binding dye base real-time DNA amplification experiment (Table 3). Primers were purchased from Sigma-Aldrich (St. Louis, MO) with the sequences shown in Table 4. Each reaction mixture contained 10µl of Apex qPCR GREEN Master Mix, 0.5µl of 10µM forward/reverse primers, 3µl of 50ng template cDNA and nuclease-free water to a final volume of 20µl. GAPDH and β-actin were used as housekeeping genes for relative gene expression analyses. The cycle threshold (Ct) value or cycle number obtained from single reactions for each standard reaction were all values that fell within a linear portion of the standard curve. The obtained Ct values from the qRT-PCR experiment were exported to Excel for data analyses. Fold change in signals of expression of the genes of interest relative to GAPDH and β-Actin were determined using the ΔΔCt method. The results are expressed as mean ± SD.

Results

Viability of MA104 cells in the presence of DMSO, A1 and A3.

The percentage of live/dead cells calculated using the trypan blue exclusion dye assay (Ball et al., 2015). RV-infected cells showed an average viability of 89.4% demonstrating, a viral effect on the cells; RV with 0.002% DMSO showed 91.5% cell viability. Untreated cells (NV) containing 0.002% DMSO showed 97.5% and NV alone demonstrated 93% viability. Cells treated with RV + 20 µM A1 displayed a viability of 90% and 20 µM A1 alone had a 91.3% viability. Cells treated with RV + 20 µM A3 displayed a viability of 92.5% and 20 µM A3 alone had a 95.8% viability (Figure 1).

The effects of A1 and A3 on the production of infectious RV particles.

Supernatants were collected at 18 hpi from the RV-infected and RV-infected with 20µM concentrations of A1 or A3 and used for plaque forming assays. Plaques were counted and the average of three experiments was calculated and graphed as PFU/mL (Figure 2). Data are expressed as mean +/-SD, and comparisons were statistically evaluated by analysis of variance (ANOVA) and Student t tests using Excel (significance level, $p \leq 0.05$). The PFU assays demonstrated no statistical difference between RV and RV with DMSO ($p = 0.631$). The A1 and A3 experiments demonstrated one hundred twenty-seven and one hundred twenty-fold differences, respectively, from the RV only that were statistically significant ($p = 0.014$ for both A1 and A3). Correspondingly, A1 and A3 demonstrated one hundred thirty-six and one hundred thirty-one-fold differences, respectively, from RV with DMSO that were statistically significant ($p = 0.006$ for both A1 and A3) (Figure 2). This suggests that by 18 hpi, a large amount of infectious RV is released into the media from RV infected cells, but there is a significant decrease in the released infectious RV with the addition A1 or A3.

TEM morphometric analyses of MA104 cells.

Morphometric analyses of uninfected, A1 and A3 only treated MA104 cells were compared to RV infected cells as well as infected cells treated with A1 or A3. The ratio of nucleus to cytoplasm was calculated using twelve representative cells from each treatment. At 18 hpi, the mean ratios of the control cells treated with A1 (0.44) and A3 (0.39) were similar to those of the cells with no treatment (0.48) (Figure 3). The RV-infected cells demonstrated an increased nucleus to cytoplasm ratio as well as plasma membrane blebbing, both of which have been described as apoptotic characteristics (Elmore, 2007). RV-infected cells treated with A1 and A3 had mean ratios, 0.49 and 0.54 respectively, that were like the ratios of the control cells. However, both arachidin treated RV infected cells displayed different ultrastructure characteristics from the control cells. RV-infected cells treated with A1 had many autophagosomes and large sized mitochondria, while the A3 treated cells exhibited many small mitochondria and many vesicles in the cytoplasm (Figure. 3).

RV particle size measurements with TEM.

RV particles of two different populations were seen at 18hpi, enveloped RV particles ($_e$RV) and non-enveloped RV particles ($_{ne}$RV) (Fig.ure 4A). To determine an accurate size of the particles, micrographs were taken at high magnification, and twenty-two RV particles from each group were measured. Data was expressed as mean +/-SD, and statistically evaluated by analysis of variance (ANOVA) to be two significantly different populations ($p = 1.96E\text{-}31$), $_e$RV and $_{ne}$RV, with average diameters of $_{ne}$RV 112.74nm and $_e$RV 72.39nm, respectively (Figure 4B).

Autophagosome content in RV infected MA104 cells.

MA104 cells from each treatment (n = 12 each) were scored positive or negative for the presence of autophagosomes. Control treatments showed autophagosomes in 23.1% of the NV cells, 8.3% of the A3 treated cells, and 66.7% of the A1treated cells (Figure 5). Comparatively, 5.9% of RV-infected cells were positive, 84.6% of RV-infected cells treated with A1 were positive for, and 7.7% of RV-infected cells treated with A3 were positive for autophagosomes (Figure 5).

Quantification of RV particles and size distribution by TRPS analysis.

TRPS analysis was performed on the RV infected cell supernatants to display the concentration of virus particles/mL, diameter of RV particles and size distribution of particles. TRPS allow for high-throughput single particle measurements as virus particles are driven through pores, one at a time, causing a blockade event that can be measured for individual size; the number of blockades is used to determine concentration (Vogel et al., 2011). The RV only samples showed a concentration of 1.71E13 particles/mL at 18hpi (Figure 5A). Also, the particles had a dispersed range in diameter from approximately 60-120nm. At the same time, RV-infected cells treated with A3 demonstrated particles with diameters between 90-140nm (Figure 6B). Additionally, RV-infected cells treated with A1 displayed a concentration of 1.42E12, and the particles were between 70-150nm (Figure 6C).

Quantification of Transcripts for Apoptosis and Autophagy Genes MA104 treated with Arachidins.

Multiple connections exist between autophagy and apoptosis (Dang et al., 2015; Kroemer & Levine, 2009; Nikoletopoulou et al., 2013; Wang et al., 2015). This data led us to explore the molecular and functional connections between the apoptosis and autophagy pathways in RV infected MA104 cells with and without the arachidins. We focused on the expression of caspases that initiate the apoptosis death pathway (initiator caspases 8 and -9) and genes that execute the apoptosis death pathway (caspase -3 and 7). Also, we detected the presence of autophagy genes (*Beclin-1, Bcl2, atg3, atg 5*) that are decisive in the progression to autophagy (Noguchi & Hirata, 2015). In our experiments, there was no significant changes in the regulation of either the apoptosis or autophagy pathways with the addition of A1 and A3

(Figure 7A –D). This demonstrates that at 8 hpi, the two death pathways are not regulating an RV infection in MA104 cells.

Immunoblot assays to detect cannabinoid receptors.

Slot blot assays were performed to confirmed the presence of both A) cannabinoid receptor 1 (CBR1) and B) cannabinoid receptor 2 (CBR2) on MA104 cells (Figure 8). Both uninfected cell lysates (Figure 8 lane 1) and RV-infected cell lysates (Figure 8 lane 2) were positive for both receptors.

Discussion

Previous studies in our lab using a simian RV, SA11.4f, revealed that A1 and A3 generate antiviral effects by reducing the amount of released infectious RV particles, suggesting a decrease in viral replication (Ball et al., 2015). This is the first study to investigate the A1 and A3 induced changes in a human RV (Wa) infected African green monkey kidney cell line, MA104.

The viability assay verified no adverse effects on the survival of MA104 cells treated with both arachidins (A1 and A3), therefore 20μM concentrations of A1 and A3 are not toxic to MA104 cells. Any alterations in patterns observed in RV-infected cells treated with the arachidins can be attributed to effects of the arachidins on RV and viable host cells.

Furthermore, the decreased amount of infectious RV produced in Wa-infected arachidin treated cells corresponds to the decreases in progeny RV produced in the simian RV, SA11.4f, infected human intestinal cell line, HT29.f8 (Ball et al., 2015) with arachidin treatments. This indicates that A1 and A3 have antiviral properties that effect both simian and human RV strains.

Morphometric examination of intracellular RV particles demonstrated two size populations that corresponded to the sizes of extracellular RV particles measured using TRPS analysis. This indicates that immature noninfectious large RV particles are released from the infected cells. Furthermore, even though the number of extracellular particles detected among treatments with and without arachidins were similar, the size distribution of particles varied significantly. Additionally, RV-infected, arachidin treated samples released RV particles that were the same size as the immature, non-infectious, large particles with ER membrane envelopes (eRV) observed in previous studies (Teimoori et al., 2014). Likewise, RV only samples released a distribution of smaller, noneveloped particles (neRV) that are the size of mature infectious RV(M.K. Estes & Greenberg, 2013).

MA104 cells infected with RV only demonstrated characteristics of apoptotic cells which was altered with the addition of A1 or A3 demonstrating an increased nuclear size and membrane blebbing seen in previous studies (Nikoletopoulou et al., 2013). This suggests that the apoptosis pathway was regulated by A1 and A3. Additionally, many autophagosomes were present in the cells with A1 alone and RV with A1, which suggested the autophagy pathway was initiated with A1 treatments. Autophagy is a conserved mechanism that produces autophagosomes to degrade damaged proteins in the cytoplasm and is believed to be a pro-survival pathway (Noguchi & Hirata, 2015). Observations of increased numbers of autophagosomes in A1 treated cells suggests that A1 modulates an RV infection by stimulating cells to utilize the autophagy cell death pathway. This observation led us to examine the apoptosis and autophagy gene transcript by qRT-PCR to confirm the involvement of these pathways in the modulation of the RV infection. However, no significant changes in the gene transcripts were observed at 8 hpi from the treated MA104 cells (RV, RV with A1, RV with A3, A1 only and A3 only).

This finding is contradictory to data obtained using the same treatments at 8 hpi in a human intestinal cell line, HT29.f8 (Parr laboratory, personal communications), suggesting that two cell types use different signaling pathways, or have differences in the timing of regulation of apoptosis and autophagy. Further studies will be performed to answer this question.

A previous study has confirmed the binding of A1 and A3 to cannabinoid receptors 1 and 2 (Brents et al., 2012). The presence of these receptors on MA104 cells suggests a signaling pathway that could be used to modulate an RV infection. This will be further investigated to determine the signaling pathways used in RV-infected MA104 cells treated with A1 or A3.

In summary, data collected from RV-infected MA104 cells treated with A1 or A3 exhibited a more normal ultrastructural appearance than untreated infected cells, as well as a decrease in the number of extracellular infectious RV particles with a shift to larger, immature, $_e$RV particle size. However, the fact that A1 produced numerous autophagosomes while A3 did not infers that different mechanisms of action modulate an RV infection, thus broadening the anti-RV therapeutic potential of the arachidins.

Table 1. cDNA Master Mix.

	Volume	Final Concentration
5x cDNA synthesis buffer	4µL	1x
dNTP Mix	2µL	500µM each
Anchored oligo dT	1µL	
Verso Enzyme Mix	1µL	
Template (RNA)	5µL	5µg
Nuclease-free Water	7µL	
Total Volume	20µL	

Table 2. cDNA synthesis thermocycler parameters.

	Tempeture	Time	Number of cycles
cDNA synthesis	42°C	30 min	1 cycle
Inactivation	95°C	2 min	1 cycle

Table 3. PCR cycle conditions used for qRT-PCR.

Initial denaturation	94°C	3 minutes
PCR (34 cycles)	94°C	30 seconds
	58°C	30 seconds
	72°C	1 minutes

Table 4. Primers used for the amplification of MA104 apoptosis and autophagy genes

Genes	Primer name	Primer sequence (5'-3')[a]	% GC	T_m(°C)	PCR productSize (bp)
Caspase 3	Casp3forAGM	AGGTATCCATGGAGAACACTGA	45.45	62.3	210
	Casp3RevAGM	CTGTACCAGACCGAGATGC	60	60.9	
Caspase 7	Cas7forAGM	GGTGGATGCTAAGCCAGA	55	61.5	230
	Cas7revAGM	CGAACACCCATACCTGTCA	50	62.1	
Caspase 8	Cas8forAGM	GGTCACTTGAACCTTGGGA	52.7	62.6	146
	Cas8frevGM	TGGGATGCAGTCCAGG	62.5	62.1	
Caspase 9	Cas9forAGM	ACGGCAGAAGTTCACATTG	47.4	61.4	147
	Cas9revAGM	ACACCCAGACCAGTGGAC	61.2	61.2	
GAPDH	GAPDHfor	GAGTCCACTGGCGTCTTCA	57.9	51	190
	GAPDHrev	GGGGTGCTAAGCAGTTGGT	57.8	50	
β-Actin	β-Actin for	ATCCTCACCCTGAAGTACCC	55	61.7	183
	β-Actin rev	TAGAAGGTGTGGTGCCAGAT	50	62.1	
BCL2	BCL2ForAGM	CAGTTGGGCAACAGAAAACCAT	50	60.5	171
	BCL2RevAGM	AGCCCTTGACCCCAATTTGGAA	45	60.1	
ATG3	atg3 ForAGM	CCCGGTCCTCAAGGAATCAAA	50	61.3	207
	atg3 RevAGM	TCCATCTGTTTGCACCGCTT	53	61.1	
ATG5	atg5 ForAGM	TCGGGTAGGTTTGGCTTTGG	55.6	61.9	220
	atg5 RevAGM	CCAATTGGATAATGCATAGTATGGT	47.7	60.2	
BCLN1	belcin-1 ForAGM	CTACAAACGCTGTTTGGAG	50	61.3	189
	belcin-1 RevAGM	TGATCCAGTCTCTCAGCCTCA	55	62.2	

a-Primer sequences obtained from the NCI Primer data base. All oligonucleotides were ordered from Sigma-Genosys (Sigma-Aldrich Corp).

Figure 1

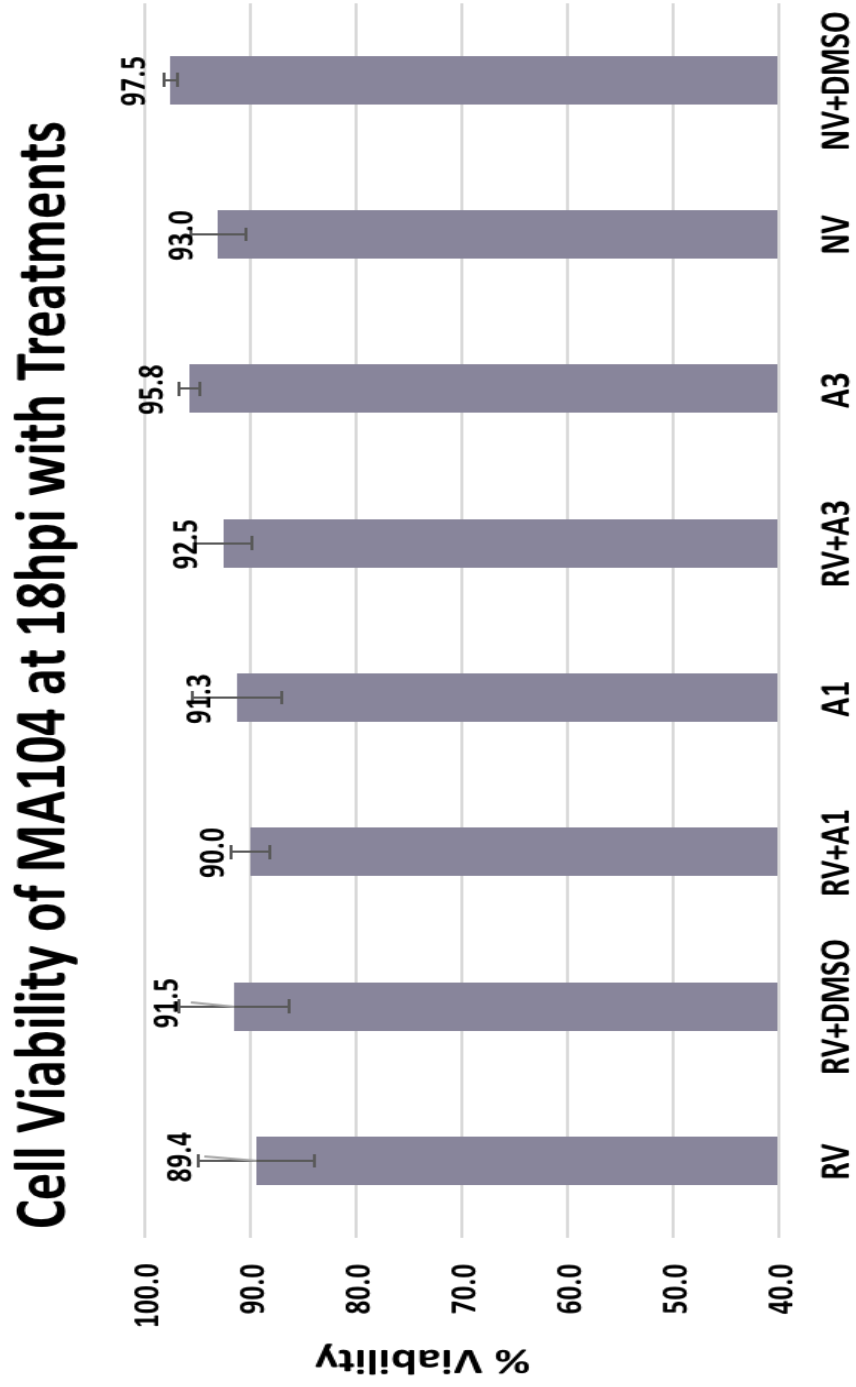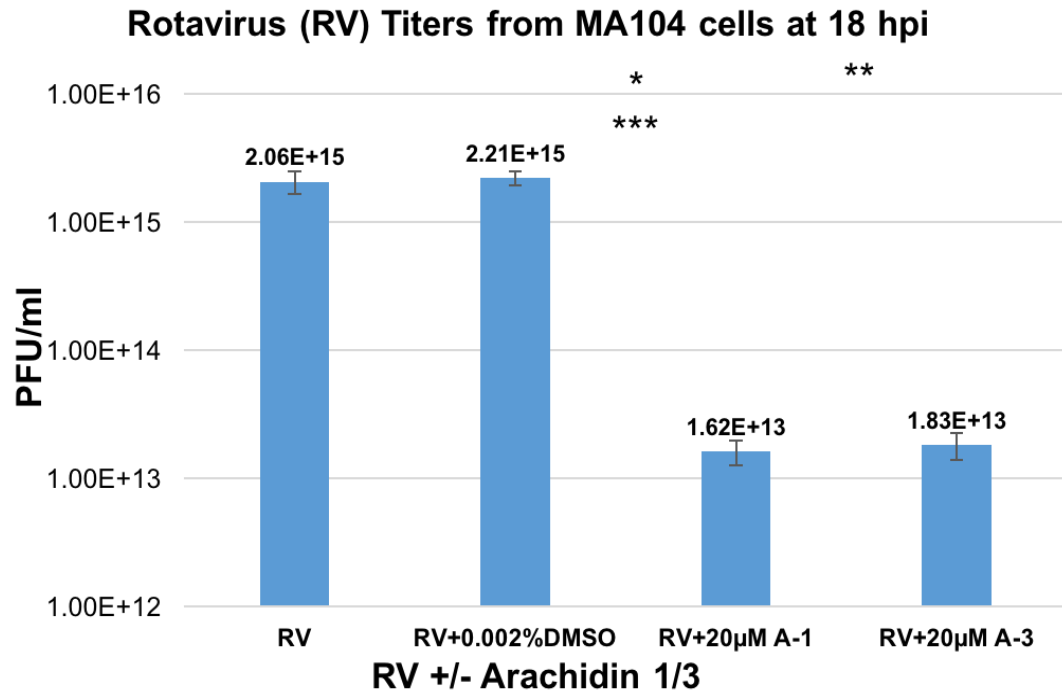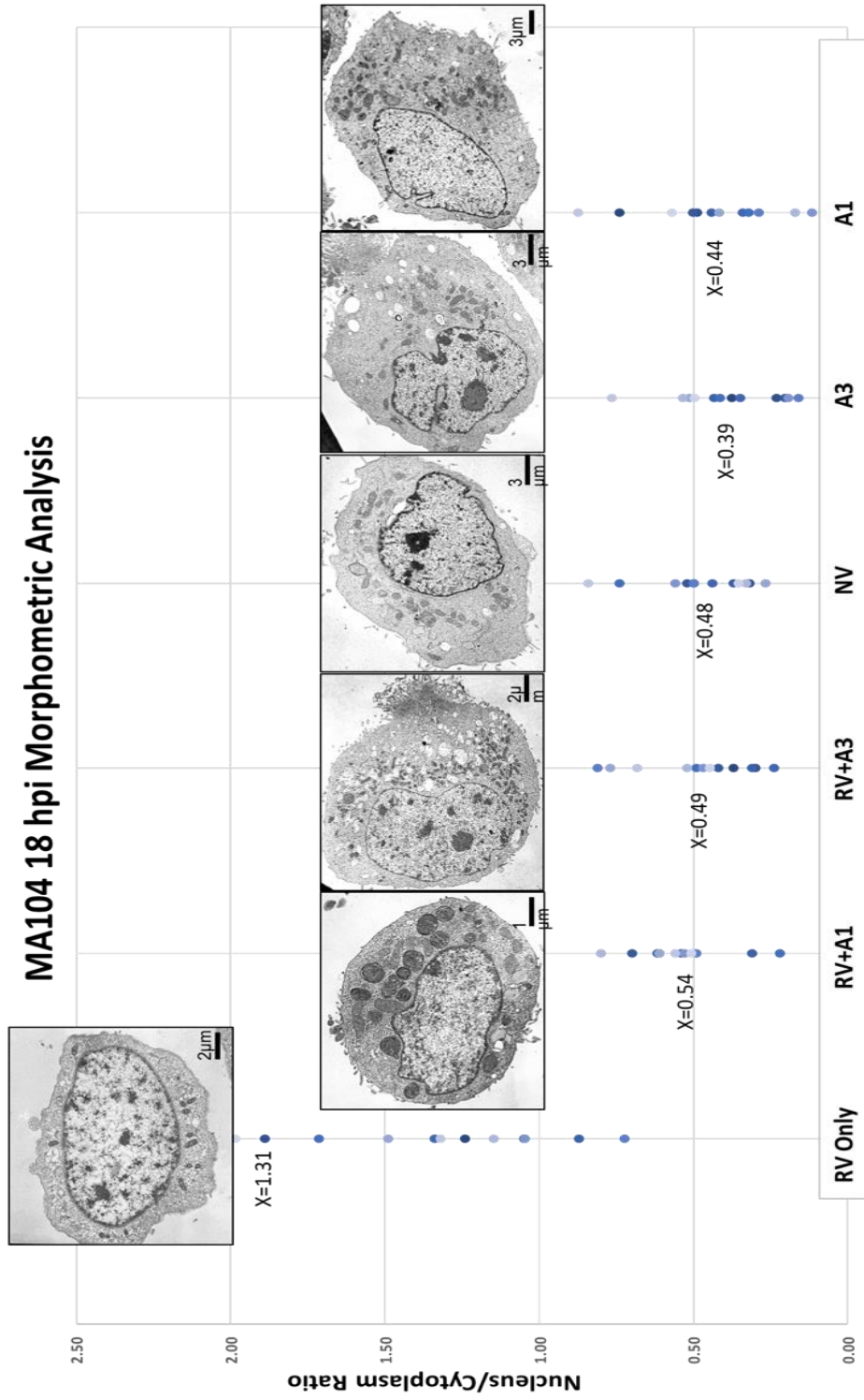

Cell Viability of MA104 at 18hpi with Treatments

Figure 2

Rotavirus (RV) Titers from MA104 cells at 18 hpi

Figure 3

Figure 4

Figure 5

Percent MA104 cells with Autophagic Vesicles at 18hpi

Figure 6

Figure 7

Apoptosis and Autophagy transcripts from MA104 treated with A3

Apoptosis and Autophagy Transcripts from MA104 Treated with A1
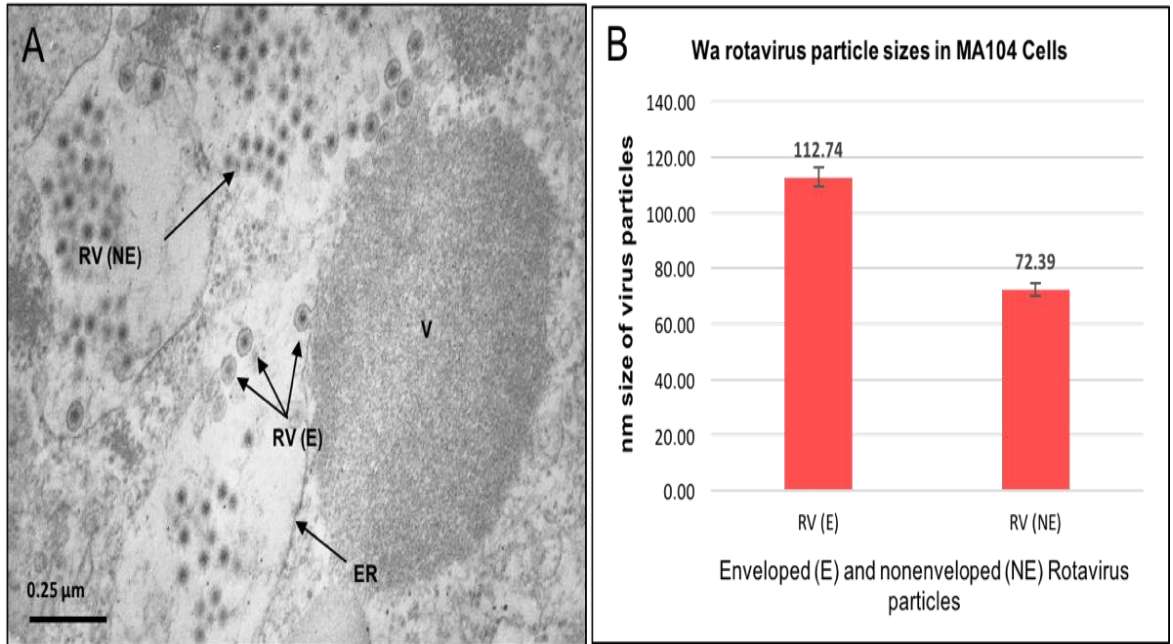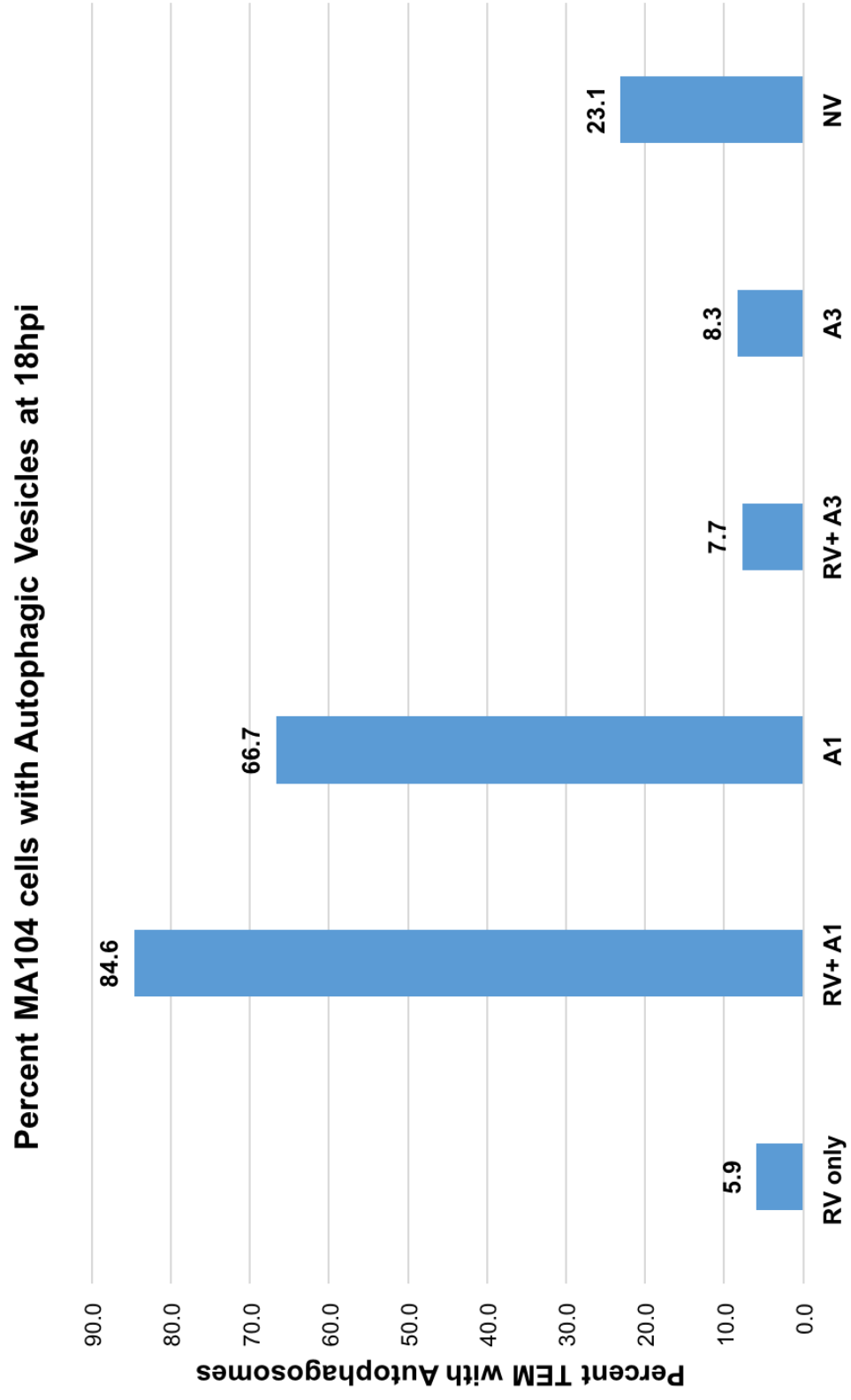
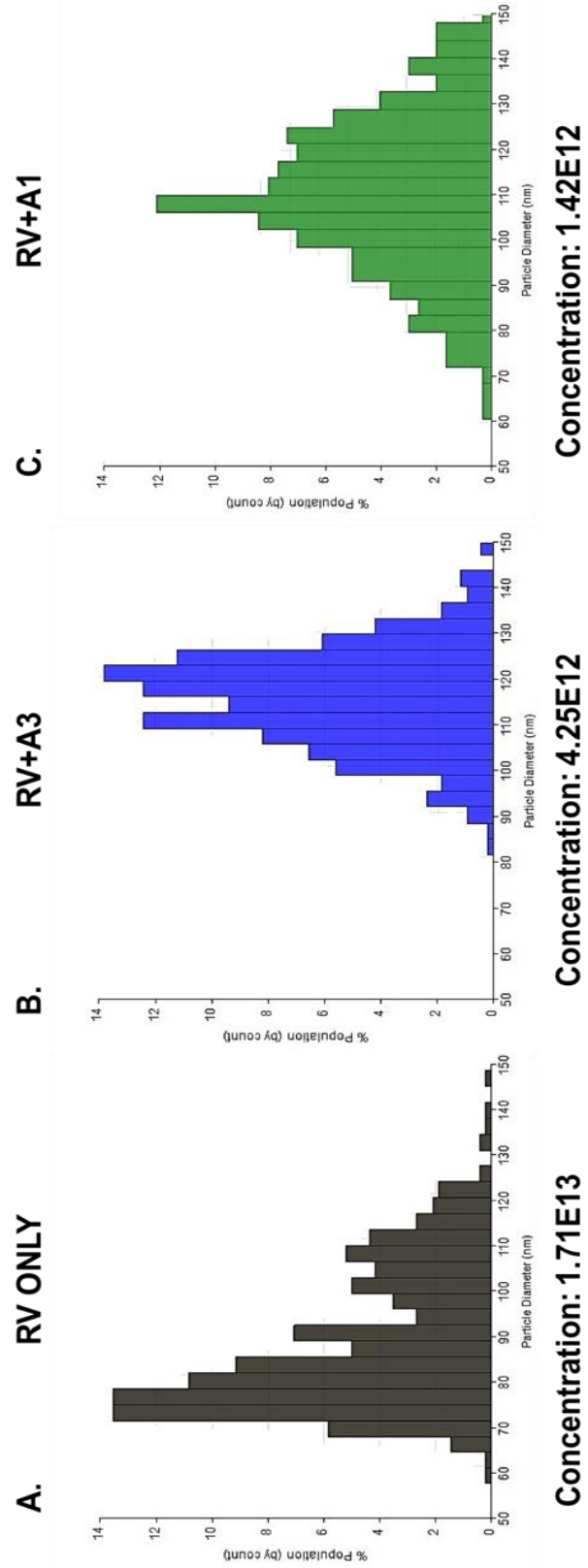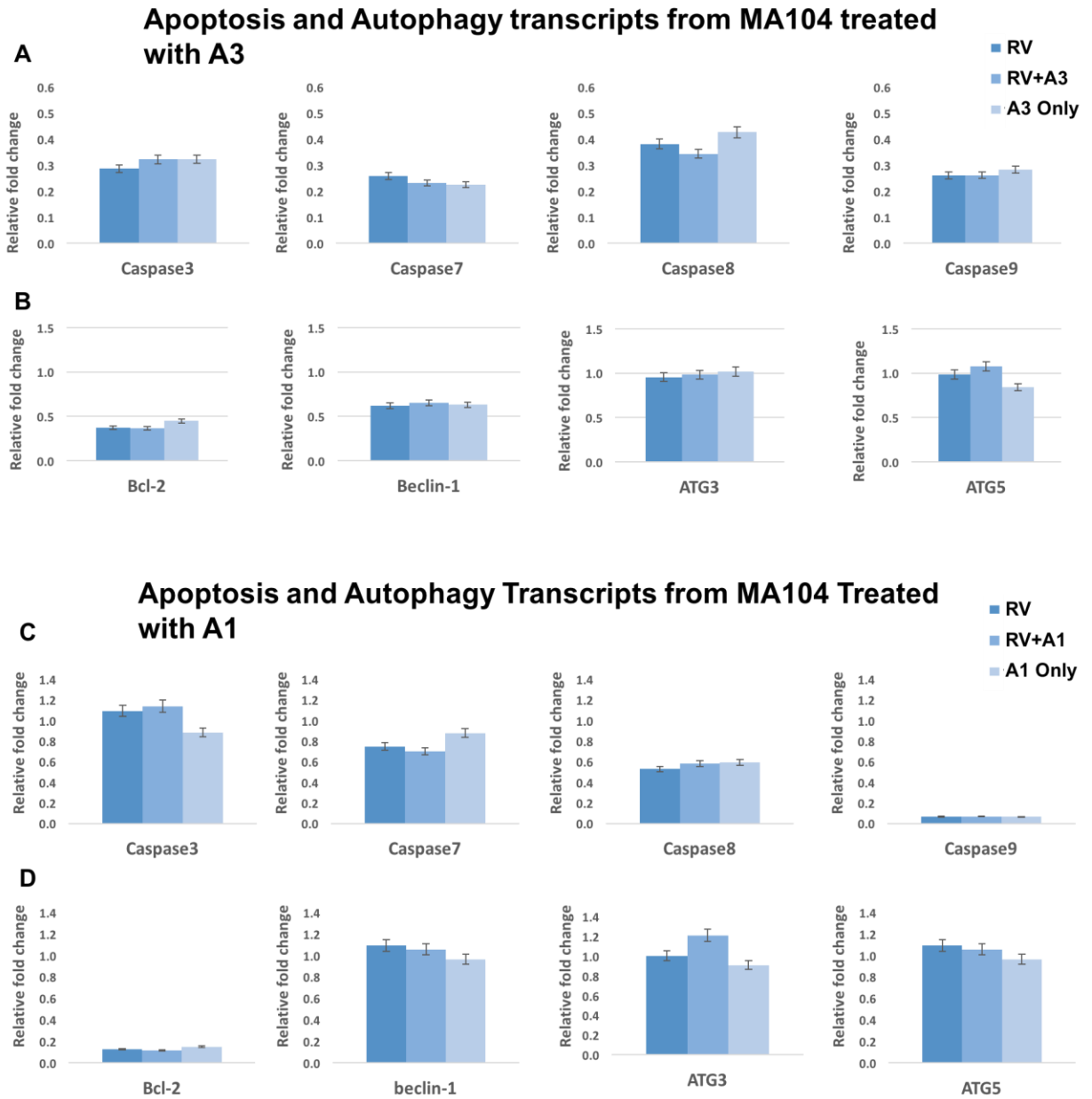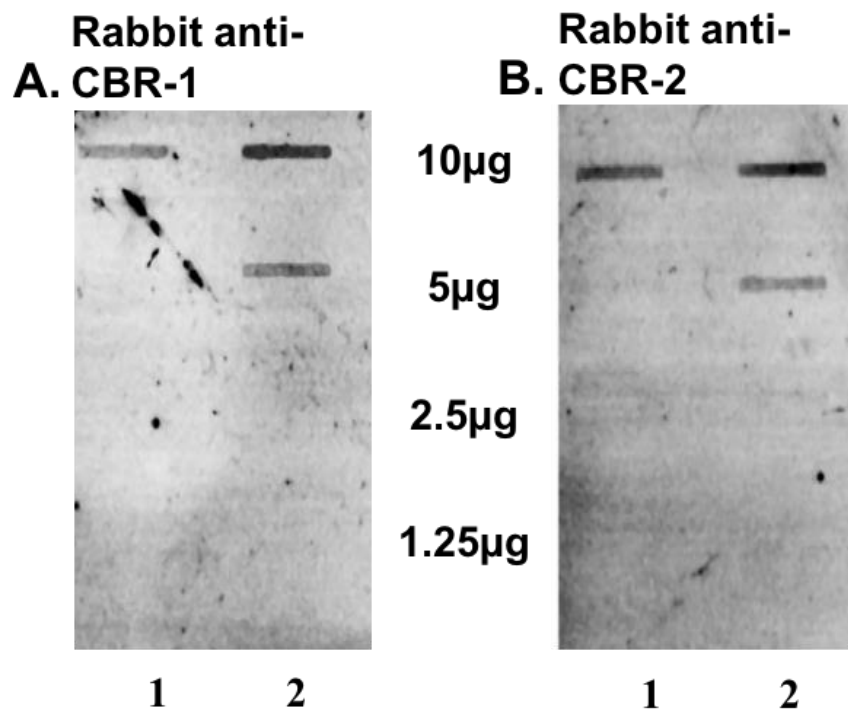**Figure 8**

Fig. 1. MA104 cell viability assay. Using Trypan blue exclusion dye, the cells were counted in triplicate with and without treatments at 18hpi and percent live/dead cells were calculated. Data are expressed as mean ± SD, and comparisons were statistically evaluated by Student's *t*-tests using Excel (significance level, $p \leq 0.05$).

Fig. 2. Plaque forming assays using supernatants from RV-infected and arachidin treated MA104 cells. MA104 cells were infected with a human RV (Wa) treated with/without A1 or A3. The inoculum was replaced with serum-free DMEM supplemented with 1 µg/mL trypsin. At 18hpi, the cells & media were collected, centrifuged, and stored at -80°C. To titer the RV from the supernatants, MA104 cells were incubated with serial dilutions of the test samples & plaque forming assays were used to determine the number plaque forming units (PFU/mL). * Comparison on RV only to RV + A1, $p = 0.014$. ** Comparison of RV to RV + A3, $p = 0.014$ *** Comparison on RV + DMSO to RV + A1, $p = 0.006$ **** Comparison of RV + DMSO to RV + A3, $p = 0.006$.

Fig. 3. Morphometric analysis of RV-infected MA104 cells treated with and without arachidins at 18 hpi. Cells were collected and processed for TEM analysis and the nucleus and whole cell were measured with Macnification (Orbicule, Inc). Nucleus to cytoplasm ratios were obtained and compared for 10 cells of each treatment.

Fig. 4. RV particle size populations. A) Transmission electron micrograph (TEM) of Wa rotavirus infected MA104 cells at 18hpi). Final Magnification = 57,000x. Endoplasmic reticulum (ER), Viroplasm (V), Enveloped virus particles (E), and non-enveloped virus particle (NE). B) Measurements of RV particles in TEM micrographs of MA104 cells infected with Wa rotavirus at 18 hpi, n = 22 per group. Statistically significant p = 1.96E-31.

Fig. 5. Percent MA104 Cells with Autophagic Vesicles at 18 hpi. The presence of autophagosomes in the cytoplasm of RV and RV treated cells were scored and compared to the three controls, NV, A1 and A3 only. The percent positive cells (n=12 for each treatment) were calculated and graphed.

Fig. 6. TRPS analysis of arachidin treat MA104 cells. The size variations, virus concentrations and population distribution of extracellular RV particles were measured from supernatants of RV-infected cells treated with/without A1 and A3 at 18 hpi. A) RV-infected supernatants, B) Supernatants from RV-infected cells treated with 20µM A3, and C) Supernatants from RV-infected cells treated with 20µM A1.

Fig.7. Real-time quantitative PCR (qRT-PCR) data for gene transcripts in apoptosis and autophagy signaling pathways. Total RNA was extracted from MA104 cells with RV,

RV+20µM A1, RV+20µM A3, 20µM A1 or 20µM A3 at 8 hpi. cDNA for each treatment was synthesized and used for qRT-PCR experiments. Fold change in expression of the genes of interest relative to GAPDH and β-actin were determined using the $2^{\Delta\Delta CT}$ method. The results are expressed as mean ± SD from three separate experiments.

Fig. 8. Cannabinoid Receptors 1 & 2 on MA104 cells. MA104 cell lysates [1-uninfected and 2-RV-infected (Wa)] were added to nitrocellulose membranes, probed with a 1:1000 dilution of rabbit anti-CBR1 (A) or anti-CBR-2 (B) antibodies from Antibodies Online (Atlanta, GA) and reactive bands were visualized by the addition and excitation of goat anti-rabbit antibodies Alexa Fluor®546 (Life Technologies) using the Typhoon 9500 Plus laser scanner.

Conflict of interest

The authors declare that there is no conflict of interest regarding the publication of this paper.

Acknowledgements

Style: ACMAP

References

Abbott, J. A., Medina-Bolivar, F., Martin, E. M., Engelberth, A. S., Villagarcia, H., Clausen, E. C., & Carrier, D. J. (2010). Purification of resveratrol, arachidin-1, and arachidin-3 from hairy root cultures of peanut (Arachis hypogaea) and determination of their antioxidant activity and cytotoxicity. *Biotechnology Progress*, *26*(5), 1344–1351. http://doi.org/10.1002/btpr.454

Adams, W. R., & Kraft, l. M. (1963). Epizootic diarrhea of infant mice: indentification of the etiologic agent. *Science (New York, N.Y.)*, *141*(3578), 359–360.

Aggarwal, B. B., Bhardwaj, A., Aggarwal, R. S., Seeram, N. P., Shishodia, S., & Takada, Y. (2004). Role of resveratrol in prevention and therapy of cancer: preclinical and clinical studies. *Anti- Cancer Research*, *24*, 2783–2840.

Anderson, E. J., & Weber, S. G. (2004). Rotavirus infection in adults. *The Lancet Infectious Diseases*, *4*(February), 91–99.

Arnold, M., Patton, J. T., & McDonald, S. M. (2009). Culturing, storage, and quantification of rotaviruses. *Current Protocols in Microbiology*, *SUPPL. 15C*. http://doi.org/10.1002/9780471729259.mc15c03s15

Arnold, M., Patton, J. T., & Mcdonald, S. M. (2012). Culturing, Storage, and Quantification of Rotavirus. *Current Protocols in Microbiology*, *15C.3*, 1–29. http://doi.org/10.1002/9780471729259.mc15c03s15.Culturing

Athar, M., Back, J. H., Tang, X., Kim, K. H., Kopelovich, L., Bickers, D. R., & Kim, A. L. (2007). Resveratrol: a review of preclinical studies for human cancer prevention.

Toxicology and Applied Pharmacology, *224*, 274–283.

Ayala-Breton, C., Arias, M., Espinosa, R., Romero, P., Arias, C. F., & López, S. (2009). Analysis of the kinetics of transcription and replication of the rotavirus genome by RNA interference. *Journal of Virology*, *83*(17), 8819–8831. http://doi.org/10.1128/JVI.02308-08

Bakare, N., Menschik, D., Tiernan, R., Hua, W., & Martin, D. (2010). Severe combined immunodeficiency (SCID) and rotavirus vaccination: Reports to the Vaccine Adverse Events Reporting System (VAERS). *Vaccine*, *28*(40), 6609–6612. http://doi.org/10.1016/j.vaccine.2010.07.039

Ball, J. M., Medina-Bolivar, F., Defrates, K., Hambleton, E., Hurlburt, M., Fang, L., Parr, R. (2015). Investigation of stilbenoids as potential therapeutic agents for rotavirus gastroenteritis. *Advances in Virology*.

Berardi, V., Ricci, F., Castelli, M., Galati, G., & Risuleo, G. (2009). Resveratrol exhibits a strong cytotoxic activity in cultured cells and has an antiviral action against polyomavirus: potential clinical use. *Journal of Experimental & Clinical Cancer Research : CR*, *28*, 96. http://doi.org/10.1186/1756-9966-28-96

Bernstein, D. I. (2009). Rotavirus overview. *The Pediatric Infectious Disease Journal*, *28*, S50–S53. http://doi.org/10.1097/INF.0b013e3181967bee

Bhandari, N., Rongsen-Chandola, T., Bavdekar, A., John, J., Antony, K., Taneja, S., Bhan, M. K. (2014). Efficacy of a monovalent human-bovine (116E) rotavirus vaccine in Indian infants: A randomised, double-blind, placebo-controlled trial. *The Lancet*, *383*(9935),

2136–2143. http://doi.org/10.1016/S0140-6736(13)62630-6

Bishop, R. (2009). Discovery of rotavirus: Implications for child health. *Journal of Gastroenterology and Hepatology*, *24 Suppl 3*, S81–S85. http://doi.org/10.1111/j.1440-1746.2009.06076.x

Bishop, R., Davidson, G. P., Holmes, I. H., & Ruck, B. J. (1973). Virus particles in epithelial cells of duodenal mucosa from children with acute non-bacterial gastroenteritis. *The Lancet*, *302*(7841), 1281–1283.

Bo, A. N., Pol, E. Van Der, & Grootemaat, A. E. (2014). Single-step isolation of extracellular vesicles by size-exclusion chromatography. *Journal of Controlled Release : Official Journal of the Controlled Release Society*, *1*, 1–11. http://doi.org/10.3402/jev.v3.23430

Bobek, V., Kolostova, K., Pinterova, D., Kacprzak, G., Adamiak, J., Kolodziej, J., Hoffman, R. M. (2010). A clinically relevant, syngeneic model of spontaneous, highly metastatic B16 mouse melanoma. *Anticancer Research*, *30*(12), 4799–4804. http://doi.org/10.1002/jmv

Brents, L. K., Medina-Bolivar, F., Seely, K. a., Nair, V., Bratton, S. M., Ñopo-Olazabal, L., Radominska-Pandya, A. (2012). Natural prenylated resveratrol analogs arachidin-1 and -3 demonstrate improved glucuronidation profiles and have affinity for cannabinoid receptors. *Xenobiotica*, *42*(2), 139–156. http://doi.org/10.3109/00498254.2011.609570

Chang, J. C., Lai, Y. H., Djoko, B., Wu, P. L., Liu, C. D., Liu, Y. W., & Chiou, R. Y. Y. (2006). Biosynthesis enhancement and antioxidant and anti-inflammatory activities of peanut (Arachis hypogaea L.) arachidin-1, arachidin-3, and isopentadienylresveratrol.

Journal of Agricultural and Food Chemistry, *54*(26), 10281–10287.

http://doi.org/10.1021/jf0620766

Chong, J., Anne, P., & Hugueney, P. (2009). Metabolism and roles of stilbenes in plants. *Plant Science*, *177*(3), 143–155.

Condori, J., Sivakumar, G. Hubstenberger, J., Dolan, M. C., Sobolev, V. S., & Medina-Bolivar, F. (2010). Induced biosynthesis of resveratrol and the prenylated stilbenoids arachidin-1 and arachidin-3 in hairy root cultures of peanut: effects of culture medium and growth stage. *Plant Physiology and Biochemistry*, *48*(5), 310–318.

Cook, S. M., Glass, R. I., LeBaron, C. W., & Ho, M. S. (1990). Global seasonality of rotavirus infections. *Bulletin of the World Health Organization*, *68*(2), 171–177.

Crawford, S. E., Hyser, J. M., Utama, B., & Estes, M. K. (2012). Autophagy hijacked through viroporin-activated calcium/calmodulin-dependent kinase kinase-β signaling is required for rotavirus replication. *Proceedings of the National Academy of Sciences of the United States of America*, *109*(50), E3405–13. http://doi.org/10.1073/pnas.1216539109

Dang, S., Yu, Z., Zhang, C., Zheng, J., Li, K., Wu, Y., Wang, R. (2015). Autophagy promotes apoptosis of mesenchymal stem cells under inflammatory microenvironment. *Stem Cell Research & Therapy*, 1–9. http://doi.org/10.1186/s13287-015-0245-4

DeBlois, R. W. (1970). Counting and Sizing of Submicron Particles by the Resistive Pulse Technique. *Review of Scientific Instruments*, *41*(7), 909. http://doi.org/10.1063/1.1684724

Desselberger, U. (2014). Rotaviruses. *Virus Research*, *190*, 75–96.

http://doi.org/10.1016/j.virusres.2014.06.016

Di Fiore, I. J. M., Holloway, G., & Coulson, B. S. (2015). Innate immune responses to rotavirus infection in macrophages depend on MAVS but involve neither the NLRP3 inflammasome nor JNK and p38 signaling pathways. *Virus Research*, *208*, 89–97. http://doi.org/10.1016/j.virusres.2015.06.004

Djoko, B., Chiou, R. Y. Y., Shee, J. J., & Liu, Y. W. (2007). Characterization of immunological activities of peanut stilbenoids, arachidin-1, piceatannol, and resveratrol on lipopolysaccharide-induced inflammation of RAW 264.7 macrophages. *Journal of Agricultural and Food Chemistry*, *55*(6), 2376–2383. http://doi.org/10.1021/jf062741a

Elmore, S. (2007). Apoptosis: a review of programmed cell death. *Toxicologic Pathology*, *35*(4), 495–516. http://doi.org/10.1080/01926230701320337

Estes, M. K., Graham, D. Y., & Mason, B. B. (1981). Proteolytic enhancement of rotavirus infectivity: molecular mechanisms. *Journal of Virology*, *39*(3), 879–888. http://doi.org/10.1016/0042-6822(80)90456-0

Estes, M. K., & Greenberg, H. . (2013). Rotaviruses. In *Fields Virology* (6th ed., pp. 1347–1401). Wolters Kluwer Health/Lippincott Williams & Wilkins, Philadelphia, PA.

Flewett, T. H., & Woode, G. N. (1978). The rotaviruses. *Archives of Virology*, *57*(1), 1–23.

Freshney, R. I. (1994). *Culture of Animal Cells: A Manual of Basic Technique.* (3rd ed.). New York: Wiley-Liss.

Frias, A. H., Jones, R. M., Fifadara, N. H., Vijay-Kumar, M., & Gewirtz, A. T. (2012).

Rotavirus-induced IFN-β promotes anti-viral signaling and apoptosis that modulate viral replication in intestinal epithelial cells. *Innate Immunity*, *18*(2), 294–306. http://doi.org/10.1177/1753425911401930

Gambini, J., Inglés, M., Olaso, G., Abdelaziz, K. M., Vina, J., & Borras, C. (2015). Properties of Resveratrol: In Vitro and In Vivo Studies about Metabolism, Bioavailability, and Biological Effects in Animal Models and Humans. *Oxidative Medicine and Cellular Longevity*, *2015*.

Gardet, A., Breton, M., Fontanges, P., Trugnan, G., & Chwetzoff, S. (2006). Rotavirus spike protein VP4 binds to and remodels actin bundles of the epithelial brush border into actin bodies. *Journal of Virology*, *80*(8), 3947–3956. http://doi.org/10.1128/JVI.80.8.3947-3956.2006

Glass, R. I., Parashar, U., Patel, M., Gentsch, J., & Jiang, B. (2014). Rotavirus vaccines: Successes and challenges. *Journal of Infection*, *68*, S9–S19. http://doi.org/10.1016/j.jinf.2013.09.010

Greenberg, H. B., & Estes, M. K. (2009). Rotaviruses: From Pathogenesis to Vaccination. *Gastroenterology*, *136*(6), 1939–1951. http://doi.org/10.1053/j.gastro.2009.02.076

Halasz, P., Holloway, G., Turner, S. J., & Coulson, B. S. (2008). Rotavirus replication in intestinal cells differentially regulates integrin expression by a phosphatidylinositol 3-kinase-dependent pathway, resulting in increased cell adhesion and virus yield. *Journal of Virology*, *82*(1), 148–160. http://doi.org/10.1128/JVI.01980-07

Hall, G. A., Bridger, C., Chandler, R. L., & Wwde, G. N. (1976). Gnotobiotic Piglets

Experimentally Infected with Neonatal Calf Diarrhoea Reovirus-Like Agent (Rotavirus

), *210*, 197–210.

Hammerschimidt, R., & Dann, E. K. (1999). The role of phytoalexins in plant protection. *Novartis Foundation Symposium*, *223*, 175–87. http://doi.org/223

Holloway, G., & Coulson, B. S. (2006). Rotavirus activates JNK and p38 signaling pathways in intestinal cells, leading to AP-1-driven transcriptional responses and enhanced virus replication. *Journal of Virology*, *80*(21), 10624–10633. http://doi.org/10.1128/JVI.00390-06

Holloway, G., & Coulson, B. S. (2013). Innate cellular responses to rotavirus infection. *Journal of General Virology*, *94*(Pt_6), 1151–1160. http://doi.org/10.1099/vir.0.051276-0

Hsieh, Y. C., Wu, F. T., Hsiung, C. A., Wu, H. S., Chang, K. Y., & Huang, Y. C. (2014). Comparison of virus shedding after lived attenuated and pentavalent reassortant rotavirus vaccine. *Vaccine*, *32*(10), 1199–1204. http://doi.org/10.1016/j.vaccine.2013.08.041

Huang, C.-P., Au, L.-C., Chiou, R. Y.-Y., Chung, P.-C., Chen, S.-Y., Tang, W.-C., Lin, S.-B. (2010). Arachidin-1, a peanut stilbenoid, induces programmed cell death in human leukemia HL-60 cells. *Journal of Agricultural and Food Chemistry*, (16), 12123–12129. http://doi.org/10.1021/jf102993j

Jeandet, P., Delaunois, B., Conreux, A., Donnez, D., Nuzzo, V., Cordelier, S., … Courot, E. (2010). Biosynthesis, metabolism, molecular engineering, and biological functions of

stilbene phytoalexins in plants. *BioFactors*, *36*(5), 331–341.

Jiang, V., Jiang, B., Tate, J., Parashar, U. D., & Patel, M. M. (2010). Performance of rotavirus vaccines in developed and developing countries. *Human Vaccines*, *6*(7), 532–542. http://doi.org/10.4161/hv.6.7.11278

John M Chirgwin, Przybyla, A. E., MacDonald, R. J., & Rutter, W. J. (1979). Isolation of biologically active ribonucleic acid from sources enriched in ribonuclease. *Biochemistry*, *18*(24), 5294–5299. http://doi.org/10.1021/bi00591a005

Jones, C. L. (2015). Characterization of Vesicular stomatitis virus populations by tunable resistive pulse sensing Fulya, *33*(4), 395–401. http://doi.org/10.1038/nbt.3121.ChIP-nexus

Kozak, D., Anderson, W., Vogel, R., & Trau, M. (2011). Advances in resistive pulse sensors: Devices bridging the void between molecular and microscopic detection. *Nano Today*, *6*(5), 531–545. http://doi.org/10.1016/j.nantod.2011.08.012

Kroemer, G., & Levine, B. (2009). Autophagic cell death: the story of a misnomer. *Apoptosis*, *9*(12), 1004–1010. http://doi.org/10.1038/nrm2527.Autophagic

Leshem, E., Lopman, B., Glass, R., Gentsch, J., Banyai, K., Parashar, U., & Patel, M. (2014). Distribution of rotavirus strains and strain-specifi c eff ectiveness of the rotavirus vaccine after its introduction: a systematic review and meta-analysis, (August 2015).

Light, J. S., & Hodes, H. L. (1943). Studies on epidemic diarrhea of the new-born: isolation of a filtrable agent causing diarrhea in calves. *American Journal of Public Health*, *33*(12), 1451.

Marsh, Z., Yang, T., Nopo-Olazabal, L., Wu, S., Ingle, T., Joshee, N., & Medina-Bolivar, F. (2014). Effect of light, methyl jasmonate and cyclodextrin on production of phenolic compounds in hairy root cultures of Scutellaria lateriflora. *Phytochemistry*, *107*, 50–60. http://doi.org/http://dx.doi.org/10.1016/j.phytochem.2014.08.020

Matthews, R. (1979). The classification and nomenclature of viruses. *Intervirology*, *11*, 133–135.

Matthijnssens, J., Ciarlet, M., Heiman, E., Arijs, I., Delbeke, T., McDonald, S. M., … Van Ranst, M. (2008). Full genome-based classification of rotaviruses reveals a common origin between human Wa-Like and porcine rotavirus strains and human DS-1-like and bovine rotavirus strains. *Journal of Virology*, *82*(7), 3204–3219. http://doi.org/10.1128/JVI.02257-07

McNulty, M., Curran, W., & McFerran, J. (1976). The morphogenesis of a cytopathic bovine rotavirus in Madin-Darby bovine kidney cells. *Journal of General Virology*, *33*(3), 503–508.

Mebus, C. A., Wyatt, R. G., Sharpee, R. L., Sereno, M. M., Kalica, A. R., & Twiehaus, M. J. (1976). Diarrhea in gnotobiotic calves caused by the reovirus-like agent of human infantile Diarrhea in Gnotobiotic Calves Caused by the Reovirus-Like Agent of Human Infantile Gastroenteritis1, *14*(2), 471–474.

Mitchell, D. M., & Ball, J. M. (2004). Characterization of a spontaneously polarizing HT-29 cell line, HT-29/cl.f8. *In Vitro Cellular & Developmental Biology. Animal*, *40*(10), 297–302. http://doi.org/10.1290/04100061.1

Moss, R., Mao, Q., Taylor, D., & Saucier, C. (2013). Investigation of monomeric and
oligomeric wine stilbenoids in red wines by ultra-high-performance liquid
chromatography/electrospray ionization quadrupole time-of-flight mass spectrometry.
Rapid Communications in Mass Spectrometry, *27*, 1815–1827.
http://doi.org/10.1002/rcm.6636

Nakamura, M., Saito, H., Ikeda, M., Hokari, R., Kato, N., Hibi, T., & Miura, S. (2010). An
antioxidant resveratrol significantly enhanced replication of hepatitis C virus. *World
Journal of Gastroenterology*, *16*(2), 184–192. http://doi.org/10.3748/wjg.v16.i2.184

Nikoletopoulou, V., Markaki, M., Palikaras, K., & Tavernarakis, N. (2013). Crosstalk
between apoptosis, necrosis and autophagy. *Biochimica et Biophysica Acta - Molecular
Cell Research*, *1833*(12), 3448–3459. http://doi.org/10.1016/j.bbamcr.2013.06.001

Noguchi, M., & Hirata, N. (2015). Intersection of apoptosis and autophagy cell Death
pathways. *Austin Journal of Molecular and Cellular Biology*, *2*(1), 1–7.

Otto, P. H., Reetz, J., Eichhorn, W., Herbst, W., & Elschner, M. C. (2015). Isolation and
propagation of the animal rotaviruses in MA-104 cells—30 years of practical
experience. *Journal of Virological Methods*, *223*, 88–95.
http://doi.org/10.1016/j.jviromet.2015.07.016

Palamara, A. T., Nencioni, L., Aquilano, K., De Chiara, G., Hernandez, L., Cozzolino, F.,
Garaci, E. (2005). Inhibition of influenza A virus replication by resveratrol. *The Journal
of Infectious Diseases*, *191*, 1719–1729. http://doi.org/10.1086/429694

Parashar, U. D., & Glass, R. I. (2009). Rotavirus Vaccines - Early Success, Remaining

Questions. *New England Journal of Medicine*, *360*(11), 1063–1065. http://doi.org/10.1056/NEJMp0810154

Park, M., Yun, Y. J., Woo, S. Il, Lee, J. W., Chung, N. G., & Cho, B. (2015). Rotavirus-associated hemophagocytic lymphohistiocytosis (HLH) after hematopoietic stem cell transplantation for familial HLH. *Pediatrics International*, *57*(2), e77–e80. http://doi.org/10.1111/ped.12567

Patel, N. C., Hertel, P. M., Estes, M. K., de la Morena, M., Petru, A. M., Noroski, L. M., Abramson, S. L. (2010). Vaccine-acquired rotavirus in infants with severe combined immunodeficiency. *The New England Journal of Medicine*, *362*(4), 314–9. http://doi.org/10.1056/NEJMoa0904485

Pattingre, S., Tassa, A., Qu, X., Garuti, R., Xiao, H. L., Mizushima, N., Levine, B. (2005). Bcl-2 antiapoptotic proteins inhibit Beclin 1-dependent autophagy. *Cell*, *122*(6), 927–939. http://doi.org/10.1016/j.cell.2005.07.002

Patton, J. T. (1995). Structure and function of the rotavirus RNA-binding proteins. *Journal of General Virology*, *76*(11), 2633–2644. http://doi.org/10.1099/0022-1317-76-11-2633

Patton, J. T. (2012). Rotavirus diversity and evolution in the post-vaccine world. *Discovery Medicine*, *13*(68), 85–97. Retrieved from http://www.pubmedcentral.nih.gov/articlerender.fcgi?artid=3738915&tool=pmcentrez&rendertype=abstract

Payne, C., Thomas, B., Skillicorn, C., & Charles, G. (2012). Anti-Apoptotic and Pro-Apoptotic Molecular and Cellular Pathways Induced by Viral Agents of Human and Animal

Gastroenteritis: A Comprehensive Review. Retrieved from http://www.viralem.com/wp-content/uploads/2012/08/How-G.I.-Viruses-Kill-Cells.pdf

Payne, D., Staat, M., Edwards, K., Szilagyi, P., Gentsch, J., Stockman, L., Parashar, U. (2006). Rotavirus Proteins: Structure and Assembly. *CTMI*, *309*, 189–219.

Roupe, K. A., Remsberg, C. M., Yanez, J. A., & Davies, N. M. (2006). 2006. Pharmacometrics of stilbenes: seguing towards the clinic. *Current Clinical Pharmacology*, *1*, 81–101.

Ruiz, M. C., Leon, T., Diaz, Y., & Michelangeli, F. (2009). Molecular biology of rotavirus entry and replication. *TheScientificWorldJournal*, *9*, 1476–1497. http://doi.org/10.1100/tsw.2009.158

Rzeżutka, A., & Cook, N. (2004). Survival of human enteric viruses in the environment and food. *FEMS Microbiology Reviews*, *28*(4), 441–453. http://doi.org/10.1016/j.femsre.2004.02.001

Saxena, K., Blutt, S. E., Ettayebi, K., Zeng, X., Broughman, J. R., Crawford, S. E., Estes, K. (2016). Human Intestinal Enteroids : a New Model To Study Human Rotavirus Infection , Host Restriction , and Pathophysiology, *90*(1), 43–56. http://doi.org/10.1128/JVI.01930-15.Editor

Sobolev, V. S., Potter, T. L., & Horn, B. W. (2006). Prenylated stilbenes from peanut root mucilage. *Phytochemical Analysis*, *17*(5), 312–322. http://doi.org/10.1002/pca.920

Stokley, S., Jeyarajah, J., Yankey, D., Cano, M., Gee, J., Roark, J., Markowitz, L. (2014). Human papillomavirus vaccination coverage among adolescents, 2007-2013, and postlicensure vaccine safety monitoring, 2006-2014 - United States. *MMWR. Morbidity*

and Mortality Weekly Report, *63*(29), 620–4. Retrieved from
http://www.ncbi.nlm.nih.gov/pubmed/25055185

Superti, F., Ammendolia, M. G., Tinari, A., Bucci, B., Giammarioli, A. M., Rainaldi, G.,
Donelli, G. (1996). Induction of apoptosis in HT-29 cells infected with SA-11 rotavirus.
Journal of Medical Virology, *50*(4), 325–334. http://doi.org/10.1002/(SICI)1096-
9071(199612)50

Takacs-Vellai, K., Vellai, T., Puoti, A., Passannante, M., Wicky, C., Streit, A., Müller, F.
(2005). Inactivation of the autophagy Gene bec-1 triggers apoptotic cell death in C.
elegans. *Current Biology*, *15*(16), 1513–1517. http://doi.org/10.1016/j.cub.2005.07.035

Tate, J. E., Burton, A. H., Boschi-Pinto, C., Steele, A. D., Duque, J., & Parashar, U. D. (2012).
2008 estimate of worldwide rotavirus-associated mortality in children younger than 5
years before the introduction of universal rotavirus vaccination programmes: a systematic
review and meta-analysis. *The Lancet. Infectious Diseases*, *12*(2), 136–141.
http://doi.org/10.1016/S1473-3099(11)70253-5

Teimoori, A., Soleimanjahi, H., & Makvandi, M. (2014). Characterization and transferring of
human rotavirus double-layered particles in MA104 cells. *Jundishapur Journal of
Microbiology*, *7*(6), 1–5. http://doi.org/10.5812/jjm.10375

Uzri, D., & Greenberg, H. B. (2013). Characterization of Rotavirus RNAs That Activate Innate
Immune Signaling through the RIG-I-Like Receptors. *PLoS ONE*, *8*(7), 1–15.
http://doi.org/10.1371/journal.pone.0069825

Velayudhan, L., Van Diepen, E., Marudkar, M., Hands, O., Suribhatla, S., Prettyman, R.,

Bhattacharyya, S. (2014). Therapeutic potential of cannabinoids in neurodegenerative disorders: a selective review. *Current Pharmaceutical Design*, *20*(13), 2218–30. http://doi.org/10.2174/13816128113199990434

Vitaglione, P., Sforza, S., & Galaverna, G. (2005). Bioavailability of trans-resveratrol from red wine in humans. *Molecular Nutrition*, *49*(5), 495–504.

Vogel, R., Willmott, G., Kozak, D., Roberts, G. S., Anderson, W., Groenewegen, L., Trau, M. (2011). Quantitative Sizing of Nano/ Microparticles with a Tunable Elastomeric Pore Sensor. *Analytical Chemistry*, *83*(9), 3499–3506.

Vogelstein, B., & Gillespie, D. (1979). Preparative and analytical purification of DNA from agarose. *Proceedings of the National Academy of Sciences of the United States of America*, *76*(2), 615–619. http://doi.org/10.1073/pnas.76.2.615

Wang, H., Ramakrishnan, A., Fletcher, S., Prochownik, E. V, & Genetics, M. (2015). Current questions and possible controversies in autophagy. *Cell Death Discov.*, *2*(2), 1–20. http://doi.org/10.14440/jbm.2015.54.A

Ward, R. L. (1996). Mechanisms of protection against rotavirus in humans and mice. *The Journal of Infectious Diseases*, *174 Suppl* (3), S51–S58. http://doi.org/10.1097/INF.0b013e3181967c16

Weatherall, E., Hauer, P., Vogel, R., & Willmott, G. R. (2016). Pulse Size Distributions in Tunable Resistive Pulse Sensing. *Anal. Chem*, *88*(17), 8648–8656. http://doi.org/10.1021/acs.analchem.6b01818

Weinberg, G., Teel, E. N., Mijatovic-Rustempasic, S., Payne, D. C., Roy, S., Foytich, K.,

Bowen, M. D. (2013). Detection of novel rotavirus strain by vaccine postlicensure surveillance. *Emerging Infectious Diseases*, *19*(8), 1321–1323. http://doi.org/10.3201/eid1908.130470

World Health Organization. (2013). Weekly epidemiological record Relevé épidémiologique hebdomadaire. *Weekly Epidemiological Record*, (5), 49–64. Retrieved from http://www.who.int/wer/2013/wer8805.pdf

Wright, R. (2000). Transmission electron microscopy of yeast. *Microsc Res Tech.*, *51*(6), 496–510.

Yakshe, K. a, Franklin, Z. D., & Ball, J. M. (2015). *Rotaviruses: Extraction and Isolation of RNA, Reassortant Strains, and NSP4 Protein. Current Protocols in Microbiology*. http://doi.org/10.1002/9780471729259.mc15c06s37

Yang, T., Fang, L., Nopo-Olazabal, C., Condori, J., Nopo-Olazabal, L., Balmaceda, C., & Medina-Bolivar, F. (2015). Enhanced Production of Resveratrol, Piceatannol, Arachidin-1, and Arachidin-3 in Hairy Root Cultures of Peanut Co-treated with Methyl Jasmonate and Cyclodextrin. *Journal of Agricultural and Food Chemistry*, *63*, 3942–3950. http://doi.org/10.1021/jf5050266

Yen, C., Jakob, K., Bsn, R. N., Esona, M. D., Rausch, J., Hull, J. J., Jon, R. (2015). HHS Public Access, *29*(24), 4151–4155. http://doi.org/10.1016/j.vaccine.2011.03.074.Detection

Yen, C., Tate, J. E., Hyde, T. B., Cortese, M. M., Lopman, B. A., Jian, B., … Parashar, U. D. (2014). RV Vaccines.

Yin, Y., Metselaar, H. J., Sprengers, D., Peppelenbosch, M. P., & Pan, Q. (2015). Rotavirus in organ transplantation: Drug-virus-host interactions. *American Journal of Transplantation*, *15*(3), 585–593. http://doi.org/10.1111/ajt.13135

CONCLUSIONS

Historically, rotavirus (RV) infections have been shown to be detrimental to host cells due to increased cellular stress that can lead to several cell death pathways, including apoptosis (Payne et al., 2012). In a previous study, simian RV-infected human intestinal cells (HT29.f8) exhibited a decrease in the production of infectious RV that suggested a decrease in viral replication when treated with A1 or A3 (Ball et al., 2015). This implies that the arachidins have an effect on the cells and the RV particles. To identify the effects of the arachidins on RV-infected cells, two cell lines, the African green monkey kidney cell line (MA104) and the human intestinal cells (HT29.f8), were infected with a human RV, Wa, and treated with A1 or A3. At 18 hpi, progeny infectious RV particles along with host cell ultrastructure were altered with the addition of the arachidins, thus indicating that the arachidins have antiviral activity against the human strain in both cell lines.

The production and release of infectious RV progeny decreased when both MA104 and HT29.f8 cells were treated with A1 and A3. Also, intracellular RV particles were measured and shown to have similar diameters representing two populations of particles [enveloped ($_e$RV) and nonenveloped ($_{ne}$RV)] in both cell lines. Furthermore, at 18 hpi, the populations of extracellular particles released from RV-infected cells exhibited similar diameters to the intracellular particles. This suggests that the smaller $_{ne}$RV population represents infectious RV particles. However, at 18 hpi, the extracellular population identified from RV-infected cells with A3 were of a larger size ($_e$RV), consistent with that of more immature noninfectious particles. At the same time point, the extracellular population identified from RV-infected cells with A1 were broad

in sizes ranging from the smaller more mature particles $_{ne}$RV to a larger size ($_e$RV), a more immature noninfectious population of particles.

Likewise, at 18 hpi, both cell lines demonstrated similar ultrastructural characteristics of apoptosis which appeared to be regulated to a more normal state with the addition of the arachidins. In addition, A1 treated cells presented increased numbers of autophagosomes, suggesting an initiation of autophagy, a pro-survival pathway that degrades and recycles damaged proteins and organelles when exposed to cellular and metabolic stress (Noguchi & Hirata, 2015).

To further explore the regulation of the apoptosis and autophagy death pathways, gene transcripts representing both pathways were quantified. HT29.f8 cells demonstrated an upregulation of the apoptosis genes and two autophagy genes (Bcl-2 and Beclin-1) which were significantly decreased with the addition of either A1 or A3. This indicates a cross-talk between the pathways is modulated in the presence of the arachidins in the human intestinal cell line at 8 hpi. However, we detected no regulation of either pathway during RV infection in MA104 cells at 8hpi. This implies that the cells use different mechanisms of action to achieve a reduction in infectious RV particles at 18 hpi or that there is a different temporal regulation of these cell death pathways in MA104 cells.

Gathered from this data we can conclude that, even without the regulation of apoptosis and autophagy transcripts in the MA104 cells, the arachidins play a significant role in regulating RV infections by decreasing the amount of virus produced and preserving host cell ultrastructure, advocating the need to look further at the progression of an RV infection to learn more about the antiviral capabilities of the arachidins.

The HT29.f8 study employed time course experiments to observe RV production and host cell ultrastructure over the course of an infection treated with arachidins. Morphological changes in cell ultrastructure were seen from 12-18 hpi that revealed a progression to apoptosis by 18 hpi in RV infected cells while RV-infected cells treated with either arachidin exhibited an increase in nuclear size that returned to normal by 18 hpi. Interestingly, between 16 and 18 hpi, a switch was observed in nucleus to cytoplasm ratios between the RV only cells and those treated with arachidins. This data shows an important time point where the arachidins are triggering a change in the host cell. Moreover, throughout the time course, the number of cells with autophagosomes increased with the addition of A1 but not with A3. This suggest A1 and A3 employ different mechanisms of action.

Analysis of the extracellular RV particles released from 12-18 hpi from RV-infected HT29.f8 cells demonstrated a concentration of a broad RV particle size range to particles that correspond to $_{ne}$RV seen intracellularly, but A1 treatments produced particles that ranged in size from $_e$RV to $_{ne}$RV. Conversely, A3 treated cells displayed a more focused group of $_e$RV particles, suggesting that particles released from these treatments did not mature completely before leaving the cell. Taken together, both studies demonstrated ultrastructural regulations of apoptosis with both arachidins, the initiation of autophagy with A1 treatments, and a decrease in RV production with either arachidin with a shift in RV population to a more immature size. Future studies will explore the receptors on host cells to discover how the arachidins enter or start a signaling pathway in the cells. Collectively, RV infections have been differentially modulated with the arachidins in cell lines from two different tissues and two different species. Further studies will be performed to identify the mechanisms of

actions and temporal regulation of the arachidins as their potential development as broad acting anti-RV therapeutics is explored.

VITA

Caleb Witcher graduated from Stephen F. Austin State University with a Bachelors in Animal Science in December 2014. He entered graduate school at Stephen F. Austin State University, Nacogdoches, Texas in January 2015 and will receive a Master of Science degree in Biology with a Minor in Biotechnology in May 2017.

Permanent Address: 686 County Road 715

    Nacogdoches, Tx 75964

Email Address: witchercm@gmail.com

Style: Virus Research and ACMAP

This thesis was typed by Caleb Michael Witcher.